

INAUGURAL – DISSERTATION

**zur Erlangung der Doktorwürde
der
Naturwissenschaftlich-Mathematischen Gesamtfakultät
der
Ruprecht-Karls-Universität
Heidelberg**

vorgelegt von
Anne Weiser, Diplom Molekulare Medizin
aus Saalfeld

Tag der mündlichen Prüfung:

Impact of mast cell deficiency on immunological parameters and autoimmunity

Gutachter: Prof. Dr. Hans-Reimer Rodewald
Prof. Dr. Bernd Arnold

Hiermit erkläre ich, dass ich die vorgelegte Dissertation selbst verfasst und mich dabei keiner anderen, als der von mir ausdrücklich bezeichneten Quellen bedient habe.

Heidelberg, den

Anne Weiser

Contents

SUMMARY	III
ZUSAMMENFASSUNG	IV
ABBREVIATIONS	VI
1 INTRODUCTION	1
1.1 A HARMFUL RELATIONSHIP: MAST CELLS, HISTAMINE AND IGE	1
1.2 ORIGIN AND DEVELOPMENT OF MAST CELLS	2
1.3 CELL BIOLOGY OF MAST CELLS	4
1.4 MAST CELLS AS PLAYERS IN IMMUNE RESPONSES TO PATHOGENS	5
1.5 LESSONS LEARNED FROM KIT MUTANT MOUSE MODELS OF MAST CELL FUNCTION	8
1.6 KIT-INDEPENDENT MAST CELL-DEFICIENT MOUSE MODELS	13
AIMS OF THE STUDY	16
2 MATERIAL AND METHODS	17
2.1 MATERIAL	17
2.1.1 CHEMICALS	17
2.1.2 KITS	18
2.1.3 ENZYMES	18
2.1.4 PEPTIDES	18
2.1.5 OLIGONUCLEOTIDES	18
2.1.6 ANTIBODIES AND SECOND STEPS	19
2.1.7 MEDIA AND SUPPLEMENTS FOR MURINE CELLS	21
2.1.8 BUFFERS AND SOLUTIONS	22
2.1.9 CELL LINES AND ANIMALS	23
2.1.10 EQUIPMENT	25
2.1.11 COMPUTER ANALYSIS	25
2.2 METHODS	26
2.2.1 MOLECULAR BIOLOGY	26
2.2.2 CELL CULTURE	28
2.2.3 PREPARATION OF CELLS FROM MURINE ORGANS	30
2.2.4 FLOW CYTOMETRY	33
2.2.5 HISTOLOGY	35
2.2.6 WORKING WITH MICE	37
2.2.7 STATISTICAL ANALYSIS	40
3 RESULTS	41
3.1 COMPLETE ABSENCE OF CTMC IN $CPA3^{CRE/+}$ MICE	41
3.1.1 ANALYSIS OF CTMC BY HISTOLOGY AND FLOW CYTOMETRY	41
3.1.2 $CPA3^{CRE/+}$ MICE LACK EXPRESSION OF MAST CELL PRODUCTS IN PERITONEAL CAVITY AND EAR SKIN	43
3.1.3 $CPA3^{CRE/+}$ MICE ARE RESISTANT TO IGE-MEDIATED ANAPHYLAXIS	45
3.2 CHARACTERIZATION OF THE IMMUNOLOGICAL STATUS OF $CPA3^{CRE/+}$ MICE	48

3.2.1 LYMPHOID CELL SUBSETS ARE NORMAL IN <i>CPA3</i> ^{CRE/+} MICE	49
3.2.2 NUMBERS OF MYELOID CELL SUBSETS ARE NORMAL IN <i>CPA3</i> ^{CRE/+} MICE EXCEPT FOR A REDUCTION IN BASOPHILS	53
3.2.3 CORRELATION BETWEEN <i>CPA3</i> -DRIVEN CRE EXPRESSION AND CELL ABLATION IN THE BASOPHIL/MAST CELL LINEAGES	56
3.2.4 BASOPHIL-DEPENDENT ANAPHYLAXIS IS SUPPRESSED IN <i>CPA3</i> ^{CRE/+} MICE	59
3.3 K/BxN SERUM TRANSFER ARTHRITIS AND EXPERIMENTAL AUTOIMMUNE ENCEPHALOMYELITIS IN <i>CPA3</i>^{CRE/+} MICE	61
3.3.1 <i>CPA3</i> ^{CRE/+} MICE ARE FULLY SUSCEPTIBLE TO K/BxN SERUM TRANSFER ARTHRITIS	61
3.3.2 MOLECULAR RESPONSES TO SERUM TRANSFER ARTHRITIS	64
3.3.3 <i>CPA3</i> ^{CRE/+} AND <i>KIT</i> ^{W/W^v} MICE ARE FULLY SUSCEPTIBLE TO EAE	66
3.3.4 NEITHER MAST CELL NOR KIT DEFICIENCY AFFECT MOG-SPECIFIC T CELL RESPONSES	68
3.3.5 MAST CELL AND KIT DEFICIENCY HAVE NO IMPACT ON THE INFLAMMATORY IMMUNE RESPONSE IN THE CNS	70
4 DISCUSSION	73
SELECTIVE MAST CELL DEFICIENCY MODELS VERSUS KIT MUTANTS	73
<i>CPA3</i>^{CRE/+} MICE FULFIL THE CRITERION OF COMPLETE MAST CELL DEFICIENCY	74
IMPLICATIONS OF REDUCED BASOPHIL NUMBERS IN <i>CPA3</i>^{CRE/+} MICE	75
CONSIDERATIONS ON THE MECHANISM OF LINEAGE ABLATION IN <i>CPA3</i>^{CRE/+} MICE	78
KIT DEFICIENCY RATHER THAN MAST CELL DEFICIENCY IMPACTS SUSCEPTIBILITY TO K/BxN SERUM TRANSFER ARTHRITIS	80
EAE DEVELOPMENT IS INDEPENDENT OF MAST CELLS AND KIT SIGNALLING	82
5 REFERENCES	84
ACKNOWLEDGEMENTS	97

Summary

Mast cells originate from hematopoietic stem cells and leave the bone marrow as early lineage progenitors. After entering peripheral tissues they differentiate into mature cells expressing the stem cell factor receptor Kit and the high-affinity receptor for immunoglobulin IgE FcεRI. Mast cells have long been recognized as the principle effector cells in IgE-mediated type I hypersensitivity. In recent years several lines of evidence have suggested that mast cells might be involved in other disease models as well, including autoimmune models for multiple sclerosis and rheumatoid arthritis. So far, these studies have relied on mice lacking mast cells due to naturally occurring mutations of the tyrosine kinase Kit. However, impaired Kit signalling as in *Kit^{W/W^v}* mice does not only result in mast cell deficiency, but causes many defects in multiple other cell types inside and outside of the immune system.

Thorsten Feyerabend in our laboratory generated a new Cre knock-in strain by insertion of Cre recombinase into the *mast cell carboxypeptidase A (Cpa3)* locus. Surprisingly, *Cpa3^{Cre/+}* mice selectively lack mast cells in connective and mucosal tissues due to genotoxic effects of sustained Cre expression and hence represent a novel mast cell deficiency model with intact Kit function. The present study demonstrated the entire absence of mast cells in skin and peritoneal cavity by flow cytometry, histology and mRNA expression profiling. *Cpa3^{Cre/+}* mice were fully refractory to IgE-mediated anaphylaxis, and this defective response was rescued by reconstitution with cultured mast cells. With exception of the complete ablation of mast cells and a partial reduction in basophils, other hematopoietic lineages in *Cpa3^{Cre/+}* mice developed normally. Contrasting previous studies in *Kit^{W/W^v}* mice, Kit-proficient *Cpa3^{Cre/+}* mice were fully susceptible to antibody-mediated K/BxN arthritis and experimental autoimmune encephalomyelitis (EAE). The different results obtained from *Kit* mutant mice compared to selectively mast cell-deficient *Cpa3^{Cre/+}* mice call for a careful re-evaluation of the immunological function of mast cells beyond allergy.

Zusammenfassung

Mastzellen stammen von hämatopoetischen Stammzellen ab und verlassen das Knochenmark als undifferenzierte Vorläuferzellen. Sie differenzieren erst im Gewebe zu reifen Zellen aus und exprimieren dann neben dem Stammzellfaktor-Rezeptor Kit auch den hochaffinen IgE-Rezeptor FcεRI auf ihrer Oberfläche. Mastzellen wurden bisher hauptsächlich als Effektorzellen in der IgE-vermittelten allergischen Reaktion vom Soforttyp wahrgenommen. Es gibt jedoch vermehrt Hinweise, dass Mastzellen auch in anderen Krankheitsmodellen, unter anderem in den experimentellen Autoimmun-Modellen für Multiple Sklerose oder Rheumatoider Arthritis, involviert sein könnten. Diese Erkenntnisse beruhen auf Studien mit Mausstämmen, wie dem *Kit^{W/W^v}* Stamm, welche bedingt durch eine natürlich auftretende Mutation in der Rezeptor-Tyrosinkinase Kit keine Mastzellen besitzen. Allerdings führt die verminderte Signalweiterleitung durch den mutierten Kit-Rezeptor nicht nur zu Mastzell-Defizienz sondern verursacht auch Defekte in zahlreichen weiteren Zelltypen innerhalb und außerhalb des Immunsystems.

Thorsten Feyerabend aus unserer Arbeitsgruppe hat einen neuen Cre knock-in Stamm generiert, der Cre-Rekombinase unter Kontrolle des Mastzell-spezifischen *carboxypeptidase A (Cpa3)* Locus exprimiert. Überraschenderweise fiel bei histologischen Untersuchungen im Bindegewebe und in den Schleimhäuten von *Cpa3^{Cre/+}* Mäusen ein selektiver Verlust von Mastzellen auf, was auf die genotoxische Wirkung lang anhaltender Cre-Expression zurückgeführt werden kann. Somit repräsentiert der *Cpa3^{Cre/+}* Stamm ein neues Mastzell-defizientes Mausmodell mit funktionell intaktem Kit-Rezeptor. In der vorliegenden Arbeit wurde die komplette Mastzell-Ablation in Haut und Peritonealhöhle anhand von Durchflusszytometrie, Histologie und mRNA Expressions-Analysen demonstriert. Weiterhin konnte gezeigt werden, dass *Cpa3^{Cre/+}* Mäuse keine IgE-vermittelte Anaphylaxie-Reaktion ausbilden. Dieser Phänotyp konnte durch den adoptiven Transfer von kultivierten Mastzellen aufgehoben werden. Mit Ausnahme der kompletten Ablation der Mastzell-Linie und einer partiellen Reduktion von Basophilen, bildeten sich alle weiteren hämatopoetischen

Linien in *Cpa3^{Cre/+}* Mäusen normal aus. Im Gegensatz zu bisherigen Studien mit *Kit^{W/W^v}* Mäusen, entwickelten Kit-kompetente *Cpa3^{Cre/+}* Mäuse einen normalen Krankheitsverlauf in der experimentellen autoimmunen Enzephalomyelitis (EAE) und der K/BxN Serumtransfer-Arthritis. Aufgrund der unterschiedlichen Ergebnisse aus Experimenten mit Kit-Mutanten und selektiv Mastzell-defizienten *Cpa3^{Cre/+}* Mäusen sollte eine umfassende Re-Evaluierung der immunologischen Funktion von Mastzellen außerhalb ihrer Beteiligung in allergischen Reaktionen vorgenommen werden.

Abbreviations

ANP	atrial natriuretic peptide
APC	allophycocyanin
bio	biotinylated
BMCP	basophil mast cell progenitor
BMMC	bone marrow-derived mast cells
bp	base pairs
CAI	chronic allergic inflammation
CD	cluster of differentiation
CFA	complete Freund's adjuvant
CFSE	carboxyfluorescein succinimidyl ester
CNS	central nervous system
Cpa3	carboxypeptidase A
CTMC	connective tissue mast cells
Cy	cychrome
DC	dendritic cell
ddH ₂ O	double distilled water
DMEM	Dulbecco's Modified Eagle's Medium
DNA	deoxyribonucleic acid
DNP	dinitrophenyl
dNTP	deoxynucleotide trisphosphate
DT	diphtheria toxin
DTR	diphtheria toxin receptor
EAE	experimental autoimmune encephalomyelitis
EDTA	Ethylenediaminetetraacetic acid
ER	estrogen receptor
ES-cells	embryonic stem cells
FACS	fluorescence-activated cell sorting
Fc	constant region of an immunoglobulin
FcR	Fc (α , γ , ϵ) receptor
FCS	fetal calf serum
FITC	fluorescein
fwd	forward (5' PCR primer)

GPI	glucose-6-phosphate isomerase
ham	hamster
HBSS	Hank's Balanced Salt Solution
hCD4	artificial chimeric human CD4
HSA	human serum albumin
HSC	hematopoietic stem cell
IE	enhancer element
IFN- γ	Interferon-gamma
Ig	immunoglobulin
IL	interleukin
IMDM	Iscove's Modified Dulbecco's Medium
KI	knock-in
KO	knock-out
Lin ⁻	lineage negative
loxP	locus of X-over P1
LPS	lipopolysaccharide
m	mouse
MC	mast cell
Mc-cpa	mast cell carboxypeptidase A
Mcl-1	myeloid cell leukaemia sequence 1
MCP	mast cell progenitor
Mcpt	mast cell protease
β -ME	2-mercaptoethanol
MHC	major histocompatibility complex
MFI	mean fluorescence intensity
MMC	mucosal mast cells
MOG	myelin oligodendrocyte glycoprotein
mRNA	messenger ribonucleic acid
MS	multiple sclerosis
Nb	<i>Nippostrongylus brasiliensis</i>
n.s.	nonsignificant
OD	optical density
o/n	overnight
PAMPs	pathogen-associated molecular patterns

PBS	phosphate-buffered saline
PCA	passive cutaneous anaphylaxis
PCR	polymerase chain reaction
PE	phycoerythrin
PEC	peritoneal exudate cells
PMA	phorbol-12-myristate-13-acetate
polyA	polyadenylation signal
PSA	passive systemic anaphylaxis
RA	rheumatoid arthritis
rev	reverse (3' PCR primer)
RNA	ribonucleic acid
RT	room temperature
SCF	stem cell factor
SEM	standard error of the mean
Sl	steel locus
SPF	specific pathogen-free
TBE	Tris Borate EDTA
TCR	T cell receptor
Th cell	T helper cell
TLR	toll-like receptor
TNF- α	tumor necrosis factor alpha
TRECK	toxin receptor-mediated conditional knock-out
Tris	Tris-(hydroxymethyl)-aminomethan
w/o	without
wt	wild type

1 Introduction

1.1 A harmful relationship: Mast cells, histamine and IgE

The mast cell research begins with Paul Ehrlich's description of aniline-reactive granular cells, which he found in connective tissues¹. He emphasized that the identification of these cells should not solely be based on cell morphology but also consider their histochemical reactivity, a novel concept at that time. Basic aniline dyes like toluidine blue interact with the highly acidic glycosaminoglycan residues contained within mast cell granules. The resulting characteristic change in the colour of the staining dye is called metachromasy. This histochemical phenotype determines the unique purple staining characteristics of mast cells. Their prominent granules led Paul Ehrlich to the conclusion that these cells had a nutritional function for the surrounding tissue. For this reason, he coined the term 'Mastzelle' (mast cell) according to the German word 'Mast', which denotes a 'fattening' or 'suckling' function. Today, more than 130 years after their first description, it is clear that mast cells do not provide nutrients. They still remain one of the most enigmatic cells of the immune system.

Studies in the 1950s recognized a link between mast cells, histamine and anaphylactic responses. Histamine increases the vascular permeability, causes smooth muscle contraction and decreases cardiac output. Effects of histamine are manifested as urticaria, hypotension, dyspnoea and abdominal cramps. A severe allergic reaction with these symptoms is also named anaphylaxis, a term that was introduced in 1902². Riley and West established mast cells as predominant source of histamine in many tissues³⁻⁵. The connection to anaphylaxis was established following reports that certain polymeric compounds like the so-called compound 48/80 induced degranulation of mast cells, and the thereby released histamine-elicited symptoms of an anaphylactic shock^{6,7}. At the same time, an independent line of experiments led to the conclusion that the aggregation of antibodies in antigen-antibody complexes on the cell surface of tissue cells initiates passive cutaneous anaphylaxis⁸. About ten years later, the reaginic antibody in this reaction was finally identified by Kimishige and Teruko Ishizaka as immunoglobulin (Ig) E⁹.

In search for the corresponding receptor, Metzger and colleagues characterized the high-affinity Fc receptor for IgE (FcεRI), which is expressed on mast cell-tumor lines and normal mast cells^{10,11}. Aggregation of just two or three receptors with chemically cross-linked dimers and higher oligomers of IgE triggered degranulation with histamine release of FcεRI-bearing cells^{12,13}. These findings have directly linked mast cells and IgE-associated immune responses following secondary contact with allergens. Since then mast cells have been recognized as key effector cells in allergic conditions such as hay fever, asthma and anaphylactic shock. Focus of the current research is to understand the physiological function of mast cells beyond their role in allergic responses.

1.2 Origin and development of mast cells

Paul Ehrlich believed that mast cells differentiate from fibroblast and are therefore a component of the connective tissue. Only in the 1970s it was found that mast cells arise from pluripotent hematopoietic stem cells in the bone marrow¹⁴. The earliest committed mast cell precursor was identified in mouse fetal blood and was characterized as Kit^{high}Thy-1^{lo}FcεR1⁻ cells containing few metachromatic granules¹⁵. In 2005, three independent groups identified mast cell progenitors in adult murine hematopoiesis and proposed divergent mast cell developmental pathways¹⁶⁻¹⁸. Arinobu et al. characterized granulocyte/monocyte progenitor (GMP)-derived β7^{high} cells in the spleen that gave rise only to basophil and mast cell colonies. This newly isolated population in the adult spleen was named basophil/mast cell progenitor (BMCP) and provided the formal proof for a common origin of the basophil and mast cell lineage. Furthermore, unipotent progenitors for either the basophil or the mast cell lineage were isolated from the bone marrow and the intestine, respectively¹⁸. Under physiological conditions, only very low frequencies of committed mast cell progenitors and no circulating mature mast cells are found in peripheral blood of adult mice¹⁹. These observations imply that in contrast to other cells of the hematopoietic stem cell lineage, mast cell precursors leave the bone marrow before their terminal maturation and become fully differentiated after entering diverse vascularized peripheral tissues (Figure 1). It has been shown that mature tissue-

resident mast cells proliferate locally in certain situations²⁰. Thus, mast cell populations in the peripheral tissues are controlled by the recruitment of committed progenitors from the bone marrow, maturation of tissue-resident precursors, and local proliferation. Once migrated into tissues, rodent mast cells can have a long lifespan. The cytokine stem cell factor (SCF) is essential for development and survival of mast cells *in vivo*. Mice carrying loss of function mutations in SCF or its receptor Kit suffer from a profound mast cell deficiency (see also chapter 1.5), emphasizing that mast cell development *in vivo* is critically dependent on the presence of SCF and functional Kit signalling^{21,22}. Interleukin 3 (IL-3) is an important co-factor influencing the number and function of mast cells. *In vitro*, IL-3 is sufficient for the generation and maintenance of bone marrow-derived mast cells (BMMC), even from *Kit* mutant bone marrow cells^{23,24}. The *in vivo* role of IL-3, however, is more complex. *IL-3*-deficient mice exhibit insufficiencies in the increase of tissue mast cell populations only during parasite infections, but show normal mast cell numbers under physiological conditions²⁵.

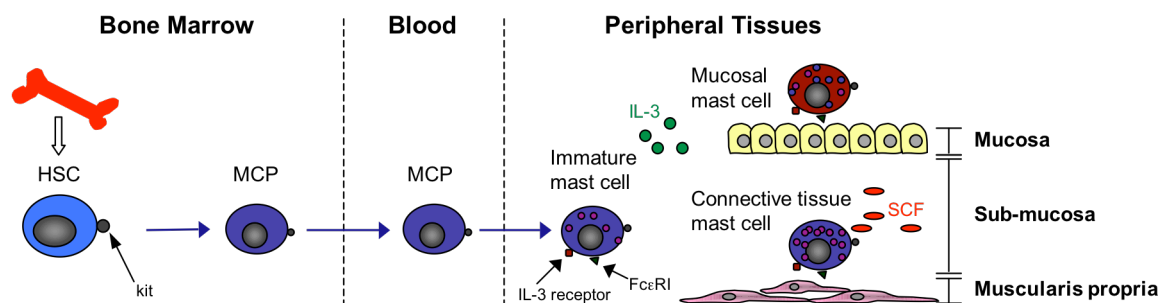


Figure 1 | Mast cell development and tissue distribution

Mast cells are derived from hematopoietic stem cells (HSCs), which give rise to mast cell progenitors (MCPs). Immature progenitors circulate in the blood and enter the peripheral tissues, where they undergo differentiation and maturation. Stem cell factor (SCF) is required to maintain mast cell survival in the tissues. The phenotype of mature mast cells can vary depending on microenvironmental factors such as IL-3. Mucosal mast cells (MMC) are found in the mucosa of the gut and can markedly increase during a Th2 response to parasitic infections. Connective tissue mast cells (CTMC) reside constitutively in the sub-mucosa and muscularis propria (Figure modified from Galli et al.²⁶).

1.3 Cell biology of mast cells

Cross-linking of FcεRI on the surface of mast cells by IgE-bound antigen results in a signalling cascade that finally culminates in degranulation and rapid release of pre-formed granule-associated mediators such as histamine, proteases²⁷⁻²⁹ and tumour necrosis factor (TNF) alpha³⁰. Although proteases are the major protein constituents in mast cell granules, their biologically relevant substrates are not obvious. Experiments in mice suggest that mast cell-derived proteases enhance host resistance to reptile and insect venoms and might have an important role in limiting the harmful effects of endogenous toxic peptides like endothelin 1 or neurotensin³¹⁻³⁴. Exposure to these substances induces mast cell degranulation and rapid release of the stored mediators, some of which can degrade the activation causing peptides. Moreover, several lines of evidence implicate a role of mast cell proteases in the recruitment of neutrophils³⁵ and in the innate protection against parasite infestation^{36,37} and bacterial peritonitis³⁸. Upon activation, mast cells can also synthesize inflammatory lipid mediators (eicosanoids) including prostaglandins³⁹ and leukotrienes⁴⁰ and a large number of cytokines and chemokines⁴¹ which are all secreted in a delayed fashion. Their equipment with a wide variety of biologically active mediators and their potential to release pre-stored products very quickly, within seconds or minutes after activation, supports the idea that mast cells might be involved in the modulation of immune responses beyond allergic reactions.

The observation of distinct histochemical staining properties^{42,43} of rodent mast cells led to the concept of mast cell 'heterogeneity'. This idea was reinforced by heterogenous lipid mediator and glycosaminoglycan (e.g. heparin) contents in mast cell granules, as well as differences in the protease expression profiles of mast cells localized at distinct anatomical sites⁴⁴. Mast cells in the mucosa of the small intestine express mast cell protease (Mcpt) 1 and Mcpt2 and have only little or no heparin, whereas those present in the intestinal sub-mucosa express Mcpt4, -5, -6 and mast cell carboxypeptidase A (Mc-cpa or Cpa3), and contain abundant heparin in their granules^{45,46}. Based on their varied granule composition and their different tissue localization, the two sub-populations of mast cells are defined as mucosal mast cells (MMC) and connective tissue mast cells (CTMC)^{47,48} (Figure 1). A recent study

analyzing the mast cell phenotype in the lung and trachea revealed a more complex picture regarding the protease expression patterns in MMC and CTMC. Tracheal CTMC and intraepithelial MMC in the trachea displayed the same protease expression pattern whereas protease expression overlapped in both mast cell sub-populations that are located in the large airways of the lung⁴⁹. Hence, the tissue seems to determine the protease profile for CTMC and MMC, e.g. protease phenotype differences in the airways compared to those in the small intestine.

Variations in the expression of proteoglycans account for the distinct histochemical staining properties of CTMC and MMC. But the two mast cell types also differ functionally with regard to their degranulation responses to pharmacological stimulation⁵⁰ and their ability to proliferate in response to parasitic challenge⁵¹. Particularly, CTMC are constitutively present in connective tissues like skin and peritoneal cavity whereas the numbers of physiologically less abundant MMC can significantly increase upon Th2-driven allergic inflammation in the lung or during nematode infections in the intestine. It is likely that MMC and CTMC do not reflect fixed subclasses but that mast cell heterogeneity is rather shaped by the cytokine environment under normal and pathological conditions⁵². Collectively, the differences in mediator profiles and the diverse biological responses of MMC and CTMC point towards distinct functional roles of mast cell sub-populations, which might further change in the context of inflammation or infection.

1.4 Mast cells as players in immune responses to pathogens

Mast cells are widely distributed throughout peripheral tissues, such as the skin, the respiratory and gastrointestinal tract, and thus at interfaces to the environment. At these sites they are located in close proximity to blood vessels, lymphatic vessels and nerve fibres⁵³. Their tissue location positions them to potentially function as sentinel cells in host defence and to interact effectively with the vasculature⁵⁴ (Figure 2). Multiple locally released mast cell-derived mediators, such as vasoactive amines and chemoattractant compounds, can regulate vascular permeability and selective recruitment of immune effector cells⁵⁵. Furthermore, mediators that are produced by

mast cells can also modulate the behaviour of neighbouring cells that are resident in the same tissue sites, for example Langerhans cells in the epidermis of the skin^{56,57}. The long lifespan of mast cells and thus their long-term location in pathogen-exposed tissues would allow sustained effector functions in response to pathogens. Consistent with the proposed view of mast cells as sentinel cells in host defence⁵⁴, they express a wide variety of cell surface receptors that directly detect pathogens or recognize molecules that are produced in the context of an ongoing immune response. Toll-like receptors (TLRs) directly interact with bacterial-, viral- or fungal-associated molecular patterns and are mainly expressed by antigen-presenting cells. Functional expression of TLR1, TLR2, TLR3, TLR4, TLR6, TLR7 and TLR9 has also been described for murine mast cells^{58,59}. So far, a functional role of TLR activation on mast cells in vivo exists for TLR2, TLR3, TLR4 and TLR7⁶⁰⁻⁶³. Altogether, activation of mast cells by ligand binding to TLRs results in the selective production of inflammatory cytokines and chemokines rather than degranulation^{59,60}. Other receptors that are found on mast cells, such as Fc receptors⁶⁴, complement receptors⁶⁵, cytokine and chemokine receptors⁶⁶, might sense by-products of the pathogen-specific immune response and may therefore indirectly activate mast cells during infections (Figure 2).

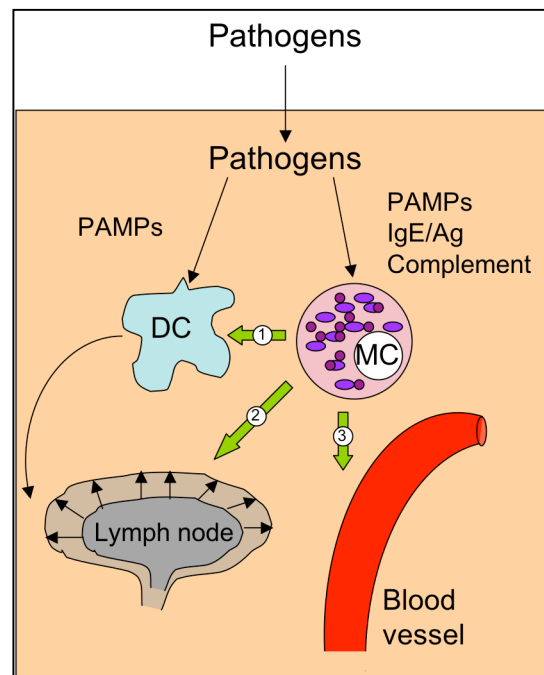


Figure 2 | The location of mast cells in tissues

Mast cells (MC) are common at sites of the body that are exposed to the environment, such as the skin. In these tissues, they are found in close proximity to blood vessels and local populations of antigen-presenting cells. Mast cells are activated by pathogens through receptors specific for pathogen-associated molecular patterns (PAMPs), IgE-bound antigen (Ag) and complement. Mast cell-derived mediators promote the maturation and migration of immature dendritic cells (DCs) from the skin to the lymph node (1), and can drive lymph node hypertrophy (2). Also, mast cell-derived products can regulate vascular permeability and recruitment of effector cells from the circulation (3) (Figure adopted from Dawicki and Marshall⁶⁷).

The majority of the described functional and structural features are not unique to mast cells. In particular, mast cells share localization, receptor expression, as well as cytokine and chemokine profiles with several other immune effector cells including macrophages and dendritic cells. But their ability for rapid mediator release has mainly pathogenic consequences, emphasizing the unique role of mast cells as key modulators in promoting harmful IgE-mediated type I hypersensitivity reactions. Nevertheless, it is an appealing idea that IgE-independent agonists, such as pathogen-associated molecules or inflammatory cytokines, might activate mast cells to rapidly and selectively respond to pathogens. However, the involved mechanisms were hitherto mainly examined in cell culture systems using phenotypically

'immature' mast cells derived in vitro from mouse hematopoietic stem cells, and the reported in vivo studies relied on mouse models that are not selectively mast cell-deficient (see chapter 1.5). The importance of mast cells in host defence against pathogens needs to be affirmed in an appropriate experimental system.

1.5 Lessons learned from *Kit* mutant mouse models of mast cell function

The in vivo functions of mast cells were widely studied in genetically mast cell-deficient *Kit* mutant mouse models, such as *WBB6F1-Kit^{W/W^v}* and more recently the *C57BL/6-Kit^{W-sh/W-sh}* mice^{68,69}. Both mouse strains carry spontaneous loss-of-function mutations in both alleles of the dominant *white spotting (W)* locus, which encodes for the receptor tyrosine kinase Kit. The transmembrane receptor Kit (CD117) binds the growth factor SCF, also known as steel factor, or Kit ligand. Ligand binding results in dimer formation of the Kit receptor, which turns on its intrinsic tyrosine kinase activity. The physiological kinase activation triggers signalling cascades like STAT and MAPK pathways and thereby regulates cell survival, proliferation and differentiation of Kit-expressing cells. The *Kit^W* allele contains a deletion mutation of 78 amino acids, resulting in a truncated Kit protein, which lacks the transmembrane domain and is therefore not expressed on the cell surface. The *Kit^{W^v}* allele encodes for a point mutation in the Kit tyrosine kinase domain that markedly decreases the kinase activity of the receptor. Therefore heterozygous *Kit^{W/W^v}* mice show reduced expression of a hypofunctional tyrosine kinase²¹. Kit is expressed on hematopoietic stem and progenitor cells and at all maturation stages of mast cells. Its expression is not restricted to the hematopoietic lineage because Kit is also found on melanocytes in the skin, germ cells, and interstitial cells of Cajal in the gastrointestinal tract. Since development and long term survival of mast cells is critically dependent on proper Kit signalling, *Kit* mutant mice are mast cell-deficient. However, they also suffer from additional phenotypic abnormalities inside and outside of the immune system that are unrelated to the mast cell deficiency. *Kit^{W/W^v}* mice exhibit macrocytic anaemia, neutropenia, and lack melanocytes, intraepithelial $\delta\gamma$ T lymphocytes, and interstitial cells of Cajal (reviewed in Grimbaldston et al.⁶⁹). They also develop a high

incidence of spontaneous dermatitis⁷⁰, squamous papillomas of the forestomach⁷¹, gastric ulcers⁷², and dilatation of the duodenum⁷³. *Kit^{W/W^v}* mice have very low but measurable numbers of mast cells in the skin and numbers can be strongly increased following chemically induced chronic dermatitis^{74,75}, demonstrating an active role of the *Kit^{W^v}* protein in regulating mast cell numbers under steady-state and inflammatory conditions. Furthermore, *Kit^{W/W^v}* mice are sterile. Therefore colony maintenance and breeding of these animals are laborious. Restriction to the F1 WB x C57BL/6 (WBB6F1) background impedes crossing with other mouse strains carrying mutations of interest, or an inherent disease susceptibility that might help to define the in vivo roles of mast cells. Altogether, this limits the capability of *Kit^{W/W^v}* mice as a model of mast cell deficiency.

During the last years, the use of mast cell-deficient *Kit^{W-sh/W-sh}* mice became increasingly popular among mast cell researchers. The *Kit^{W-sh}* allele⁷⁶ contains a large genetic inversion including the transcriptional regulatory elements upstream of the *Kit* transcription start site on chromosome five^{77,78}. *Kit^{W-sh/W-sh}* mice are neither anaemic nor sterile, but they exhibit elevated numbers of neutrophils, thrombocytosis, splenomegaly, lack interstitial cells of Cajal and show significant bile reflux into the stomach⁷⁹. However, they do not exhibit a high incidence of spontaneous pathology affecting the skin, stomach or duodenum as described for *Kit^{W/W^v}* mice⁶⁹. In *Kit^{W-sh/W-sh}* mice like in *Kit^{W/W^v}* mice, melanocytes are deficient, resulting in animals with a white coat but black eyes. Mast cell ablation in *Kit^{W-sh/W-sh}* mice appears to be age-dependent as *Kit*-expressing mast cell can be found in the skin of embryonic stages⁸⁰. In summary, *Kit*-related developmental abnormalities that affect lineages others than mast cells are milder in *Kit^{W-sh/W-sh}* mice. For that reason and because of their C57BL/6 strain background and their breeding, *Kit^{W-sh/W-sh}* mice are commonly used as mast cell-deficient mice. However, a recent report demonstrated that the *W^{sh}* inversion disrupts the gene *corin*, which encodes a cardiac protease responsible for the activation of atrial natriuretic peptide (ANP) that acts to reduce the systemic blood pressure^{79,81}. Consistent with this result, *Kit^{W-sh/W-sh}* mice develop symptoms of cardiomegaly and may also display spontaneous hypertension, a condition associated to *corin* ablation^{79,82}. Given the

size and the complexity of the genetic inversion, *Kit*^{W-sh/W-sh} mice may exhibit additional defects that have not been noticed yet.

Mutations affecting the Kit ligand, which is encoded at the *Steel* (*Sl*) locus, also result in mast cell deficiency in *WCB6F1/J-Kit*^{Sl/Kit}^{Sl-d} mice that lack SCF on the surface of fibroblasts and other cells^{22,68,83}. But mice with mutations affecting *Kit* rather than *SCF* are preferentially used to study mast cell functions because lack of mast cells in *Kit* mutant mice can be selectively corrected by adoptive transfer of cultured mast cells⁸⁴. This so-called ‘mast cell knock-in’ approach is widely accepted in the field of mast cell research and is thought to allow for the separation of general Kit-dependent abnormalities in *Kit* mutants from effects that might be exclusively attributed to their mast cell deficiency. Based on studies using the mast cell reconstitution system, mast cells have been implicated in a broad range of pathophysiologic processes beyond allergic diseases that range from allograft tolerance⁸⁵ to angiogenesis in tissue repair⁸⁶ and carcinogenesis⁸⁷, as well as vascular diseases⁸⁸. In addition, contributions of mast cells to autoimmune diseases such as multiple sclerosis (MS) or rheumatoid arthritis (RA) belong to the still expanding catalogue of potentially harmful or protective mast cell functions (Figure 3).

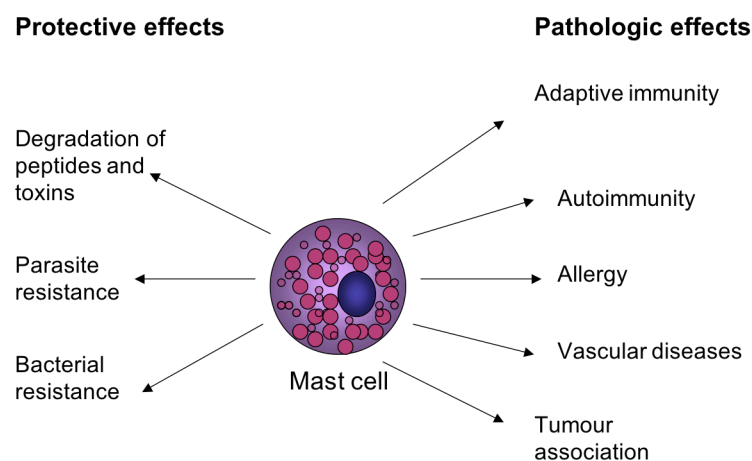


Figure 3 | Overview of potential mast cell functions

A complex picture of mast cell functions has emerged over the past decade, extending beyond their role in mediating allergy and asthma. See text for details and references.

The idea that mast cells might be involved in the pathogenesis of multiple sclerosis, a chronic inflammatory disorder of the central nervous system (CNS), was promoted by the frequently observed correlation between disease progression and localization of mast cells^{89,90}. The first observation of mast cells in the CNS of patients with MS was made already shortly after the first description of mast cells⁹¹. The technical progress in clinical diagnostics allowed the identification of mast cell-associated transcripts in MS brain lesions⁹², accompanied by high levels of mast cell tryptase in the cerebrospinal fluid of MS patients⁹³. A contribution of mast cells in inflammatory diseases of the CNS was also concluded from studies with experimental autoimmune encephalomyelitis (EAE) in mice. EAE is considered to be an experimental counterpart of MS and it is induced by immunization of genetically susceptible mice with myelin peptides in the context of complete Freund's adjuvant. EAE and MS are characterized by a breach of the blood-brain barrier, massive infiltration of inflammatory cells into the CNS, and demyelination. The local inflammatory response in the CNS provokes tissue damage, leading to neurological deficits including paralysis. In acute EAE, the percentage of degranulated mast cells increases with the clinical onset of disease symptoms⁹⁴. In addition, it has been reported that mast cell-stabilizing drugs can ameliorate the severity of EAE⁹⁵. But the strongest evidence for the involvement of mast cells in EAE was the delayed onset and diminished severity of EAE in mast cell-deficient *Kit*^{W/W^v} mice⁹⁶. The restoration of disease susceptibility by reconstitution of mice with in vitro-derived mast cells further supported the harmful role of mast cells in EAE.

Rheumatoid arthritis (RA), a chronic inflammatory disease of the diarthrodial joints, also shows hallmarks of a mast cell-dependent autoimmune disease. Accumulations of mast cells in arthritic synovial fluid and production of several mast cell-associated inflammatory mediators in human patient samples indicate that mast cells might be involved in the disease development of RA⁹⁷. Experiments in *Kit* mutant mast cell-deficient mice corroborated this assumption since in contrast to wild type mice, *Kit*^{W/W^v} and *Kitl*^{Sl}/*Kitl*^{Sl-d} mice were resistant to disease induction when injected with serum from arthritic K/BxN mice⁹⁸. Mice expressing the transgenic T cell receptor (TCR) KRN and the MHC class II allele I-A⁹⁷ (K/BxN mice) uniformly develop a joint disorder that shares many similarities with RA⁹⁹. Serum from these mice reliably

causes severe inflammatory arthritis in a wide range of recipient strains (serum transfer model) due to high titres of IgG antibodies against the glycolytic enzyme glucose-6-phosphate isomerase (GPI)¹⁰⁰. The immune complexes consisting of GPI and autoantibodies aggregate at the surface of the articular cavity where they initiate an inflammatory cascade involving complement factor C5a, Fc receptors, neutrophils, and inflammatory cytokines, such as TNF- α and IL-1^{101,102}. Reconstitution of *Kit*^{W/W^v} mice with cultured mast cells restored the sensitivity to disease induction by K/BxN serum transfer, suggesting an involvement of mast cells in this arthritis model. The observation of mast cell degranulation in the joints of wild type mice immediately after arthritogenic serum injection prompted the conclusion that mast cells might have an early, initiating role in this model of RA⁹⁸. This conclusion was also supported by findings in other mouse models of arthritis. Mast cells, for example, accumulate in the swollen paws of mice suffering from collagen-induced arthritis and inhibition of their degranulation by Salbutamol had a strong therapeutic effect on the disease progression in this model¹⁰³. Moreover, a link between mast cells and inflammatory joint disease was demonstrated in a study showing that IL-33 exacerbates collagen-induced arthritis via activating mast cells¹⁰⁴. But the pathogenic role of mast cells in animal models of MS and RA is not as clear as it might seem at first glance. Recent reports showed that mast cell deficiency in the context of *Kit*^{W-sh/W-sh} mice or in the context of modified experimental settings do not necessarily impair K/BxN serum-transferred arthritis or EAE¹⁰⁵⁻¹⁰⁸. Concerning the limitations of *Kit* mutant mast cell-deficient mouse models and the conflicting results obtained from experiments in these mice, new mouse strains exclusively deficient in mast cells would be advantageous for the field of mast cell research.

1.6 Kit-independent mast cell-deficient mouse models

The recent technical progress in gene targeting and transgenesis stimulated the development of genetically defined mouse strains that lack mast cells independent of Kit mutations. These strains represent a new generation of mast cell-deficient mouse models for the identification and characterization of mast cell functions in vivo. In 2011, four independent groups, including our own laboratory, published Kit-independent mast cell-deficient mouse strains¹⁰⁹⁻¹¹³. All four studies have chosen mast cell-specific gene loci for the manipulation of the mast cell lineage in vivo but they represent diverse mechanisms of cell ablation.

Lineage-restricted expression of diphtheria toxin fragment A or the diphtheria toxin receptor represents an efficient method of toxin-mediated cell lineage ablation in transgenic mice^{114,115}. Due to differences in cell surface receptors that recognize the DT-B fragment, humans and monkeys are sensitive to DT whereas the cells of mice and rats do not bind DT-B¹¹⁶. Transgenic expression of DT-A allows constitutive toxin-mediated cell ablation, whereas the expression of a human or simian diphtheria toxin receptor (DTR) in combination with DT administration is an effective method for inducible cell depletion. When combined with the Cre/loxP system, the expression of DT-A or DTR can be targeted to a specific cell type. The bacteriophage P1-derived Cre/loxP system is a genetic tool that is used to control site-specific recombination events in genomic DNA¹¹⁷. Cre/loxP recombination involves the targeting of so-called *loxP* (locus of X-over P1) sequences and their recombining with the help of the enzyme Cre recombinase.

Dudeck et al. generated mouse models of inducible and constitutive mast cell ablation by driving conditional expression of DT-A and DTR in the mast cell lineage¹⁰⁹. Crossing the *Mcpt5-Cre* line to a Cre-inducible DTR transgenic strain (iDTR)¹¹⁸ renders mast cells diphtheria toxin-sensitive after Cre-mediated deletion of the *loxP*-flanked stopper cassette. This Cre-inducible system requires repeated administration of diphtheria toxin for efficient mast cell ablation. To generate a model of constitutive mast cell deficiency, Dudeck et al. crossed *Mcpt5-Cre* mice with the *R-DTA* line, which encodes DTA under control of a *loxP*-flanked stop cassette in the ubiquitously expressed ROSA26 locus¹¹⁹. In both models, *Mcpt5*-expressing mast

cells are ablated due to diphtheria toxin-mediated cell death. Since *Mcpt5* is specifically expressed in CTMC, only mast cells in the peritoneal cavity, skin and sub-epithelial part of the intestine but not in the intestinal mucosa were efficiently depleted¹⁰⁹.

Otsuka et al. and Sawaguchi et al. also established an inducible DTR-based transgenic system of mast cell ablation, which they termed 'toxin receptor-mediated conditional knock-out' (TRECK)^{111,112}. In their system, a human diphtheria toxin receptor is expressed under the control of a mast cell-specific intronic enhancer (IE) element, which normally regulates *Il4* gene expression in mast cells (Mas-TRECK). However, repetitive injection of diphtheria toxin into Mas-TRECK mice does not only conditionally deplete connective tissue and mucosal mast cells, but also the basophil lineage, probably because it also uses the same *Il4* enhancer¹¹².

Lilla et al. reported a toxin-independent approach of conditional cell ablation, which is based on the disruption of a gene required for the survival of the mast cell lineage. They developed transgenic mice that express Cre recombinase under the control of a 780 bp region of the mast cell carboxypeptidase A3 (*Cpa3*) promoter¹¹⁰. In order to selectively deplete mast cells in vivo, they mated *Cpa3-Cre* mice to mice bearing a floxed allele of the myeloid cell leukaemia sequence 1 (*Mcl-1*) gene, which serves as intracellular anti-apoptotic factor in a variety of hematopoietic cells including mast cells^{110,120}. Indeed, conditional Cre-mediated deletion of *Mcl-1* expression in *Cpa3-Cre x Mcl-1^{fl/fl}* mice resulted in significant but not complete mast cell deficiency. However, as in the Mas-TRECK system¹¹¹, cell depletion is not entirely mast cell-specific since *Cpa3-Cre x Mcl-1^{fl/fl}* mice display also a marked reduction of basophils (58% - 78%)¹¹⁰.

Our laboratory has chosen the *Cpa3* locus for Cre-mediated manipulation of the mast cell lineage in vivo¹²¹. In contrast to Lilla et al., we used a gene targeting approach and thus introduced a Cre-expression construct into the first exon of the *Cpa3* locus by homologous recombination in embryonic stem cells^{121,122}. Originally, it was aimed to use *Cpa3^{Cre}* mice to focus on mast cell development since their intercross with a Cre-inducible fluorescent protein reporter strain would result in a mast cell lineage reporter line. Surprisingly, gene targeted heterozygous *Cpa3^{Cre/+}* mice were deficient in mast cells¹²². An initial characterization confirmed the

histological absence of mast cells in peritoneal cavity, skin and small intestine¹²². Earlier reports of Cre-toxicity^{123,124} led to the conclusion that potential genotoxic effects of Cre result in constitutive mast cell ablation in *Cpa3^{Cre/+}* mice. This unexpected finding provided the basis to establish and characterize a novel mast cell-deficient mouse strain. *Cpa3^{Cre/+}* mice represent a promising tool to draw the yet open secrets from the 'gorged cells' that were initially described more than 130 years ago by Paul Ehrlich.

Aims of the study

Mast cells have long been recognized as key effector cells in allergic disorders, but they receive increasing attention as crucial players of the immune system in general. Much of the groundwork for the understanding of mast cell functions in a broad range of diverse physiological and pathological conditions was established in mouse strains lacking mast cells due to defects in either stem cell factor or its receptor Kit. Major pro-pathogenic roles of mast cells had been reported in models of autoimmunity in *Kit* mutant mice. However, in addition to mast cells, defective Kit signalling affects many other lineages inside and outside of the immune system. Our laboratory has generated a new mouse strain that selectively lacks mast cells independent of Kit-related defects. Targeted insertion of Cre recombinase into the mast cell carboxypeptidase A locus constitutively deletes mast cells by a genotoxic mechanism in heterozygous *Cpa3^{Cre/+}* mice.

The objectives of this study were:

- Demonstration of the complete absence of mast cells in *Cpa3^{Cre/+}* mice by means of flow cytometry, histochemistry and gene expression analyses.
- Analysis of IgE-driven anaphylactic reactions in the absence of mast cells in *Cpa3^{Cre/+}* mice.
- Detailed comparison of immunological parameters in naïve *Cpa3^{Cre/+}* mice and wild type mice in search for immunological consequences of the absence of mast cells under steady-state conditions.
- Investigation of the influence of mast cell deficiency under inflammatory conditions by subjecting *Cpa^{Cre/+}* mice to K/BxN serum transfer arthritis and experimental autoimmune encephalomyelitis (EAE).

2 Material and Methods

2.1 Material

2.1.1 Chemicals

Unless otherwise noted, all standard chemicals not listed below were purchased from Riedel-de Haën, Merck and Fluka (liquid reagents) or Sigma-Aldrich (solid reagents) in 'pro analysis' grade.

Reagent	Company
Agarose	Biozym
Bromphenol blue	Merck
Complete Freund's Adjuvant	Sigma-Aldrich
Chloroform	Roth
DirectPCR Lysis Reagent Tail	peqlab
DNA molecular weight marker VI	Roche
DNP ₁₁ -OVA	BioCat
dNTPs (100mM each)	GE Healthcare
Dynabeads Sheep Anti-Rat IgG	Invitrogen
EDTA disodium salt	AppliChem
Ethidium bromide	AppliChem
Eukitt	O. Kindler GmbH
Fast Garnet GBC Base solution	Sigma-Aldrich
Fluoromount G	Southern Biotech
Heparin	Ratiopharm
Ketavet	Pfizer
Mycobacterium tuberculosis, H37Ra	Difco Laboratories
Naphthol AS-D Chloroacetate solution	Sigma-Aldrich
Paraformaldehyde	Serva
PBS (Dulbecco's)	Gibco
Percoll (1.130 g/ml)	GE Healthcare
Pertussis toxin	List Biological Laboratories
Readiload	Invitrogen
RNAzol	WAK-Chemie
Rompun 2 %	Bayer HealthCare
Sodium chloride solution 9 %	Diaco
Sodium nitrite solution	Sigma-Aldrich
SYTOX Blue Dead Cell Stain	Invitrogen
Tris	USB
TRIZMAL 6.3 pH	Sigma-Aldrich
Trypanblue	Fluka

2.1.2 Kits

Kit	Company
AmpliTaq DNA polymerase (incl. 10x buffer II, 25mM MgCl ₂)	Applied Biosystems
CFSE Cell Proliferation Kit	Invitrogen
Fixation/Permeabilization Kit with GolgiStop	BD Bioscience
Foxp3 Staining Buffer Set	eBioscience
innuPREP RNA Mini Kit	Analytik Jena AG
LIVE/DEAD Fixable Dead Cell Staining Kit	Invitrogen

2.1.3 Enzymes

Enzymes	Company
Collagenase D	Roche
Collagenase Type IV	Sigma-Aldrich
Dispase I	Roche
DNase I	Sigma-Aldrich
Proteinase K	Invitrogen

2.1.4 Peptides

Peptide	Supplier
MOG ₃₅₋₅₅ peptide (MEVGWYRSPFSRVVHLYRNGK)	Charité - Institute for Medical Immunology, Berlin, Germany

2.1.5 Oligonucleotides

Synthetic oligonucleotides were purchased from ThermoHybaid Ulm and were delivered HPLC-purified and lyophilized. Oligonucleotides were dissolved at a concentration of 100 pmol/μl in ddH₂O (HPLC grade). These stock solutions were stored at -20 °C.

A combination of the following three oligonucleotides was used for genotyping of *Cpa3^{Cre}* mice:

common 5': GGA CTG TTC ATC CCC AGG AAC C

3'-WT: CTG GCG TGC TTT TCA TTC TGG

3'-KI: GTC CGG ACA CGC TGA ACT TG;

yielding 320 base pairs (*Cpa3⁺*) and 450 base pairs (*Cpa3^{Cre}*) products.

2.1.6 Antibodies and second steps

Table 1 | Antibodies, Sera and Second Step reagents

Antibody	Clone	Working Dilution	Isotype	Supplier
ChromPure Mouse IgG		1:20	mouse IgG	Jackson ImmunoResearch
CD3-APC-Cy7	17A2	1:25	ratIgG2b, k	
CD4-PE-Cy7	GK1.5	1:800	ratIgG2b, k	
CD8-APC	53-6.7	1:100	ratIgG2a, k	
CD8-biotin	53-6.7	1:400	ratIgG2a, k	
CD8-PE-Cy7	53-6.7	1:400	ratIgG2a, k	
CD11b-PE-Cy7	M1/7	1:400	ratIgG2b, k	
CD11c-FITC	N418	1:100	hamsterIgG	
CD16-PE-Cy5.5	93	1:25	ratIgG2a, l	
CD19-PE-Cy5.5	1D3	1:400	ratIgG2a, k	
CD21-PE-Cy7	8D9	1:800	ratIgG2a, l	
CD34-APC	RAM34	1:25	ratIgG2a, k	
CD44-PE-Cy5.5	IM7	1:400	ratIgG2b, k	
CD45-PE-Cy7	30-F-11	1:400	ratIgG2b, k	
CD45R-biotin	RA3-6B2	1:800	ratIgG2a, k	
CD62L-FITC	MEL-14	1:1600	ratIgG2a, k	
CD93-APC	A4.1	1:400	ratIgG2b, k	
CD117-APC-Cy7	2B8	1:800	ratIgG2b, k	
CD127-FITC	A7R34	1:25	ratIgG2a, k	
F4/80-APC	BM8	1:200	ratIgG2a, k	
F4/80-APC-Cy7	BM8	1:50	ratIgG2a, k	
FcεRI-FITC	MAR-1	1:200	hamsterIgG	
Foxp3-PE	FJK-16s	1:100	ratIgG2a, k	
IFN-γ-PE	XMG1.2	1:200	ratIgG1, k	
MHC class II-APC	M5/114.15.2	1:1000	ratIgG2b, k	
TCRγδ -APC	GL3	1:50	hamsterIgG	
Ter119-biotin	Ter119	1:100	ratIgG2b, k	
Isotype control-PE	eBRG1	1:200	ratIgG1	
Isotype control-PE	eBR2a	1:100	ratIgG2a	all eBioscience
CD4-APC	RM4.5	1:400	ratIgG2a, k	Invitrogen
CD11b-PE	M1/70.15	1:800	ratIgG2b, k	Invitrogen

Antibody	Clone	Working Dilution	Isotype	Supplier
CD11b-biotin	M1/70.15	1:500	ratIgG2b, k	Caltag Laboratories
Sca-1-PE-Cy5.5	D7	1:100	ratIgG2a, k	Caltag Laboratories
CD135-biotin	A2F10	1:100	ratIgG2a, k	BioLegend
CD3-biotin	500A2	1:100	hamIgG2, k	
CD3-PE	145-2C11	1:25	hamIgG1, k	
CD3-PE-Cy7	145-2C11	1:25	hamIgG1, k	
CD4-biotin	GK1.5	1:300	ratIgG2b, k	
CD4-FITC	H129.19	1:400	ratIgG2a, k	
CD4-PE	H129.19	1:200	ratIgG2a, k	
CD5-PE	53-7.3	1:100	ratIgG2a, k	
CD8-FITC	53-6.7	1:200	ratIgG2a, k	
CD8-PE	53-6.7	1:200	ratIgG2a, k	
CD11b-FITC	M1/70	1:800	ratIgG2b, k	
CD11c-PE-Cy7	HL3	1:50	hamIgG1, l	
CD16-biotin	2.4G2	1:100	ratIgG2b, k	
CD19-APC	1D3	1:400	ratIgG2a, k	
CD19-biotin	1D3	1:400	ratIgG2a, k	
CD19-FITC	1D3	1:800	ratIgG2a, k	
CD19-PE	1D3	1:200	ratIgG2a, k	
CD23-FITC	B3B4	1:200	ratIgG2a, k	
CD25-PE-Cy7	PC6	1:1600	ratIgG1, l	
CD34-FITC	RAM34	1:25	ratIgG2a, k	
CD45-APC-Cy7	30-F-11	1:200	ratIgG2b, k	
CD45-FITC	30-F-11	1:400	ratIgG2b, k	
CD45R-APC	RA3-6B2	1:200	ratIgG2a, k	
CD45R-FITC	RA3-6B2	1:50	ratIgG2a, k	
CD45R-PerCP-Cy5.5	RA-6B2	1:100	ratIgG2a, k	
CD49b-APC	HMa2	1:800	hamIgG1, k	
CD117-APC	2B8	1:800	ratIgG2b, k	
CD125-PE	T21	1:50	ratIgG1, l	
FcεRI-PE	MAR-1	1:200	hamsterIgG	
Gr1-APC	RB6-8C5	1:400	ratIgG2b, k	
Gr1-biotin	RB6-8C5	1:500	ratIgG2b, k	
Gr1-FITC	RB6-8C5	1:800	ratIgG2b, k	
Gr1-PE	RB6-8C5	1:400	ratIgG2b, k	
humanCD4-PE-Cy7	SK3	1:25	m IgG1, κ	
IgE-FITC	R35-72	1:200	ratIgG1, k	
IgM-PE	R6-60.2	1:50	ratIgG2a, k	
Integrinβ7-PE	M293	1:800	ratIgG2a, k	
NK1.1-APC	PK136	1:100	mIgG2a, k	
Siglec-F-PE	E50-2440	1:100	ratIgG2a, k	
TCRβ-FITC	H57-597	1:200	hamIgG2, l	
Ter119-APC	Ter119	1:25	ratIgG2b, k	
Ter119-FITC	Ter119	1:100	ratIgG2b, k	
Ter119-PE	Ter119	1:50	ratIgG2b, k	
Streptavidin-APC-Cy7		1:200		
Streptavidin-PE-Cy7		1:800		
DNP	SPE-7		IgE	all BD Bioscience
DNP	U7.6		IgG1	Sigma-Aldrich
K/BxN serum with anti-GPI antibodies			mIgG	Ascites-produced ¹²⁵ Diane Mathis, Boston ¹⁰⁰

2.1.7 Media and supplements for murine cells

Media, buffers and supplement	Supplier
DMEM with GlutaMAX I	Gibco
FCS (fetal calf serum)	HyClone
HBSS	Gibco
IL-3	Supernatant from an <i>IL-3</i> gene transfected cell line ¹²⁶
IMDM with GlutaMAX I (with Glucose 4.5g/l, w/o Pyruvate)	Gibco
MEM non-essential amino acids (100x)	Gibco
MEM sodium pyruvate (100mM = 100x)	Gibco
β -mercaptoethanol	Gibco
PBS (Dulbecco's w/o CaCl ₂ , w/o MgCl ₂)	Gibco
Penicillin-Streptomycin (100x, 10.000U penicillin/ml, 10.000 μ g streptomycin/ml)	Gibco
Stem cell factor (SCF)	Supernatant from a cell line transfected with SCF cDNA

Medium for bone marrow-derived mast cells (BMMC):

10 % FCS
 100 μ M MEM Non-essential amino acids
 1 mM MEM Sodium pyruvate
 100 U/ml Penicillin
 100 μ g/ml Streptomycin
 50 μ M β -mercaptoethanol
 1 % SCF conditioned medium
 1 % IL-3 conditioned medium
 in IMDM

Medium for murine spleen cells:

10 % FCS
100 U/ml Penicillin
100 µg/ml Streptomycin
50 µM β-mercaptoethanol
in DMEM

2.1.8 Buffers and solutions

Blue loading buffer	30 % Glycerol 0.025 % Xylene cyanol FF 0.025 % Bromphenol blue
Carnoy's fixative	60 % Ethanol absolute 30 % Chloroform 10 % Acetic acid (conc.)
Esterase staining solution	1 ml Fast Garnet CBG Base solution 1 ml Sodium Nitrite Solution 40 ml pre-warmed water 5 ml Trizmal pH 6.3 1 ml Naphthol AS-D Chloroacetate solution
Kristensen's solution	8 M formic acid 1 M sodium formate
Paraformaldehyde	1x PBS 4 % Paraformaldehyde

1x PBS	9.55 g/l of a D-PBS ready-to-use mixture (Gibco) 8 g/l NaCl, 0.2 g/l KCl 1.15 g/l Na ₂ HPO ₄ 0.2 g/l KH ₂ PO ₄
10x TBE	900 mM Tris 900 mM Boric acid 20 mM EDTA (pH 8)

2.1.9 Cell lines and animals

2.1.9.1 Eukaryotic cell lines

CHO-SCF CHO cells transfected with mouse SCF cDNA to produce the cytokine SCF, Genetics Institute, Boston

X63-IL3 X63 myeloma cell line transfected with a mouse IL-3 cDNA construct to secrete large quantities of the cytokine IL-3¹²⁶

2.1.9.2 Mouse strains

Inbred strains

The inbred mouse strains C57BL/6 and BALB/c were originally obtained from Charles River or Harlan and maintained at the specific pathogen-free (SPF) mouse facilities of the University of Ulm or the DKFZ in Heidelberg.

WB x C57BL/6J F1 Kit^{W/W^v} (WBB6F1 Kit^{W/W^v}) mice

WB Kit^{W/+} mice¹²⁷ were originally purchased from Japan-SLC Inc., Japan, and intercrossed for maintenance. *C57BL/6J Kit^{W/+}* mice were purchased from Jackson Laboratories; Maine, USA, and crossed to C57BL/6 for maintenance. Heterozygous

offspring of both parental strains were identified by presence of a white belly spot¹²⁷. For the generation of *WBB6F1 Kit^{W/Wv}* mice¹²⁸, *WB Kit^{W/+}* and *C57BL/6J Kit^{W/+}* mice were intercrossed. Animals of these three lines were kept under specific pathogen-free (SPF) conditions in individually ventilated cages (IVC) at the animal facilities of the University of Ulm and the DKFZ in Heidelberg.

***Cpa3^{Cre}* mice**

Cpa3^{Cre} mice were generated from targeted E14.1 ES-cells¹²¹. ES cell clones bearing the *Cpa3^{Cre}* knock-in allele were injected into C57BL/6 blastocysts to produce chimeric mice. Subsequent crossing to C57BL/6 transmitted the targeted allele through the germline. Heterozygous offspring were then used to backcross the *Cpa3^{Cre}* allele onto C57BL/6 and BALB/c background. Heterozygous mice on C57BL/6 background were intercrossed to obtain homozygous *Cpa3^{Cre/Cre}* mice. All these strains were kept under specific pathogen-free (SPF) conditions at the animal facilities of the University of Ulm and the DKFZ in Heidelberg.

***Cpa3^{hCD4/hCD4}* mice**

Cpa3^{hCD4/+} mice were generated from targeted E14.1 ES-cell clones following blastocyst injection. Heterozygous mice on C57BL/6 background were intercrossed to obtain homozygous *Cpa3^{hCD4/hCD4}* mice and they were kept under SPF conditions at the animal facilities of the University of Ulm and the DKFZ in Heidelberg.

2.1.10 Equipment

Laboratory equipment	Company
Biophotometer	Eppendorf
Dial thickness gauge	Kaefer
Cytospin3 (centrifuge)	Shandon
Digital thermometer Qtemp 200	VWR International
FACSCanto (FACS analyzer)	BD Bioscience
Gel documentation - printer P93D	Herolab/Mitsubishi
Gel documentation - camera DNA Filter E55	Herolab
Heraeus Fresco 17 (benchtop centrifuge)	Thermo Scientific
Heraeus Megafuge 40R	Thermo Scientific
Inverse light microscope Primo Vert	Zeiss
Light microscope DM LB2	Leica
Light microscope Lab.A1	Zeiss
LSRFortessa (FACS analyzer)	BD Bioscience
T3000 Thermocycler (Biometra)	Biometra
Ultra Turrax T25 homogenizer	IKA

2.1.11 Computer analysis

Flow cytometry data were acquired and analyzed with FACS Diva software (BD Bioscience). Microscopic images were acquired using Leica Application suite and further processed with Photoshop CS (Adobe).

Statistical analyses were done using the free software environment R (version 2.12.2), and graphs were generated with Prism 4.0c (Graphpad). Heat maps for the expression levels of selected genes were assembled with the Gene Pattern software package (Broad Institute, MIT). Hierarchical clustering was performed using Chipster CSC v1.4.7.

2.2 Methods

2.2.1 Molecular Biology

2.2.1.1 Genotyping of mice

For genotyping of mice by PCR, DNA was extracted from tail biopsies. The tail biopsies were lysed in DirectPCR Lysis Tail Reagent (peqlab), supplemented with 200 µg/ml Proteinase K (Invitrogen), according to manufacturer's protocol. One µl of the lysate was directly used as template in the PCR reactions.

Reagents from Applied Biosystems were utilized for PCR, and the total volume of the PCR was 25 µl with the following composition:

- 1 µl Primer 5' (10 pmol/ µl)
- 1 µl Primer 3' (10 pmol/ µl)
- 1 µl Primer 3' (10 pmol/ µl)
- 2.5 µl 10x PCR buffer
- 2 µl dNTP mix (0.2 mM final, each)
- 1.5 µl MgCl₂ (1.5 mM final)
- 2.5 µl Readiload (Invitrogen)
- 0.2 µl Taq polymerase
- 12.3 µl H₂O
- 1.0 µl DNA template

The PCR reaction was performed on a T3000 Thermocycler (Biometra) using the following protocol:

Step1: 94 °C, 2 min

Step2: 94 °C, 30 sec

Step3: 62 °C, 45 sec

Step4: 72 °C, 45 sec (35 repeats of steps 2 to 4)

Step5: 72 °C, 2 min

Step6: 4 °C, ∞

DNA fragments were separated according to their size by agarose (1 % in 0.5 x TBE) gel electrophoresis. The gels contained 0.15 µg/ml ethidium bromide to visualize the separated DNA bands under UV light (312 nm).

2.2.1.2 RNA extraction from cells and tissue samples

RNA was extracted from ankle joints and spleens by using the innuPREP RNA Mini Kit from Analytik Jena AG. To homogenize ankle joints, the tissue was ground to a fine powder under liquid nitrogen using mortar and pestle. Spleens were processed into single cell suspensions, and 5×10^6 cells were applied as starting material for RNA isolation. Further working steps were performed according to manufacturer's instructions.

Total RNA from peritoneal exudates cells (PEC) and ear skin was extracted with RNAzol (Wak-Chemie). Up to 1.5×10^6 PEC were directly lysed in 300 µl RNAzol, and ear tissue was homogenized in 1 ml RNAzol using an Ultra Turrax T25 (IKA) homogenizer. Aqueous and organic phase separated after addition of 1/10 volume of chloroform. The samples were mixed, incubated for 5 min on ice, and centrifuged for 15 min at 17000 g and 4 °C. Subsequently, the upper phase was extracted once with chloroform, and RNA was precipitated overnight at -20 °C by addition of an equal volume of isopropanol. The next day, the RNA was recovered by centrifugation for 15 min at 17000 g and 4 °C. The RNA pellet was washed twice with 75 % ethanol and air-dried briefly. Finally, the RNA was re-dissolved in RNase free water.

2.2.1.3 RNA expression analyses

Microarray analyses were performed at the DKFZ Genomics and Proteomics Core Facility. RNA quality control was performed by total RNA Nano chip assay on an Agilent 2100 Bioanalyzer (Agilent Technologies GmbH). For microarray gene expression analyses, RNA was biotinylated and purified using the MessageAmp II aRNA Amplification kit (Ambion Inc.). Samples were hybridized to the Mouse WG-6 v2.0 BeadChip (Illumina) and conjugated with streptavidin-Cy3 (Amersham Biosciences). Signals were read with an iScan Array scanner and normalized using the quantile normalization algorithm.

2.2.2 Cell Culture

2.2.2.1 General cell culture methods

General cell culture conditions were 37 °C, 95 % humidity and 10 % CO₂. Unless otherwise indicated, standard handling of the cells during experiments was as follows: Cells were kept on ice, standard washing buffer was PBS containing 5% FCS (PBS/5 % FCS). Standard centrifugation was 5 min at 600 g (2500 rpm) in the Heraeus Fresco 17 centrifuge, or 5 min at 314 g (1200 rpm) in the Heraeus Megafuge 40R for 50-ml tubes and accordingly 3 min at 1362 g (2500 rpm) for 96-well plates. Cells were centrifuged at 4 °C.

2.2.2.2 Determination of the cell number

An aliquot of cells was diluted in an appropriate volume of PBS/5 % FCS and 10 μ l of the cell suspension was further diluted with the same volume of trypan blue. Ten μ l of this dilution were applied to a counting chamber. Cells in at least two of the four outer large squares were counted, but blue cells were excluded from counting. The cell number was calculated as follows:

(number of counted cells x dilution factor x 10^4 chamber factor)/number of counted squares = number of cells/ml

2.2.2.3 Ex vivo re-stimulation of MOG₃₅₋₅₅-specific T cells

Eleven days after immunization with CFA/MOG₃₅₋₅₅ peptide, mice were killed and the spleens were harvested for single cell preparations. Bulk spleen cells were re-suspended in complete DMEM medium containing 5 μ M MOG₃₅₋₅₅ peptide and 5 x 10⁵ cells per well were seeded into 96-well U-bottom plates, respectively. Cells that were cultured in medium only served as controls. MOG₃₅₋₅₅ re-stimulated cells or controls were analyzed for intracellular cytokine staining and proliferation response. Incubation time of the cells was chosen according to the intended purpose.

For intracellular cytokine staining, the cells were incubated with MOG₃₅₋₅₅ peptide in the presence of 0.7 μ l/ml monensin (GolgiStop, BD Biosciences) overnight. To trace cell proliferation, CFSE-labeled cells were re-stimulated with 5 μ M MOG₃₅₋₅₅ peptide and incubated for 72 hours.

2.2.2.4 Generation of bone marrow-derived mast cells (BMMC)

Bone marrow cells were flushed out from tibia and femur of one hind limb with PBS/5 % FCS using a 25G needle. The cells were pelleted, re-suspended in 1 ml BMMC medium and counted. Cells were adjusted to 1 x 10⁶ cells/ml in BMMC medium and plated into 6-well plates (3 ml/well). One ml medium was replaced by

fresh BMMC medium on a weekly basis. After two weeks non-adherent cells were transferred into new 6-well plates. After four to five weeks of culture the purity of the differentiated mast cells (FcεRI⁺ and Kit⁺) was at least 95 % as analyzed by flow cytometry. The optimal cell density is 0.5 - 1 x 10⁶ cells/ml and BMMC were split accordingly.

2.2.2.5 Loading Fcε-receptors of BMMC with DNP-specific IgE

After six weeks of culture (2.2.2.4) BMMC were adjusted to 1 x 10⁶ cells/ml in BMMC medium, and cells were incubated overnight with 0.15 µg/ml DNP-specific IgE monoclonal antibody (clone SPE-7, Sigma-Aldrich) in cell culture flasks. On the next day cells were harvested, washed twice in a large volume PBS, adjusted to 33 x 10⁶ cells/ml and prepared for intravenous injection (2.2.5.5).

2.2.3 Preparation of cells from murine organs

2.2.3.1 Preparing single cell suspensions from lymphatic organs

Mice were killed by cervical dislocation. The organs were removed and stored in PBS/5 % FCS on ice. To obtain single cells from spleens and thymi, the organs were mechanically ground between the frosted parts of object slides. Femur and tibia were taken for the generation of single cells from the bone marrow. The bone marrow was flushed out with PBS/5 % FCS using a 25G needle, and single cell suspension was acquired by pipetting cells several times up and down. Cells were kept on ice until further use.

2.2.3.2 Recovery of peritoneal exudate cells (PEC)

Mice were euthanized by CO₂ asphyxiation. The peritoneum was freed and opened by a small cut. The peritoneal cavity was flushed successively with a total of 10 ml 37 °C pre-warmed PBS/5 % FCS and the recovered PEC were collected on ice.

2.2.3.3 Digestion of spleen and thymus for analysis of dendritic cells

Spleens and thymi were minced and re-suspended in 500 µl PBS containing 0.025 mg/ml DNase I (Sigma-Aldrich), 0.08 mg/ml dispase I (Roche) and 0.2 mg/ml collagenase D (Roche). The minced tissues were incubated at 37 °C under shaking at 700 rpm for 10 min. The supernatant, containing liberated cells, was collected on ice and 5 mM EDTA and 5 % FCS were added to inhibit remaining enzymatic activity. Undigested tissue clumps were subjected to further digestion rounds with fresh digestion mix until the tissues were completely digested. Finally, the cells were pelleted, re-suspended in PBS/5 % FCS and utilized for FACS analysis of dendritic cells.

2.2.3.4 Isolation of leukocytes from the central nervous system

Leukocytes were isolated from the central nervous system (CNS) of MOG₃₅₋₅₅-immunized mice on day 11 post-immunization. Mice were euthanized by CO₂ asphyxiation and were perfused through the left cardiac ventricle with cold heparinized (10 U/ml) PBS until the effluent ran clear. Subsequently, total brain and spinal cord were dissected, and the CNS tissue was minced in ice cold PBS. Pelleted (400 g, 10 min at 4 °C) tissue samples were re-suspended in 3 ml DMEM medium, supplemented with 10 % FCS, 1 mg/ml DNase I (Sigma-Aldrich) and 2.5 mg/ml collagenase D (Roche), and were incubated for 30 min at 37 °C under constant stirring. 5 mM EDTA was added after digest, and the liberated cells were passed through a cell strainer (70 µm). Following centrifugation (400 g for 10 min at 4 °C), the cells were re-suspended in 5 ml 40 % Percoll (GE Healthcare) and

carefully overlaid on 3 ml 70 % Percoll. Percoll gradient centrifugation was performed at 700 g for 30 min at RT with moderate deceleration. Leukocytes were collected from the 70 % to 40 % interface and washed twice in a large volume of PBS/5 % FCS before FACS analysis.

2.2.3.5 Isolation of mononuclear cells from the small intestine

The small intestines were removed, flushed with HBSS and opened alongside. The open intestines were rinsed three times in fresh ice cold HBSS and then chopped with two scalpels. The minced tissue was re-suspended in 20 ml complete IMDM medium, supplemented with 1 mg/ml collagenase type IV (Sigma-Aldrich), and incubated for 20 min at 37 °C under constant stirring. A total of three enzymatic digestion rounds were carried out. The undigested tissue clumps were collected after each digestion period and were subjected to another enzymatic digestion, while the liberated cells were processed for Percoll gradient centrifugation. Liberated cells were supplemented with 5 % FCS and 5 mM EDTA, passed through a cell strainer (70 µm), pelleted, re-suspended in 6 ml 44 % Percoll (GE Healthcare) and overlaid on 3 ml 67 % Percoll. Cells were spun at 400 g for 20 min at 4 °C, mononuclear cells were harvested from the interface and washed twice in a large volume PBS/5 % FCS. The cells from each digestion round were pooled and up to 3×10^6 mononuclear cells were isolated from one intestine.

2.2.3.6 Digestion of ear skin for the analysis of Kit⁺ cells

Both ears from one mouse were pooled and minced. The minced tissue was re-suspended in 20 ml complete IMDM medium, containing 2 mg/ml collagenase type IV (Sigma-Aldrich), and incubated for 20 min at 37 °C under constant stirring. Liberated cells were collected on ice, supplemented with 5 % FCS and 5 mM EDTA, passed through a cell strainer (70 µm), spun down and re-suspended in PBS/5 % FCS. Remaining tissue clumps were subjected to a second digestion round with fresh enzyme mix. The prepared cells were utilized for FACS analysis of skin-derived Kit⁺ cells.

Flow cytometry

2.2.3.7 General antibody staining methods

If not otherwise stated, all incubation steps were performed on ice and under light protection. Cells were stained in 96-well V-bottom plates or in 1.5-ml tubes. Up to 5×10^6 cells were incubated in 50 μ l PBS/5 % FCS, respectively. Prior antibody staining, cells were incubated for 20 min with 0.28 mg/ml mouse IgG (Jackson ImmunoResearch Laboratories) to block Fc γ -receptors. The blocked cells were spun down, re-suspended in PBS/5 % FCS with the diluted antibodies and incubated for 45 min. After staining, cells were washed once with 1 ml PBS/5 % FCS in 1.5-ml tubes, or three times with 200 μ l PBS/5 % FCS in 96-well plates. If necessary, cells were incubated for another 20 min with a secondary antibody and washed accordingly. The optimal working concentration for each antibody was determined by separate titration experiments and is listed under 2.1.6.

Finally, cells were re-suspended in PBS/5 % FCS and analyzed on a FACSCanto or LSRFortessa (BD Bioscience). Data are displayed as dot plots or histograms using FACSDiva software (BD Bioscience).

2.2.3.8 Labeling of dead cells

To exclude dead cells from FACS analysis, 1 μ M SYTOX Blue Dead Cell Stain (Invitrogen) was added to the cell samples 5 min before analysis, respectively. Since SYTOX penetrates the membranes of permeabilized cells, the LIVE/DEAD Fixable Dead Cell Staining Kit (Invitrogen) was applied for labeling of dead cells prior permeabilization. Briefly, cells were re-suspended in 1 ml PBS/5 % FCS and 1 μ l fluorescent reactive dye was added. Cells were incubated on ice for 30 min in the dark and washed afterwards with 1 ml PBS/5 % FCS buffer. The labeled cells were further subjected to permeabilization and fixation for intracellular antibody staining.

2.2.3.9 Intracellular cytokine staining

After live/dead staining with the LIVE/DEAD Fixable Dead Cell Staining Kit (Invitrogen) and staining of surface markers, cells were fixed and permeabilized using the Fixation/Permeabilization Kit from BD Biosciences according to manufacturer's instructions. Briefly, cells were fixed in Cytotfix/Cytoperm solution for 20 min. Fixed cells were washed twice with Perm/Wash buffer (BD Biosciences) and incubated with anti-IFN- γ antibody or the corresponding isotype control in Perm/Wash buffer for 1 hour at RT. Cells were washed twice in Perm/Wash buffer and re-suspended in PBS/5 % FCS for subsequent analysis.

2.2.3.10 Intracellular Foxp3 staining

After live/dead staining and staining of surface markers, cells were fixed and permeabilized using the Foxp3 Staining Buffer set from eBioscience according to manufacturer's instructions. Briefly, cells were incubated in Fixation/Permeabilization Diluent for 30 min. Fixed cells were washed twice with Permeabilization Buffer and blocked with 2 % mouse IgG (Jackson ImmunoResearch Laboratories) in Permeabilization Buffer for 15 min. The Foxp3 antibody or its corresponding isotype control were directly added to the blocked cells, and cells were incubated with the antibodies for 30 min at 4 °C in the dark. Finally, cells were washed twice with Permeabilization Buffer and re-suspended in PBS/5 % FCS for subsequent FACS analysis.

2.2.3.11 CFSE-labeling of spleen cells

Labeling of cells was modified according to the CFSE Cell Proliferation Kit from Invitrogen. Briefly, single cell suspensions of bulk spleen cells were adjusted to 2.5×10^6 cells/ml in PBS/0.1 % BSA. One μ M CFSE was directly added to the cells, cell suspensions were mixed and incubated at RT for 3 min in the dark. The staining reaction was quenched by addition of five volumes PBS/10 % FCS and incubating

the cells for 5 min on ice. Cells were spun down and washed further two times with a large volume of PBS/10 % FCS to remove excess un-conjugated CFSE. Cells were re-suspended in complete DMEM medium and subjected to MOG₃₅₋₅₅ peptide re-stimulation (2.2.2.3).

2.2.3.12 Depletion of lineage positive cells

To enrich rare hematopoietic progenitor populations in spleen or bone marrow, cells expressing surface markers of hematopoietic lineage commitment were depleted. Single cells from whole spleen or bone marrow cells from two hind limbs were blocked with 0.28 mg/ml mouse IgG (Jackson ImmunoResearch Laboratories) in 400 μ l PBS/5 % FCS for 20 min at 4 °C. Cells were spun down and stained with lineage markers (CD3, CD4, CD8, CD19, CD45R, Gr1, Ter119) in 400 μ l PBS/5 % FCS for 30 min at 4 °C, respectively. Afterwards, cells were washed twice, re-suspended in 10 ml PBS/5 % FCS, and 2×10^8 magnetic beads (Dynabeads Sheep Anti-Rat IgG, Invitrogen), coated with polyclonal sheep anti-rat IgG antibodies, were added. After incubation for 1 hour at 4 °C in the dark under gentle rotation, bead-bound lineage positive cells were separated from the unbound lineage negative fraction by magnetic field. The lineage negative cells in the supernatant were pelleted and utilized for further FACS analysis.

2.2.4 Histology

2.2.4.1 Cytospins

Histochemical analyses of total PEC were done on cytopsin preparations. Cell suspensions of 2×10^5 cells in 200 μ l PBS/5 % FCS were cytopsin onto glass slides at 28 - 55 g (500 - 700 rpm) for 5 min (Cytospin3, Shandon). The glass slides were air-dried, and cells were fixed according to the staining protocol.

2.2.4.2 Paraffin sections

For chloroacetate esterase staining on ear skin sections, ears were incubated in Carnoy's fixative at 4 °C overnight, followed by incubation in 100 % ethanol at 4 °C for 8 - 48 hours. Specimen were further processed and embedded in paraffin at the routine laboratory of the department for pathology at the University Clinic in Ulm.

Haematoxylin and eosin staining on ankle joints was done on paraformaldehyde-fixed and decalcified tissue. Therefore, tissue from the distal one-third of the tibia to the midpaw was collected and fixed in 4 % paraformaldehyde at 4 °C for 24 hours under gentle agitation. After fixation, ankles were decalcified in Kristensen's solution for 48 hours at 4 °C under gentle agitation, dehydrated and embedded in paraffin. Paraffin embedded tissue was cut in 5-µm sections, respectively.

2.2.4.3 Toluidine blue staining of cytopins

Cytopins from PEC were stained with Toluidine blue. Air-dried cytopun cells were fixed with 50 % ethanol for 15 min and stained in 0.1 % Toluidine blue/30 % ethanol solution (Sigma-Aldrich) for 10 min, respectively. Finally, cells were washed with aqua dest, air-dried and mounted with Eukitt (O. Kindler GmbH).

2.2.4.4 Chloroacetate esterase staining of ear sections

Carnoy's fixed paraffin sections were de-waxed and re-hydrated in xylol and a descending ethanol row. Subsequently, slides were incubated in esterase staining solution (Sigma-Aldrich) for 15 min at 37 °C in a water bath, counterstained with Mayer's hemalum solution (Merck) for 2 min, washed with tap water and mounted with Fluoromount G (Southern Biotech).

2.2.4.5 Haematoxylin-Eosin (HE) staining of ankle sections

Paraffin sections were de-waxed and re-hydrated as described in 2.2.4.4. The sections were stained in Mayer's hemalum solution (Merck) for 7 min and washed afterwards in tap water about 5 min. Finally, slides were stained in 0.25 % Eosin/ 50 % ethanol (Sigma-Aldrich), flushed shortly with aqua dest, de-hydrated in an ascending ethanol row and in xylol, air-dried and mounted with Eukitt (O. Kindler GmbH).

2.2.5 Working with mice

2.2.5.1 Maintenance and breeding

Mice were kept under specific pathogen-free (SPF) conditions in individually ventilated cages in the animal facilities at the University of Ulm or the DKFZ. All animal experiments were approved by the local animal committees (Regierungspräsidien Tübingen and Karlsruhe) and were performed in accordance with institutional guidelines. *Cpa3*^{+/+} and *Cpa3*^{Cre/+} mice were littermates from at least 12 backcrosses to C57BL/6 or the fourth backcross on Balb/c background. *WB Kit*^{W/+} mice¹²⁷ were crossed to *C57BL/6J*^{Wv/+} mice. The resulting *WB x C57BL/6J F1 Kit*^{W/Wv} mice¹²⁸ (referred to as *WBB6F1 Kit*^{W/Wv}) are black-eyed white animals. For all experiments, mice were age and sex-matched.

2.2.5.2 Induction and assessment of EAE

Complete Freund's adjuvant (CFA, Sigma-Aldrich), containing 1 mg/ml heat inactivated *Mycobacterium tuberculosis* strain H37Ra, was further supplemented with additional *M. tuberculosis* (Difco Laboratories) to a final concentration of 11 mg/ml. To get a viscous emulsion, equal volumes of *M. tuberculosis*-enriched CFA and in water dissolved murine MOG₃₅₋₅₅ peptide (Charité, Berlin) were

squeezed several times through a 20G needle on ice. The correct consistency was reached when the produced emulsion did not disperse in water.

Thirteen to fifteen weeks old mice were immunized subcutaneously on day 0 with 100 μ l emulsion containing 200 μ g MOG₃₅₋₅₅ peptide and CFA (with 550 μ g *M. tuberculosis*). Two injections per mouse (50 μ l one on each side of the tail base) were given. In addition, the mice received 200 ng pertussis toxin (List Biological Laboratories) intravenously in 100 μ l PBS on day 0 und 2 post-immunization. Individual animals were monitored daily for clinical signs of disease and were scored according to their clinical severity of disease as follows:

Table 2 | Scoring system for EAE

Clinical score	Phenotype
0	No signs of disease
1	Limp tail or hind limb weakness
2	Limp tail and hind limb weakness
3	Partial hind limb paralysis
4	Complete hind limb paralysis
5	Moribund or dead

Moribund animals were euthanized for ethical reasons. The data were plotted as the mean daily clinical score \pm SEM for all animals in a particular group.

2.2.5.3 Induction and evaluation of antibody-mediated arthritis

Arthritis was induced in 12 weeks old recipient mice by intraperitoneal injection of 150 μ l pooled arthritogenic K/BxN serum¹⁰⁰ (kindly provided by Mathis/Benoist lab, Harvard Medical School, Boston) on experimental days 0 and 2. Mice were monitored daily for arthritis severity. Thereby each paw was evaluated and scored individually, applying the following scoring system:

Table 3 | Scoring system for arthritis

Clinical score	Phenotype
0	No evidence of erythema and swelling
1	Erythema and mild swelling
2	Erythema and pronounced edematous swelling
3	Ankylosis of the joint

The data were plotted as mean daily clinical score (0 to 12 based on 0 - 3 scores for each of four paws) \pm SEM for all animals in a particular group. Additionally, ankle thickness of the hind limbs was measured using a precision caliber (Kaefer, dial thickness gauge), and ankle thickening was calculated by subtracting the baseline ankle thickness of each hind limb from its subsequent measurements, respectively.

2.2.5.4 Induction of passive systemic anaphylaxis

To induce passive systemic anaphylaxis, mice were sensitized with an intravenous injection of 500 μ g DNP-specific monoclonal IgG1 (U7.6) antibody or 20 μ g DNP-specific IgE monoclonal antibody (clone SPE-7, Sigma-Aldrich) in 100 μ l PBS. Three hours after IgG injection or 24 hours after IgE injection, mice were intravenously challenged with 500 μ g DNP₃₀₋₄₀-HSA (Sigma-Aldrich) or 20 μ g DNP₁₁-OVA (BioCat), respectively. Following challenge, rectal temperature was monitored in 10 min intervals with a digital thermometer (Qtemp 200, VWR International).

2.2.5.5 Induction of systemic anaphylaxis in BMDC-transplanted mice

For the transplantation with cultured mast cells, mice were intravenously injected with 10×10^6 IgE-loaded syngeneic BMDC (2.2.2.5) or 10×10^6 unloaded BMDC in 300 μ l PBS, respectively. Four hours later, mice were intravenously challenged with 20 μ g DNP₁₁-OVA (BioCat) and rectal temperature was measured in 10 min intervals.

2.2.5.6 Induction of passive cutaneous anaphylaxis

For induction of passive cutaneous anaphylaxis, mice were first narcotized by an intraperitoneal injection of 100 mg/kg Ketamine (Pfizer) and 16 mg/kg Xylazine (Bayer HealthCare) in 0.9 % NaCl solution (Diac). Narcotized mice were sensitized by intradermal injection of 20 ng DNP-specific IgE (Sigma-Aldrich), dissolved in 20 μ l PBS, into the skin of one ear. As control, the opposite ear was treated with 20 μ l PBS only. Twenty-four hours later, mice were intravenously challenged with 100 μ g DNP₁₁-OVA (BioCat) in 1 % Evan's blue (Sigma-Aldrich) in 100 μ l PBS. Mice were killed and their ears were dissected 15 min after challenge for the quantification of the extravasation of Evan's blue. Ears were placed into tubes with 1.5 ml formamide and incubated at 55 °C overnight. The optical density of extracted Evan's blue in the supernatant was measured at 620 nm.

2.2.6 Statistical Analysis

Unpaired t test and one-sample t test were performed with Prism 4 (GraphPad Software). p values are given in the figures, and p > 0.05 was considered nonsignificant (n.s.). A two-way ANOVA for longitudinal data was used to evaluate the differences in response curves of *Cpa3*^{+/+} and *Cpa3*^{Cre/+} mice in arthritis and EAE experiments. All computations were performed with the statistical software environment R, version 2.12.2. Values for p > 0.05 were considered nonsignificant. Differentially expressed genes were filtered by standard deviation (3 SDs = 99.7%), subjected to a several groups test (empirical Bayes method with Benjamini-Yakutieri test) and hierarchically clustered by Pearson correlation.

3 Results

3.1 Complete absence of CTMC in *Cpa3*^{Cre/+} mice

The *Cpa3*^{Cre} strain was initially generated for genetic mapping of mast cell development pathways. The strategy was to combine mast cell-specific Cre expression in *Cpa3*^{Cre} mice with a Cre-dependent reporter locus to create a mast cell lineage reporter mouse¹²¹. But to our surprise, first analyses of heterozygous *Cpa3*^{Cre/+} mice revealed a complete lack of mast cells in their peritoneal cavity, skin and intestinal mucosa¹²². These unexpected results led us to establish this mouse strain as novel mast cell-deficient mouse model.

Initial experiments in the *Cpa3*^{Cre/+} mice focused on the histological verification of the absence of mast cells from peritoneal cavity, ear skin and small intestine. In the present study different independent methods were applied to examine whether mast cells were entirely absent in skin and peritoneal cavity. To this end, both anatomical sites, that are normally rich in mast cells, were analyzed by flow cytometry, histology and mRNA expression arrays.

3.1.1 Analysis of CTMC by histology and flow cytometry

The surface antigens Kit and FcεRI are markers, which are in combination commonly used to characterize mast cells by flow cytometry. In the peritoneal cavity, mast cells represent about 1 – 2 % of all peritoneal exudate cells (PEC). Accordingly, a distinct population of Kit⁺FcεRI⁺ cells was identified by flow cytometry on PEC of *Cpa3*^{+/+} mice (Figure 4A, left) whereas this population was absent in *Cpa3*^{Cre/+} mice (Figure 4B, left). For a morphological confirmation of these findings cytopspins of PEC were stained with toluidine blue. Highly granulated cells with the typical metachromatic, i.e. purple staining of mast cells were detected in *Cpa3*^{+/+}, but not in *Cpa3*^{Cre/+} mice (Figure 4A and B, right side).

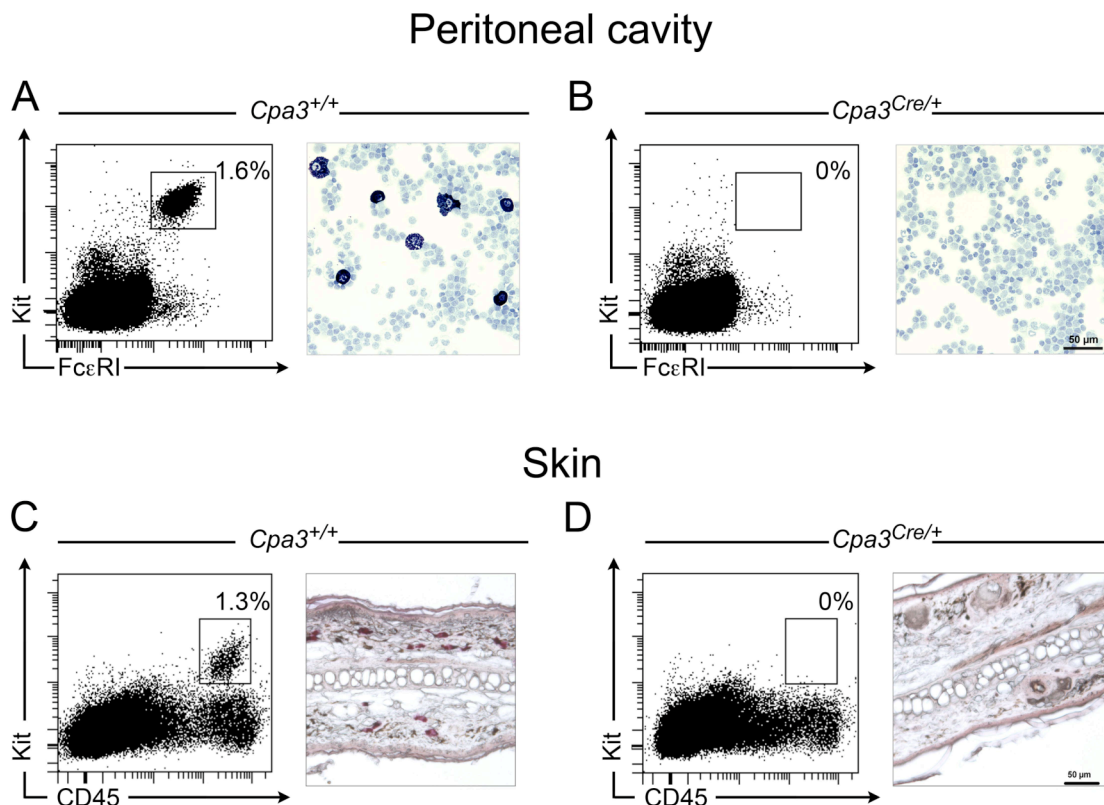


Figure 4 | Histological and flow cytometric analyses of mast cells in peritoneal cavity and skin

(A, B) Peritoneal exudate cells from *Cpa3*^{+/+} (A, left) and *Cpa3*^{Cre/+} (B, left) mice were analyzed by flow cytometry for the presence of Kit⁺FcεRI⁺ mast cells. FcεRI expression was detected by anti-IgE staining. Shown numbers represent the percentage of mast cells within total alive cells. Cytospins of total peritoneal exudate cells from *Cpa3*^{+/+} (A, right) and *Cpa3*^{Cre/+} (B, right) mice were stained with toluidine blue for metachromatic mast cells. The scale bar applies for both photographs. (C, D) Single cell suspensions from digested ear tissues of *Cpa3*^{+/+} (C, left) and *Cpa3*^{Cre/+} (D, left) mice were stained for Kit and CD45 and analyzed by flow cytometry. Numbers show percentages of gated Kit⁺CD45⁺ mast cells within total alive cells. Paraffin sections of ear skin from *Cpa3*^{+/+} (C, right) and *Cpa3*^{Cre/+} (D, right) mice were analyzed for chloroacetate esterase activity in mast cells. The shown scale bar in D applies for both photographs.

Next, ear skin was analyzed for the presence of mast cells. To test the skin for hematopoietic-derived Kit-expressing cells by flow cytometry, the tissue was digested with collagenase, and liberated cells were stained for CD45 and Kit. By this approach, 1.3 % of acquired live cells from *Cpa3*^{+/+} mice were CD45⁺Kit⁺ skin-resident mast cells (Figure 4C, left). In contrast, flow cytometry from skin of *Cpa3*^{Cre/+} mice revealed no Kit-expressing hematopoietic cells and hence further confirmed the ablation of skin mast cells in this mouse strain (Figure 4D, left). Furthermore, ear

sections from *Cpa3*^{+/+} and *Cpa3*^{Cre/+} mice were analyzed by histochemical staining for chloroacetate esterase activity. Positively stained mast cells were only identified in the dermis of wild type but not *Cpa3*^{Cre/+} mice (Figure 4C and D, right panel). In summary, mast cell deficiency of *Cpa3*^{Cre/+} mice was demonstrated for skin and peritoneal cavity by flow cytometry and histology.

3.1.2 *Cpa3*^{Cre/+} mice lack expression of mast cell products in peritoneal cavity and ear skin

A gene expression approach was chosen to comprehensively test normally mast cell-bearing tissues for the presence or absence of mast cell products. The results shown here were obtained in collaboration with Dr. Thorsten Feyerabend, who conducted RNA extraction. Total mRNAs were extracted from peritoneal lavage cells (Figure 5A) or ear skin homogenates (Figure 5B), and were analyzed by whole-genome gene expression arrays. Expression profiling of the RNA samples was performed at the DKFZ Microarray Core Facility. Dr. Markus Feuerer and Martin Teichert assisted with the preparation of the heat maps. For a direct comparison of gene expression signatures in *Cpa3*^{Cre/+} mice and conventional mast cell-deficient *Kit* mutant mice, RNA samples of *Kit*^{W/W^v} mice were included.

The CTMC-specific protease genes *Cma2*, *Cpa3*, *Mcpt4*, *Mcpt5* and *Mcpt6* were strongly expressed in peritoneal cells and skin from wild type mice but, consistent with the complete lack of mast cells, their expression was undetectable in *Cpa3*^{Cre/+} and *Kit*^{W/W^v} mice. As expected for connective tissues, protease transcripts of mucosal mast cells (*Mcpt1*, *Mcpt2*) or basophils (*Mcpt8*) as well as from mast cells of different anatomical sites e.g. the uterus (*Mcpt9*) were not detectable in peritoneal cavity or skin from any of the three analyzed strains. The mast cell products *Kit* and *FcεRI* were not expressed in the peritoneal cavity of *Cpa3*^{Cre/+} or *Kit*^{W/W^v} mice (Figure 5A). In the skin, *Kit* expression was undetectable in *Kit*^{W/W^v} mice but only reduced in *Cpa3*^{Cre/+} mice compared to wild type mice (Figure 5B). Residual *Kit* expression in *Cpa3*^{Cre/+} skin is most likely derived from cells of the melanocyte lineage, which express *Kit*. *Cpa3*^{Cre/+} mice are on the C57BL/6 background and are wild type for *Kit*. In contrast to *Kit*^{W/W^v} mice, they should therefore have normal numbers of *Kit*-

expressing skin-resident melanocytes. This is in agreement with the finding that the melanocyte-associated genes *silver* (*Si*) and *dopachrome tautomerase* (*Dct*) were expressed at normal levels in the skin of *Cpa3^{Cre/+}* mice but not in *Kit* mutant *Kit^{W/Wv}* mice (Figure 5B).

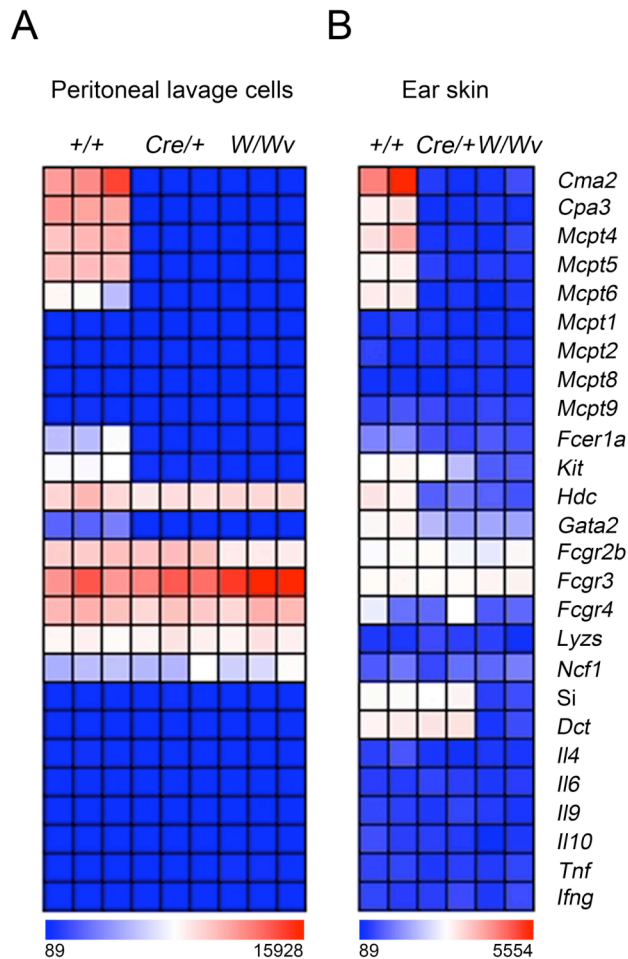


Figure 5 | Mast cell gene expression signature in peritoneal cavity and skin

Total mRNAs were isolated from peritoneal lavage cells (**A**) and ear skin (**B**) of *Cpa3^{+/+}*, *Cpa3^{Cre/+}* and *Kit^{W/Wv}* mice and analyzed by global gene expression arrays for differentially expressed genes. Analyzed genes are listed adjacent to the heat map in B. The heat maps in (**A**) and (**B**) are globally normalized for all shown genes and the color code at the bottom visualizes the corresponding differences in gene expression.

Further mast cell-associated genes like the transcription factor *Gata2*, which is important for mast cell development, and *histidine decarboxylase (Hdc)*, which is involved in histamine metabolism in mast cells and other myeloid cells, were detected in wild type mice, but were similarly reduced in mast cell-deficient *Cpa3^{Cre/+}* and *Kit^{W/Wv}* mice. Transcripts of genes that are critically involved in phagocytic defence mechanisms (*Lyzs* and *Ncf1*) as well as Fcγ receptors (*Fcgr2b*, *Fcgr3* and *Fcgr4*) and cytokines (*Il4*, *Il6*, *Il9*, *Il10*, *Tnf*, *Ifng*) were not differentially expressed in wild type mice or mast cell-deficient *Cpa3^{Cre/+}* or *Kit^{W/Wv}* mice (Figure 5).

Taken together, mRNA expression analyses revealed a loss of mast cell-specific transcripts in the peritoneal cavity and ear skin of *Cpa3^{Cre/+}* mice, confirming their complete mast cell deficiency. The direct comparison of the expression profile of mast cell-specific transcripts in *Cpa3^{Cre/+}* and *Kit^{W/Wv}* mice revealed an equal extent of mast cell deficiency in both strains. Finally, Cre-mediated mast cell ablation did not influence the expression of the analyzed immune cell-associated parameters.

3.1.3 *Cpa3^{Cre/+}* mice are resistant to IgE-mediated anaphylaxis

Next, *Cpa3^{Cre/+}* mice were subjected to IgE-mediated anaphylaxis to functionally test for the absence of mast cells.

Activation of mast cells via antigen-induced cross-linking of FcεRI-bound IgE molecules results in degranulation with rapid release of biologically active mediators including histamine, which increase vascular permeability and cause smooth muscle contraction. This severe type 1 hypersensitivity reaction is called anaphylaxis. Antigen-induced IgE-mediated anaphylaxis can be modeled in mice by first injecting an antigen-specific IgE antibody, which replaces FcεRI-bound endogenous IgE, followed by injection of the corresponding antigen. This so-called passive anaphylaxis can be induced locally or systemically.

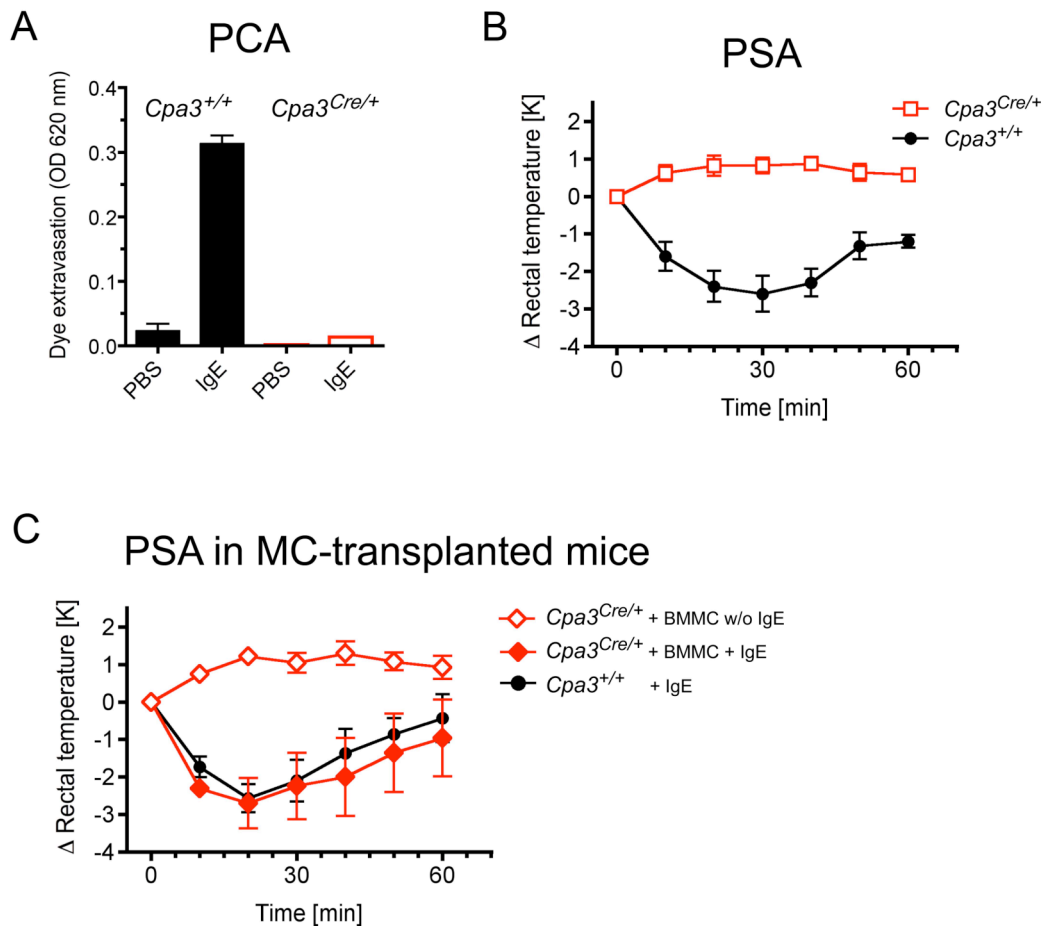


Figure 6 | IgE-mediated anaphylactic response in *Cpa3*^{Cre/+} mice

(A) Passive cutaneous anaphylaxis (PCA) in *Cpa3*^{+/+} and *Cpa3*^{Cre/+} mice. Mice were sensitized by intradermal injection of DNP-specific IgE into one ear, and the opposite ear was injected with PBS. On the next day, mice were challenged by intravenous injection of DNP-Ovalbumin together with Evan's blue. Extravasated Evan's blue was extracted from ear tissue and optical density was measured at 620 nm. Data are shown as mean ± SEM for two mice per genotype. **(B)** *Cpa3*^{+/+} and *Cpa3*^{Cre/+} mice were subjected to passive systemic anaphylaxis (PSA). Mice were intravenously injected with anti-DNP IgE and challenged on the subsequent day by intravenous injection of DNP-Ovalbumin. Anaphylactic response following challenge was measured as drop in body temperature. Rectal temperatures were monitored in 10 min intervals and are expressed as temperature difference compared to starting temperature. Shown are the mean ± SEM for five animals per genotype. **(C)** Passive systemic anaphylaxis in mast cell-transplanted mice. *Cpa3*^{Cre/+} mice were intravenously reconstituted with DNP-specific IgE-loaded bone marrow derived mast cells (BMMC + IgE). The control group was injected with untreated mast cells (BMMC w/o IgE). After a rest of four hours, mice were intravenously injected with DNP-Ovalbumin. *Cpa3*^{+/+} mice that were subjected to PSA as described in (B) served as positive control (*Cpa3*^{+/+} + IgE). Drop in rectal temperature was recorded as in (B). Data are shown as mean ± SEM for three (*Cpa3*^{+/+}) or five mice (BMMC transplanted) per group, respectively.

To elicit local passive cutaneous anaphylaxis (PCA), mice were first sensitized by intradermal injection of antigen-specific IgE into the skin of one ear. As negative control, the opposite ear was injected with PBS. Mice were challenged 24 hours later by intravenous injection of the multivalent antigen. Co-injected Evan's blue served as tracer for the mast cell-triggered local increase of vascular permeability. Five minutes after antigenic challenge, dye extravasation was observed in IgE-injected (0.313 ± 0.02 OD) but not in control-injected ears of *Cpa3*^{+/+} mice (0.023 ± 0.02 OD). In *Cpa3*^{Cre/+} mice no extravasation of Evan's blue was measured in IgE-sensitized ears (0.014 ± 0.0 OD), indicating the absence of mast cell-mediated anaphylactic response in these mice (Figure 6A). In addition, *Cpa3*^{Cre/+} mice were also subjected to a systemic anaphylaxis model. IgE-mediated passive systemic anaphylaxis relies on the same mechanisms as local anaphylaxis. However, release of vasoactive mediators from systemically activated mast cells results in a measurable drop of the body temperature due to systemic vasodilatation. To induce passive systemic anaphylaxis (PSA), mice were sensitized by intravenous injection of antigen-specific IgE and challenged one day later by intravenous antigen application. *Cpa3*^{+/+} mice responded with a transient drop in body temperature that peaked 30 minutes after antigenic challenge (-2.6 ± 1.07 K) whereas mast cell-deficient *Cpa3*^{Cre/+} mice were resistant to the induction of passive systemic anaphylaxis (Figure 6B). Of note, we noticed a slight increase in the body temperature in *Cpa3*^{Cre/+} mice, which is probably due to the repeated handling of the mice caused by the temperature measurements. To test whether defective systemic anaphylaxis was solely mast cell-dependent, *Cpa3*^{Cre/+} mice were transplanted with bone marrow-derived mast cells (BMMC) from wild type mice. In detail, cultured mast cells were incubated with antigen-specific IgE to allow loading of the high-affinity IgE receptor FcεRI. Ten million sensitized BMMC were intravenously injected into *Cpa3*^{Cre/+} mice. Control mice received cultured mast cells that were not pre-incubated with IgE. Finally, anaphylaxis was provoked in mast cell-transplanted *Cpa3*^{Cre/+} mice by systemic antigen challenge. Twenty minutes after antigen injection, *Cpa3*^{Cre/+} mice that were reconstituted with IgE-sensitized mast cells showed a temperature drop (-2.70 ± 1.50 K) that was comparable to wild type mice (-2.57 ± 0.65 K), which were subjected to normal passive systemic anaphylaxis. Body temperature did not decrease in *Cpa3*^{Cre/+} control mice that were injected with

non-sensitized mast cells, demonstrating that anaphylaxis is dependent on activated mast cells (Figure 6C).

In summary, *Cpa3*^{Cre/+} mice were refractory to IgE-driven local and systemic anaphylaxis, confirming mast cell deficiency on a functional level. The defect in systemic anaphylactic response was repaired by mast cell transplantation.

3.2 Characterization of the immunological status of *Cpa3*^{Cre/+} mice

The previous experiments have established complete Cre-mediated mast cell ablation in *Cpa3*^{Cre/+} mice. The following analyses were intended to clarify whether other immunologically relevant cell types might be affected by the absence of mast cells or by *Cpa3*-driven Cre expression in the naïve hematopoietic system. To this end, heterozygous *Cpa3*^{Cre/+} mice were subjected to a systematic evaluation of their immunological status under non-immunized steady-state conditions. The detailed analysis of splenic immune cells included subpopulations of T and B cells, NK cells, and cells of the myeloid lineage including dendritic cell subsets.

3.2.1 Lymphoid cell subsets are normal in *Cpa3^{Cre/+}* mice

Absolute numbers of lymphocyte subsets and NK cells from spleen samples of *Cpa3^{Cre/+}* mice were determined by flow cytometry and compared to samples from their wild type littermates. CD4⁺ and CD8⁺ T cell populations were further divided into naïve, activated or effector memory, and central memory cells by CD44 and L-selectin (CD62L) expression. A summary of the surface markers characterizing the respective cell subsets is depicted in Table 4:

Table 4 | Cell surface markers for the characterization of lymphoid subsets

Cell population	Surface markers
Naïve T cells	CD44 ⁻ CD62L ⁺
Activated or effector memory T cells	CD44 ^{high} CD62L ⁻
Central memory T cells	CD44 ^{low} CD62L ⁺
Regulatory T cells	CD4 ⁺ CD25 ⁺ Foxp3 ⁺
Transitional type 1 B cells	CD19 ⁺ CD93 ⁺ IgM ⁺ CD23 ⁻
Transitional type 2 B cells	CD19 ⁺ CD93 ⁺ IgM ⁺ CD23 ⁺
Transitional type 3 B cells	CD19 ⁺ CD93 ⁺ IgM ^{low} CD23 ⁺
Marginal zone B cells	CD19 ⁺ CD93 ⁻ CD21 ^{high} CD23 ⁻
Follicular B cells	CD19 ⁺ CD93 ⁻ CD21 ⁺ CD23 ⁺
B-1a B cells	CD19 ⁺ CD93 ⁻ CD5 ⁺
B-1b B cells	CD19 ⁺ CD93 ⁻ CD5 ⁻
NK cells	CD19 ⁻ CD3 ⁻ NK1.1 ^{high}
NK T cells	CD19 ⁻ CD3 ^{low} NK1.1 ⁺

None of the T cell populations differed in numbers between *Cpa3^{Cre/+}* and wild type mice (Figure 7A and 7B). Total numbers of splenic TCRαβ and TCRγδ T cells, were similar between mast cell-deficient and control mice (Figure 7C).

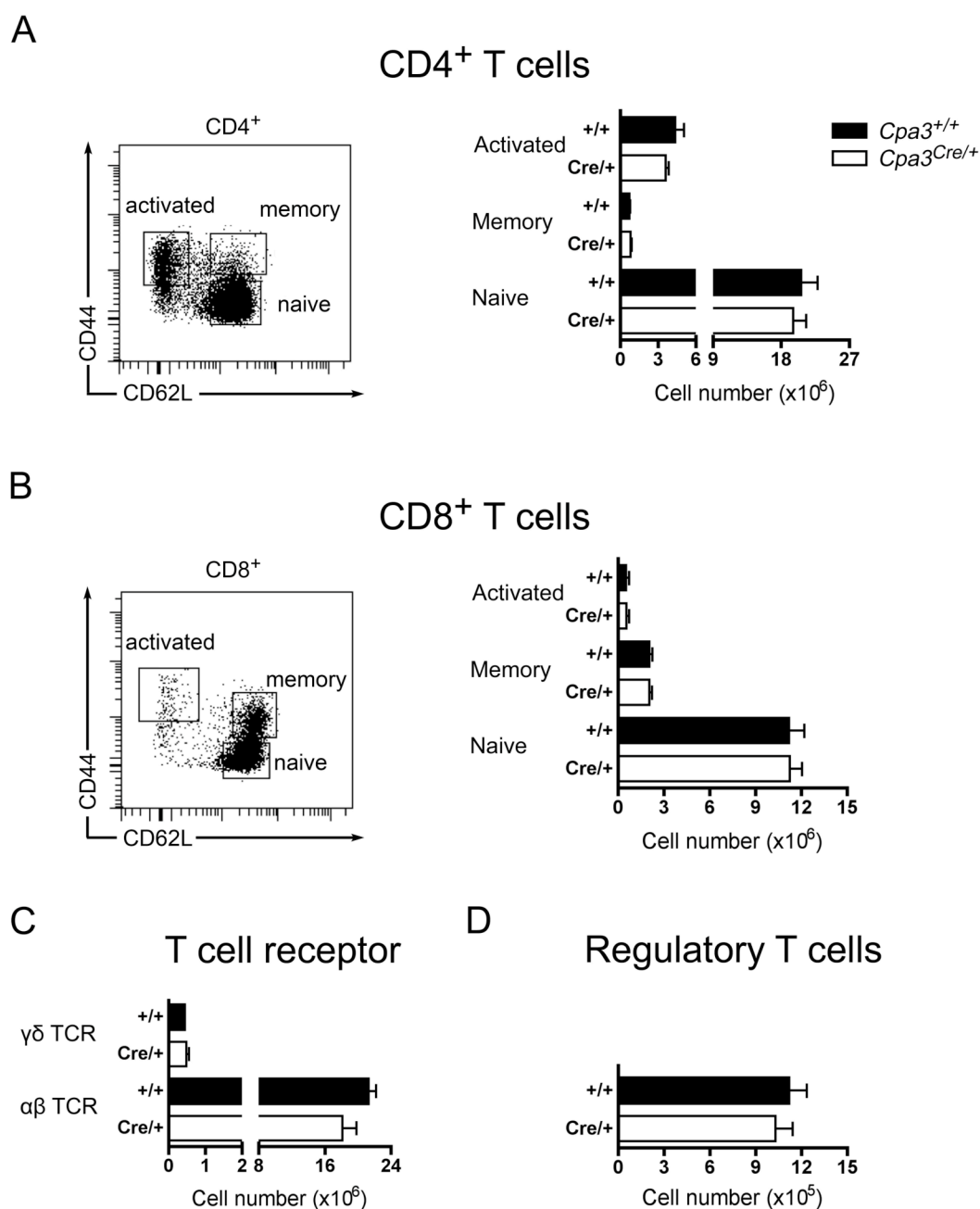


Figure 7 | Flow cytometric analysis of splenic T cell subsets

(A - D) Spleen cells from naïve *Cpa3*^{+/+} and *Cpa3*^{Cre/+} mice were analyzed for various T cell subsets by flow cytometry. (A, B) Dot plots (left) demonstrate the representative gating strategy for naïve, activated and central memory CD4⁺ (A) and CD8⁺ (B) T cell populations. Quantification for each subset is displayed on the right. Shown are the mean \pm SEM for 12 mice per genotype. (C) CD3⁺ cells were analyzed for the expression of $\alpha\beta$ and $\gamma\delta$ T cell receptors. Quantified data are shown as mean \pm SEM for eight mice per genotype. (D) Regulatory T cells were defined as CD4⁺CD25⁺Foxp3⁺ cells. Mean \pm SEM of total cell numbers from eight mice per genotype are shown.

It has been reported that mast cells can interact with regulatory T cells (Tregs) in several ways^{85,129,130}. In naïve mast cell-deficient *Kit^{W-sh/W-sh}* mice, a decrease in the Treg frequency in lymphoid organs compared to wild type mice was observed¹⁰⁶. However, the number of Tregs in the spleen of mast cell-deficient *Cpa3^{Cre/+}* mice was similar to the number of Tregs in wild type littermates (Figure 7D).

The analyses for peripheral B cells included subsets of classical immature and mature B-2 cells as well as B-1 cells in the spleen (Figure 8). Immature B cells express CD93 and their maturation process in the periphery is characterized by a sequential series of discrete stages named transitional type 1, type 2, and type 3 B cells (Table 4). The analyses of these three developmental B cell stages revealed no significant alterations in *Cpa3^{Cre/+}* mice (Figure 8A). This holds also true for the mature CD93⁻ B cell populations (Table 4), namely marginal zone B cells and follicular B cells (Figure 8B). Besides the conventional B-2 cells, the numbers of splenic B-1a and B-1b cells (Table 4) were investigated but no significant changes in numbers of these two subpopulations of B-1 cells were noticed in mast cell-deficient mice compared to wild type mice (Figure 8C). Since B-1 cells are predominantly enriched in the peritoneal cavity, peritoneal lavage cells were also analyzed for the presence of B-1 cells. The lack of peritoneal mast cells did not have an impact on cell numbers or composition of peritoneal B-1 cells in *Cpa3^{Cre/+}* mice (data not shown).

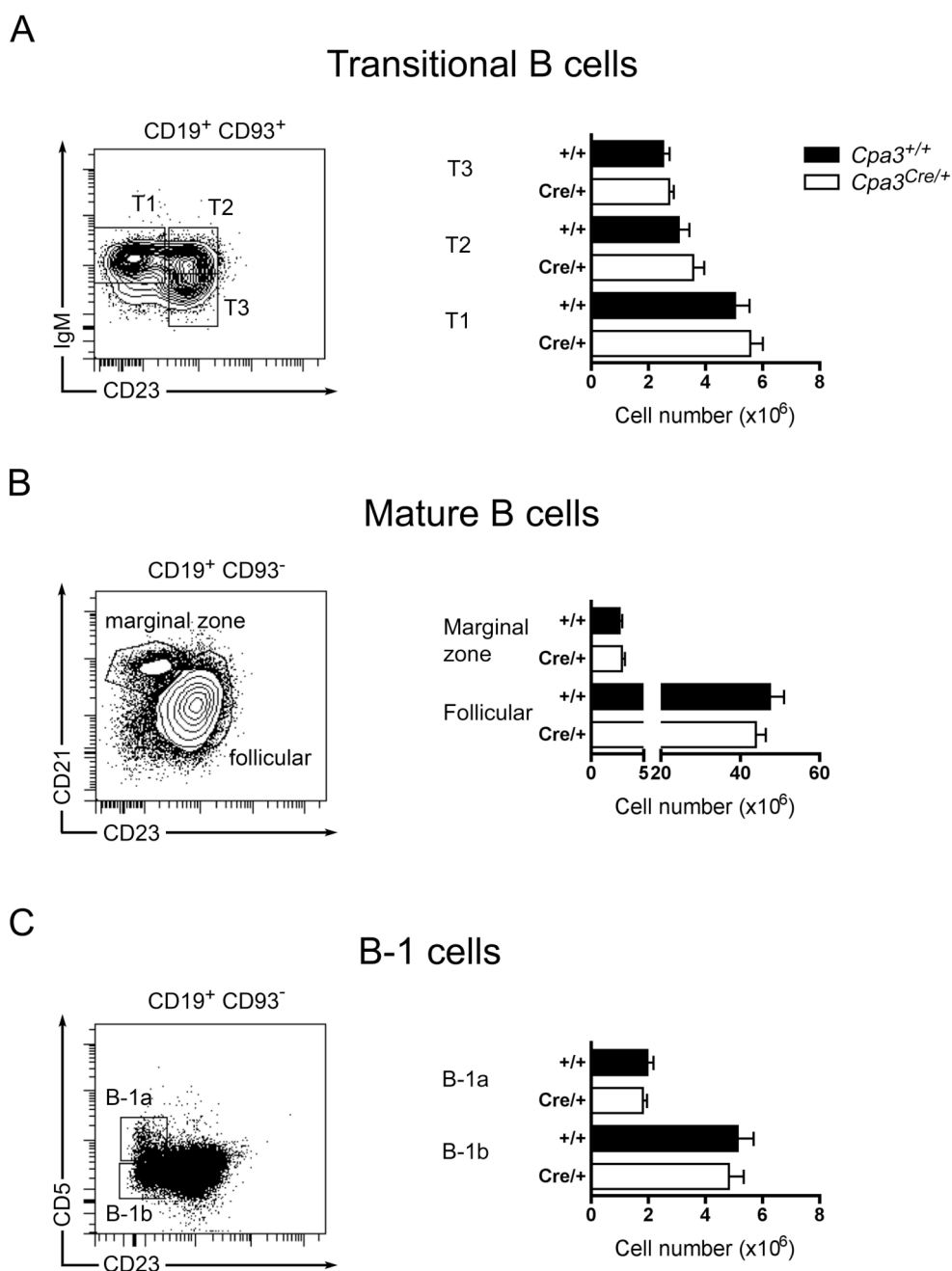


Figure 8 | Flow cytometric analysis of splenic B cell subsets

(A - C) Spleen cells from naïve *Cpa3*^{+/+} and *Cpa3*^{Cre/+} mice were analyzed for various B cell subsets by flow cytometry. (A) The dot plot (left) shows gates for flow cytometric characterization of T1, T2 and T3 cells within immature 19⁺CD93⁺ B cells. Quantified data are displayed on the right. (B) Gating for the population of CD19⁺ marginal zone and follicular B cells (left) and summary of total cell numbers (right). (C) B-1 cells were subdivided into B-1a and B-1b cells by means of their CD5 expression. Bar graphs (A - C) represent mean ± SEM of total cell numbers from 12 mice per genotype, respectively.

To further characterize lymphoid lineages, numbers of natural killer (NK) cells, and natural killer T cells (NKT), a cell type that co-expresses molecular markers of T cells and NK cells, were also determined (Table 4). No alterations in the abundance of NK and NKT cells were found in mast cell-deficient *Cpa3^{Cre/+}* mice (Figure 9).

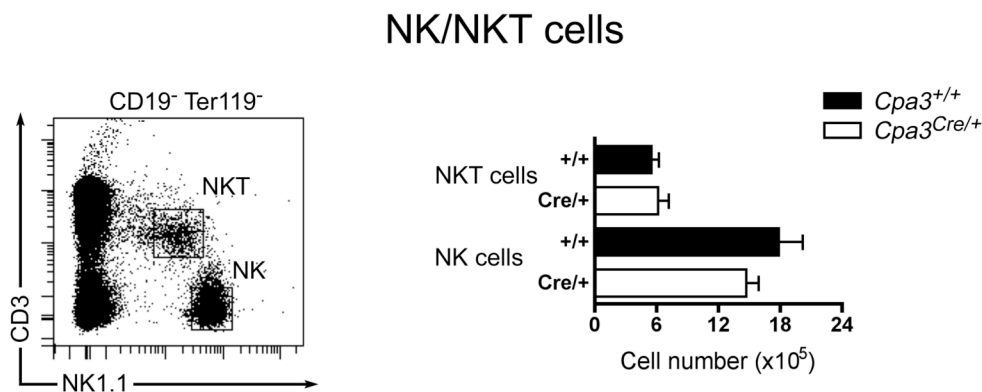


Figure 9 | Flow cytometric analysis of NK and NKT cells

Total numbers of splenic natural killer (NK) cells and natural killer T (NKT) cells were compared between *Cpa3^{+/+}* and *Cpa3^{Cre/+}* mice. The dot plot on the right shows the characterization of both subsets by means of their surface marker expression. Bar graphs show the mean \pm SEM for eight mice per genotype.

3.2.2 Numbers of myeloid cell subsets are normal in *Cpa3^{Cre/+}* mice except for a reduction in basophils

To test an impact of mast cell deficiency on myeloid lineages, dendritic cells, macrophages and granulocytes were quantified. Dendritic cells (DCs) play a dominant role in the initiation and shaping of adaptive immune responses. They are classified into myeloid DCs, lymphoid DCs, and plasmacytoid DCs (Table 5).

No significant differences were found in the spleen of *Cpa3^{Cre/+}* mice when compared to wild type spleens for either of the corresponding DC populations (Figure 10).

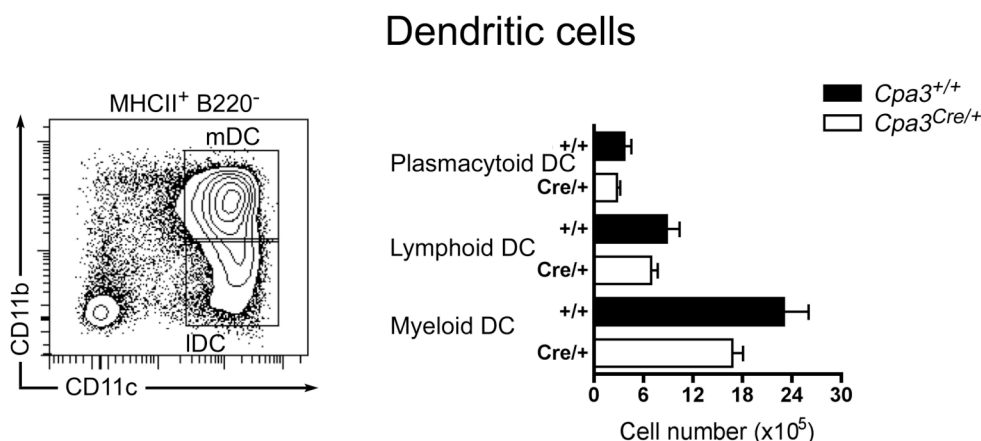


Figure 10 | Flow cytometric analysis of dendritic cells

Spleens from *Cpa3*^{+/+} and *Cpa3*^{Cre/+} mice were enzymatically digested for subsequent analyses of dendritic cell subsets. The shown dot plot is representative for the characterization of myeloid DCs (mDC) and lymphoid DCs (IDC). Plasmacytoid DCs (pDC), which are defined as MHCII^{low}B220⁺CD11b⁻CD11c⁺ cells, are not depicted in the dot plot. Quantified data of all three analyzed subsets are expressed as mean ± SEM for nine mice per genotype.

Table 5 | Cell surface markers for the characterization of myeloid subsets

Cell population	Surface markers
Myeloid dendritic cells	MHCII ⁺ B220 ⁻ CD11b ⁺ CD11c ⁺
Lymphoid dendritic cells	MHCII ⁺ B220 ⁻ CD11b ⁻ CD11c ⁺
Plasmacytoid dendritic cells	MHCII ^{low} B220 ⁺ CD11b ⁻ CD11c ⁺
Macrophages	F4/80 ⁺ CD11b ⁺
Neutrophils	Gr1(Ly6G/Ly6C) ^{high} CD11b ⁺
Eosinophils	CD11c ⁻ FcεRIα ⁻ Gr-1 ^{lo-neg} CD11b ⁺ Siglec-F ⁺
Basophils	lin ⁻ FcεRI ⁺ DX5 ⁺

Finally, total cell numbers of macrophages and granulocytes, i.e. neutrophils, eosinophils, and basophils, were determined (Table 5). Compared to wild type littermates, normal numbers of macrophages, neutrophils and eosinophils were found in *Cpa3*^{Cre/+} mice (Figure 11A). Especially the unaffected neutrophil compartment in *Cpa3*^{Cre/+} mice is worth mentioning since *Kit* mutant *Kit*^{W/W^v} and *Kit*^{W-sh/W-sh} mice suffer from neutropenia¹³¹ and neutrophilia⁷⁹, respectively.

Interestingly, splenic neutrophils are significantly increased in the recently published Kit-independent mast cell-deficient *Cpa3-Cre x Mcl-1^(fl/fl)* mouse strain¹¹⁰. These mice also have a marked reduction of basophils (58 % - 78 %) in spleen and bone marrow¹¹⁰. Lately, a similar reduction of basophils in the peripheral blood of *Kit^{W/Wv}* mice was published¹⁰⁸ whereas others reported normal numbers of basophils in *Kit^{W/Wv}* mice^{68,69}. To unravel these yet conflicting results, *Kit^{W/Wv}* mice were added to our examination of basophils. The analysis revealed a significant reduction of basophils in the spleens of *Cpa3^{Cre/+}* mice compared to wild type mice and an even more pronounced reduction in *Kit^{W/Wv}* mice (Figure 11B). While *Cpa3^{Cre/+}* mice had about one-third ($0.57 \pm 0.23 \times 10^5$) of basophils compared to *Cpa3^{+/+}* mice ($1.6 \pm 0.61 \times 10^5$), in *Kit^{W/Wv}* mice the number of basophils was further reduced down to 11.25 % (Figure 11B).

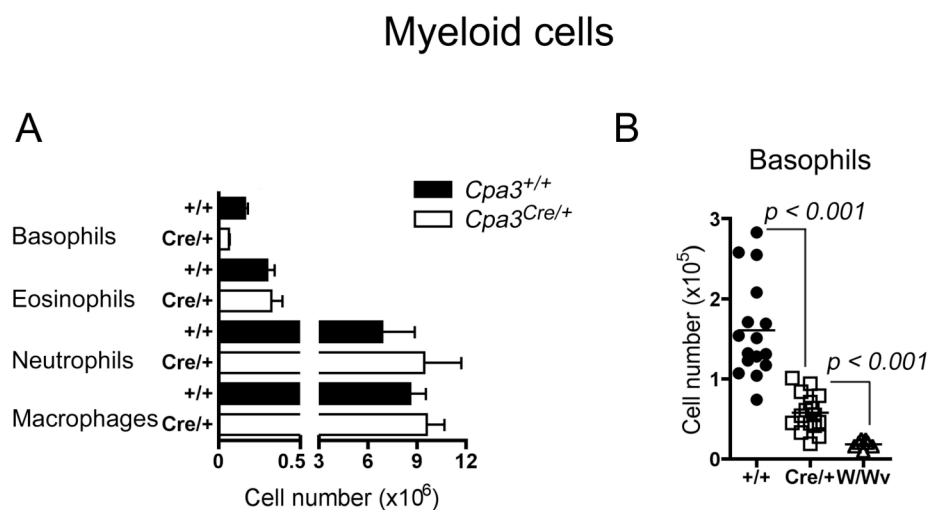


Figure 11 | Flow cytometric analysis of macrophages and granulocytes

Spleens from naïve *Cpa3^{+/+}* and *Cpa3^{Cre/+}* mice were analyzed for macrophages and granulocytes by flow cytometry. **(A)** Bar graphs show direct comparison of total numbers of basophils, eosinophils, neutrophils and macrophages between *Cpa3^{+/+}* and *Cpa3^{Cre/+}* mice. Data are expressed as mean \pm SEM for 12 animals per genotype. **(B)** The scatter plot summarizes total numbers of splenic basophils in *Cpa3^{+/+}* (+/+), *Cpa3^{Cre/+}* (Cre/+) and *Kit^{W/Wv}* (W/Wv) mice. Analyses included 16 mice per genotype except for *Kit^{W/Wv}* mice (7 animals). Data were statistically analyzed by unpaired t test and were considered as significantly different.

In summary, physical and functional mast cell deficiency combined with a reduction of basophils was demonstrated in *Cpa3*^{Cre/+} mice. Apart from the basophil reduction, this mouse strain seems to have normal cellular elements in the steady-state immune system, since no difference in any lymphoid or other myeloid cell subset was found.

3.2.3 Correlation between *Cpa3*-driven Cre expression and cell ablation in the basophil/mast cell lineages

Based on the presumed developmental relationship between the basophil and mast cell lineages in adult murine hematopoiesis¹⁸, it is conceivable that *Cpa3*-driven Cre expression might influence the development and maintenance of both lineages and consequently account for the lack of mast cells and the reduction of basophils in *Cpa3*^{Cre/+} mice. To test for *Cpa3* expression levels in both lineages, a *Cpa3* knock-in reporter strain was used that was recently developed in our laboratory by Dr. Thorsten Feyerabend. In gene-targeted *Cpa3*^{hCD4/hCD4} mice, a human CD4 surface receptor (hCD4) was inserted into the *Cpa3* locus (unpublished). The receptor expression can be specifically detected by anti-hCD4 antibody staining. Hence, *Cpa3* locus transcription can be indirectly visualized by cell surface expression of hCD4.

Table 6 | Cell surface markers for the characterization of basophil and mast cell progenitors

Cell population	Surface markers
Basophil/mast cell progenitors	lin ⁻ kit ⁺ FcγRII/III ^{high} β7integrin ⁺
Basophil progenitors	lin ⁻ CD34 ⁺ FcεRI ^{high} kit ⁺
Mast cell progenitors	lin ⁻ CD45 ⁺ CD34 ⁺ β7integrin ⁺ FcγRII/III ^{high}

Cpa3 expression was first evaluated in the known splenic bipotent basophil/mast cell progenitor (BMCP) (Table 6). The mean fluorescence intensity (MFI) of hCD4 staining reflects the expression levels of the *Cpa3* gene. Consistent with weak

expression of the *Cpa3* locus, splenic BMCPs were present in normal numbers in *Cpa3^{Cre/+}* mice ($1.34 \pm 0.57 \times 10^3$) compared to wild type littermates ($1.30 \pm 0.56 \times 10^3$) (Figure 12A). Unipotent progenitors of the basophil and the mast cell lineage (Table 6) can be isolated from the bone marrow and the small intestine, respectively¹⁸. Compared to *Cpa3* gene expression in BMCPs, expression levels were slightly increased in basophil progenitors (by a factor of 1.6) (Figure 12B) and in mast cell progenitors (by a factor of 1.3) (Figure 12C). While the abundance of basophil progenitors in the bone marrow was not affected by *Cpa3*-driven Cre expression ($1.36 \pm 0.50 \times 10^3$ in *Cpa3^{+/+}* mice and $1.52 \pm 0.67 \times 10^3$ in *Cpa3^{Cre/+}* mice) (Figure 12B), intestinal mast cell progenitors were clearly reduced in *Cpa3^{Cre/+}* mice ($1.61 \pm 0.43 \times 10^2$) compared to *Cpa3^{+/+}* mice ($14.03 \pm 7.45 \times 10^2$) (Figure 12C). *Cpa3* expression levels were elevated weakly, i.e. by a factor of 1.6, from BMCPs to mature splenic basophils (Figure 12D), but very strongly, i.e. by a factor of 14, between BMCPs and peritoneal mast cells (Figure 12E).

It has been shown that high levels of Cre expression might have a toxic effect on mammalian cells in vitro^{132,133} and in vivo^{123,124,134}. Cryptic (or pseudo) *loxP* sites in the mammalian genome can serve as functional Cre recombinase recognition sites¹³⁵, and recombination between these sites might cause accidental chromosomal rearrangements and finally loss of the affected cells¹²⁴. Thus, the partial or complete loss of cells of the basophil/mast cell lineages in *Cpa3^{Cre/+}* mice could be explained by Cre-mediated cellular toxicity.

Altogether, analyses in *Cpa3^{hCD4/hCD4}* mice indicated not only high levels of *Cpa3* expression in peritoneal mast cells but also weak *Cpa3* expression in common basophil/mast cell progenitors and in the basophil lineage. The progressive increase of *Cpa3* expression and consequently also Cre expression within the development of the basophil/mast cell lineages correlated with a concomitant loss of cells due to Cre-mediated genotoxicity. Cell deficiency in the mast cell lineage was already evident at the progenitor level while in the basophil lineage only mature basophils were reduced in number. Hence, the mast cell lineage was stronger affected by Cre-mediated cell ablation than the basophil lineage in *Cpa3^{Cre/+}* mice.

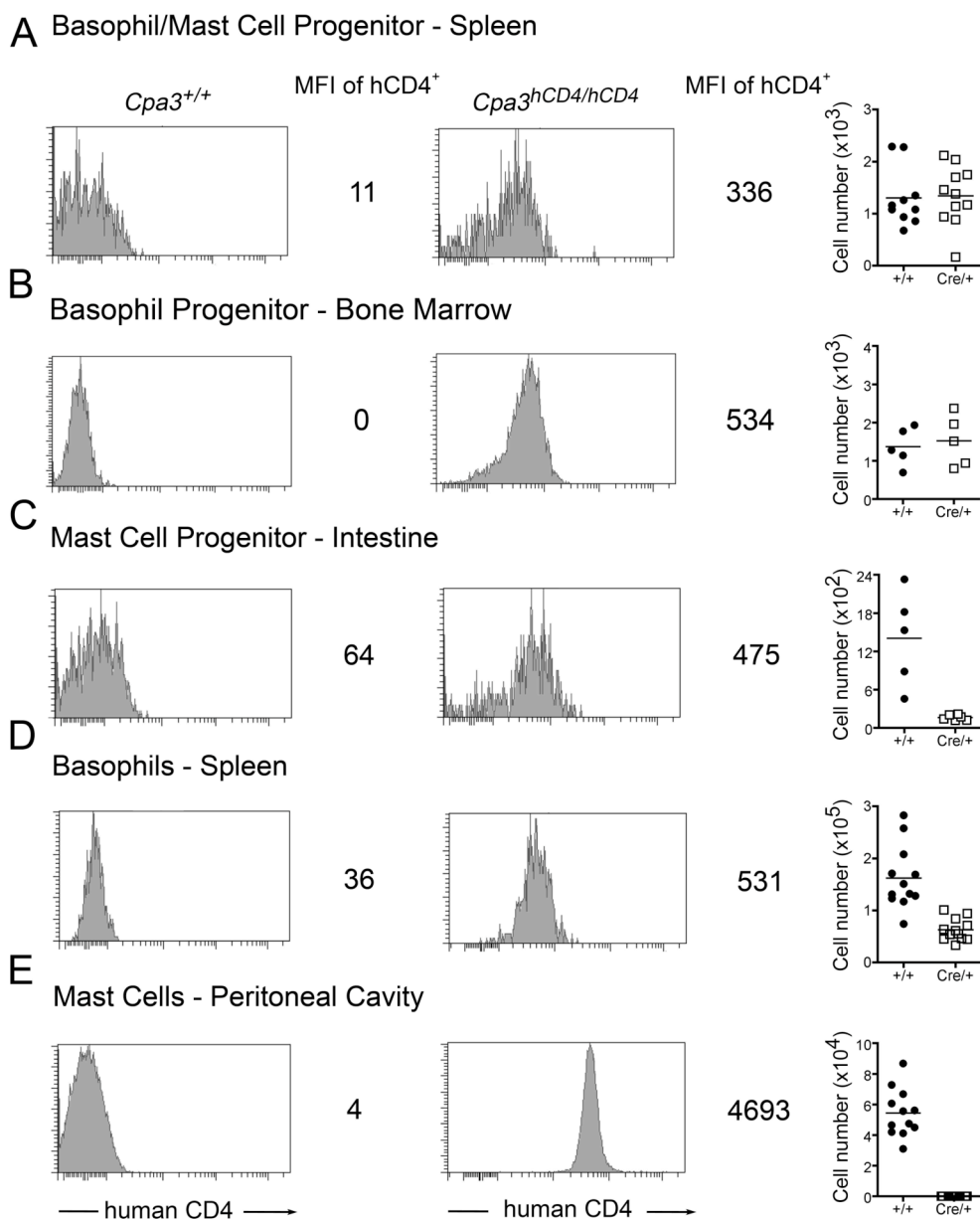


Figure 12 | Correlation between *Cpa3* expression and loss of cells in the basophil/mast cell lineages

(A - E) Cells from *Cpa3*^{hCD4/hCD4} reporter mice were analyzed for *Cpa3* expression levels by measuring the MFI of hCD4 expression (histograms in the center). Cells from *Cpa3*^{+/+} mice served as controls for the calculation of hCD4 background fluorescence (histograms on the left). Scatter plots on the right summarize numbers of cells comparing *Cpa3*^{+/+} (+/+) and *Cpa3*^{Cre/+} (Cre/+) mice at the corresponding developmental stages, respectively. MFI of hCD4 expression and cell numbers were analyzed for the following cell populations: (A) Basophil/Mast cell progenitors in the spleen, n = 10 per genotype. (B) Basophil progenitors in the bone marrow, n = 5 per genotype. (C) Mast cell progenitors in the small intestine, n = 5 per genotype. (D) Mature basophils in the spleen, n = 12 per genotype. (E) Mature mast cells in the peritoneal cavity, n = 12 per genotype.

3.2.4 Basophil-dependent anaphylaxis is suppressed in *Cpa3*^{Cre/+} mice

The partial reduction of basophils in mast cell-deficient *Cpa3*^{Cre/+} mice should be considered when immunological functions are assessed in this strain. To test the functional potential of the remaining basophils, *Cpa3*^{Cre/+} mice were subjected to a basophil-dependent IgG1-mediated anaphylaxis model. Homozygous *Cpa3*^{Cre/Cre} mice, *Kit*^{W/W^v} mice as well as wild type mice were included as control groups.

Under steady-state conditions, wild type mice have $1.74 \pm 0.45 \times 10^5$ splenic basophils (Figure 13A). It was analyzed whether homozygous *Cpa3*-driven Cre expression might further diminish the number of splenic basophils. Indeed, a higher Cre dose resulted in about 50 % higher reduction of basophils in *Cpa3*^{Cre/Cre} mice ($0.29 \pm 0.12 \times 10^5$) compared to basophil numbers in heterozygous *Cpa3*^{Cre/+} mice ($0.62 \pm 0.18 \times 10^5$). *Kit*^{W/W^v} mice had the fewest basophils ($0.18 \pm 0.05 \times 10^5$).

As stated above, mast cells are the key players in IgE-mediated anaphylactic reactions (section 3.1.3). Recent reports demonstrated that an anaphylactic response could also be induced through the IgG/FcγR pathway. In this “alternative” mast cell-independent pathway of anaphylaxis, FcγR activation of basophils, macrophages, and neutrophils elicits anaphylaxis symptoms, including a drop in core body temperature¹³⁶⁻¹³⁸. To stimulate FcγR-bearing basophils by IgG-antigen complexes, mice were first intravenously injected with antigen-specific IgG1, followed by intravenous antigen challenge three hours later. Wild type mice responded to this treatment by a persistent and severe drop in body temperature by 4 K. In contrast, IgG-mediated anaphylaxis was greatly suppressed in *Cpa3*^{Cre/+} mice, and consistent with their more severe basophil deficiency, *Cpa3*^{Cre/Cre} mice were even more protected from symptoms of anaphylaxis (Figure 13B). Surprisingly, *Kit*^{W/W^v} mice, which, in addition to a lack of mast cells, suffer from a marked reduction in basophils, responded like wild type mice but recovered much faster from temperature drop (Figure 13B). Detailed comparisons of individual temperature measurements 30 min after antigen challenge demonstrated an equal temperature drop in wild type (-3.68 ± 0.96 K) and *Kit*^{W/W^v} mice (-3.93 ± 0.59 K). Heterozygous (-2.16 ± 1.95 K) and homozygous *Cpa3*^{Cre} mice (-1.18 ± 1.66 K) were mostly resistant to IgG1-induced anaphylaxis (Figure 13C). In summary, direct comparison

of the body temperature 30 min after antigen challenge and basophil numbers revealed an inverse correlation of both parameters in all analyzed genotypes, except for *Kit^{W/Wv}* mice (Figure 13A and C).

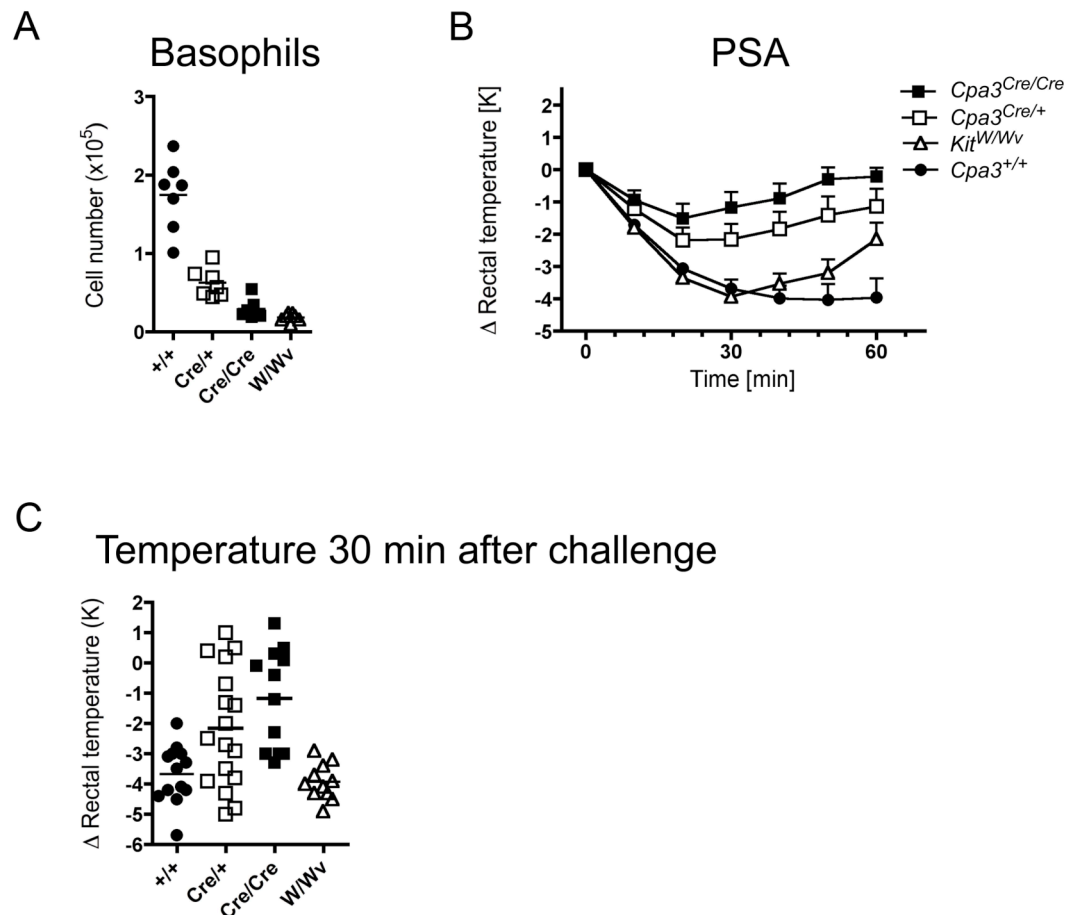


Figure 13 | Correlation between IgG1-mediated anaphylactic response and basophil numbers

(A) The scatter plot summarizes total numbers of splenic basophils in *Cpa3^{+/+}* (+/+), *Cpa3^{Cre/+}* (Cre/+), *Cpa3^{Cre/Cre}* (Cre/Cre) and *Kit^{W/Wv}* (W/Wv) mice. Analyses included 7 mice per genotype. **(B)** Mice of the indicated genotypes were subjected to IgG1-mediated PSA. Mice were intravenously injected with anti-DNP IgG1 and challenged three hours later by intravenous injection of DNP-HSA. Anaphylactic response following challenge was measured as drop in body temperature. Rectal temperatures were monitored in 10 min intervals and are expressed as temperature difference compared to starting temperature. Shown are the mean \pm SEM ($n = 13$ in *Cpa3^{+/+}*, $n = 17$ in *Cpa3^{Cre/+}*, $n = 12$ in *Cpa3^{Cre/Cre}* and $n = 13$ in *Kit^{W/Wv}* mice). **(C)** The scatter plot summarizes data from temperature measurements of individual mice 30 min after anti-DNP IgG1/DNP-HSA treatment. Numbers of analyzed mice per genotype are stated under (B).

Diminished susceptibility of *Cpa3^{Cre}* mice to IgG1-antigen treatment is compatible with the assumed involvement of basophils in IgG1-mediated anaphylaxis. The fact that *Kit^{W/W^v}* mice, which lack even more basophils compared to *Cpa3^{Cre}* mice, were not resistant to IgG1-mediated anaphylaxis, suggests that in this mutant an unknown mechanism might overcome the deficiency of basophils.

3.3 K/BxN serum transfer arthritis and experimental autoimmune encephalomyelitis in *Cpa3^{Cre/+}* mice

In the past mast cells have been mainly recognized as primary responders in allergic reactions. Several recent studies stated that they might also have a pro-inflammatory role in autoimmune diseases. Particularly, mast cell contributions to the pathology of models of rheumatoid arthritis and multiple sclerosis have been claimed¹³⁹. Due to the hitherto lack of alternative mast cell-deficient models, these reports were based on observations in *Kit* mutant mouse strains. The present study was therefore aimed for a re-evaluation of the role of mast cells in models of rheumatoid arthritis and multiple sclerosis in *Kit*-independent mast cell-deficient *Cpa3^{Cre/+}* mice on the C57BL/6 background.

3.3.1 *Cpa3^{Cre/+}* mice are fully susceptible to K/BxN serum transfer arthritis

IgG antibodies against glucose-6-phosphate isomerase (GPI), which are spontaneously produced in arthritic K/BxN mice, can passively induce a joint disorder that resembles many aspects of rheumatoid arthritis⁹⁹ upon intraperitoneal injection into naïve recipient mice¹⁰⁰. Mast cell-deficient *Kit^{W/W^v}* and *Kit^{Sl/Sl-d}* mice, however, are resistant to the induction of arthritis by transfer of antibodies against GPI⁹⁸. These data led to the conclusion that mast cells are important elements in the disease process of arthritis, at least in this serum transfer model.

To re-address disease susceptibility to serum-transferred arthritis in a mast cell-deficient but *Kit*-proficient environment, *Cpa3^{Cre/+}* mice and wild type controls on

C57BL/6 background as well as *Kit^{W/W^v}* mice were treated with intraperitoneal injections of arthritogenic K/BxN serum. Because *Cpa3^{Cre/+}* mice and their *Cpa3^{+/+}* wild type littermates appear physically identical, genotype-blind disease scoring and thus elimination of bias was feasible. This approach is impossible when using *Kit^{W/W^v}* mice and C57BL/6 controls on the same time due to the different fur of both strains. Following serum injection, disease progression was evaluated by measuring the ankle thickening as well as by clinical scoring of individual paws. For clinical scoring, individual paws were evaluated with regard to signs of swelling and erythema, and limb scores for each mouse were summed up. *Cpa3^{+/+}* and mast cell-deficient *Cpa3^{Cre/+}* mice were fully susceptible to antibody-mediated arthritis as shown by the comparable rapid onset of symptoms in both genotypes. The progression of clinical disease was also similar. The extent of ankle swelling developed in parallel and peaked around days 11 to 12 in both strains (Figure 14A). In contrast to mast cell-deficient *Cpa3^{Cre/+}* mice and in line with the literature⁹⁸, *Kit^{W/W^v}* mice were almost resistant to disease induction. This strain showed only transient symptoms of ankle joint swelling and a lower clinical score (Figure 14A). The incidence of disease was also reduced in *Kit^{W/W^v}* mice compared to the other tested genotypes, which exhibited 100 % disease incidence (Table 7).

Table 7 | Incidence of K/BxN serum transfer arthritis

Mouse genotype	Incidence
<i>Cpa3^{+/+}Kit^{+/+}</i>	10/10 (100%)
<i>Cpa3^{Cre/+}Kit^{+/+}</i>	10/10 (100%)
<i>Cpa3^{+/+}Kit^{W/W^v}</i>	3/5 (60%)

To evaluate differences in response curves, all data were analyzed by two-way ANOVA considering time and genotypes. The statistical analysis has been done in collaboration with Axel Benner from the biostatistics division. No significant differences between *Cpa3^{+/+}* and *Cpa3^{Cre/+}* genotypes were observed for clinical scores or ankle thickness (Figure 14A). A second independent experiment confirmed that mast cell-deficient *Cpa3^{Cre/+}* mice and wild type controls were comparably

susceptible to serum transfer arthritis without significant differences in their response curves (Figure 14B).

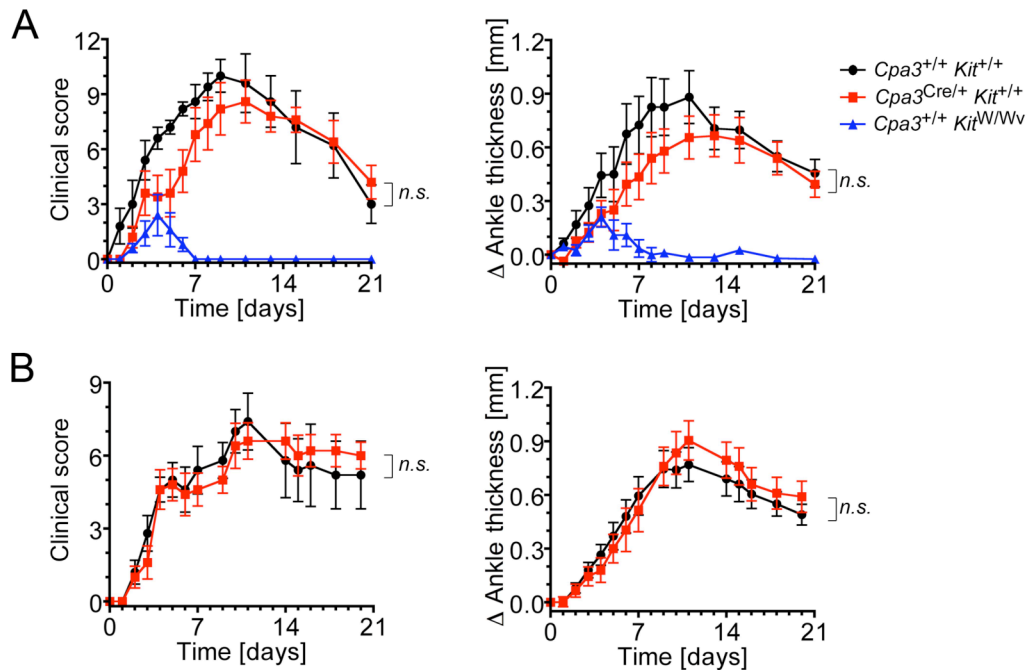


Figure 14 | Clinical disease development in K/BxN serum transfer arthritis

Kinetics of clinical scores (left) and ankle swelling (right) are shown. Mice of the indicated genotypes were treated with two intraperitoneal injections of arthritogenic K/BxN serum on day 0 and 2, respectively. The data were plotted as mean daily clinical score (0 to 12 based on 0 - 3 scores for each of four paws) \pm SEM for all animals per group (left panels). Differences in ankle thickness were calculated by subtracting the baseline ankle thickness of both hind limbs from subsequent measurements, respectively. Data are shown as mean \pm SEM (right panels). Data of *Cpa3*^{+/+} and *Cpa3*^{Cre/+} mice were statistically analyzed by two-way ANOVA and no significant differences were found for clinical scores (A, $p = 0.11$ and B, $p = 0.95$) and ankle thickness (A, $p = 0.38$ and B, $p = 0.81$). (A) *Cpa3*^{+/+}, *Cpa3*^{Cre/+}, and *Kit*^{W/Wv} mice were compared ($n = 5$ for each genotype). (B) *Cpa3*^{+/+} and *Cpa3*^{Cre/+} mice were directly compared ($n = 5$ for each genotype).

Altogether, Kit-proficient mast cell-deficient *Cpa3*^{Cre/+} mice developed severe signs of arthritis whereas mast cell-deficient *Kit*^{W/Wv} mice were largely protected from disease induction. Histopathological evaluation of affected ankle joints from arthritic mice further supported this conclusion. Particularly, histology of the swollen joints from *Cpa3*^{+/+} and *Cpa3*^{Cre/+} mice showed characteristic massive leukocyte infiltrations and pronounced synovial hyperplasia with erosion of the cartilage. None of these histopathological alterations were present in ankle joints from *Kit*^{W/Wv} or PBS-treated mice (Figure 15).

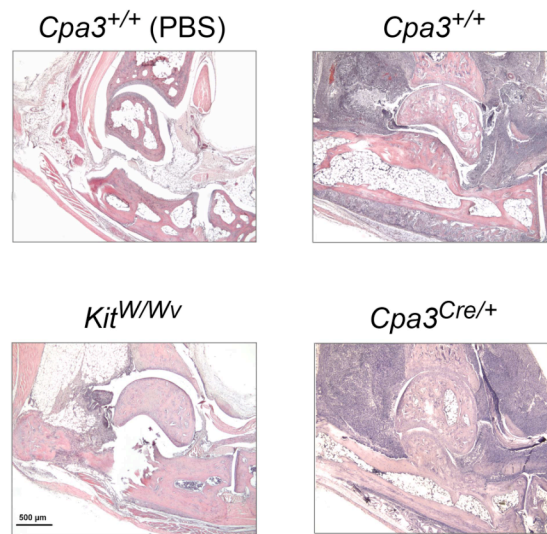


Figure 15 | Histopathological analysis of ankle joints from arthritic mice

Representative midsagittal ankle sections from $Cpa3^{+/+}$, $Cpa3^{Cre/+}$ and $Kit^{W/Wv}$ mice taken ten days after the first injection of K/BxN serum are shown. Joints from PBS-injected wild type mice (PBS) served as controls. Hematoxylin/eosin stained sections from $Cpa3^{+/+}$ and $Cpa3^{Cre/+}$ mice show severe proliferative and granulomatous rheumatoid-like arthritis with tendovaginitis and granulocytic infiltration. In contrast, ankle joints from serum-injected $Kit^{W/Wv}$ mice and controls show no pathology. The depicted scale bar applies to all photographs.

3.3.2 Molecular responses to serum transfer arthritis

Microarray analyses of RNA from ankle joints were performed to characterize molecular events underlying the pathology of K/BxN serum-transferred arthritis and to search for signs of inflammation-driven mast cell induction. Because mast cells might play an early coordinating role in the K/BxN serum transfer arthritis model⁹⁸, early time points of disease were analyzed. To this end ankle tissue from $Cpa3^{+/+}$ and $Cpa3^{Cre/+}$ mice was collected at three time points: day 0 (baseline), day 3 (disease onset) and day 7 (early disease), RNA was extracted and changes in mRNA expression were assessed. Expression profiling of the RNA samples was performed at the DKFZ Microarray Core Facility. Dr. Thorsten Feyerabend and Martin Teichert assisted with the analysis of the data. Differentially expressed genes were analyzed by hierarchical clustering. Four distinct kinetic patterns were identified: (1) genes that are upregulated towards day 7, (2) genes that are

upregulated at day three and continue to be expressed at day 7, (3) genes that are, regardless of the time point, present in *Cpa3^{+/+}* but absent in *Cpa3^{Cre/+}* mice, and (4) genes that are downregulated towards day 7 (Figure 16). Differentially expressed genes of patterns 1, 2 and 4 represent diverse functional categories including cytokines, chemokines, proteases like metalloproteases and calcium-sensitive proteases, inflammatory markers like acute-phase reactants and S100 proteins, and extracellular matrix components. Similar categories and associated kinetic patterns of expression have been described in an earlier report about gene expression profiling in K/BxN serum transfer arthritis¹⁴⁰.

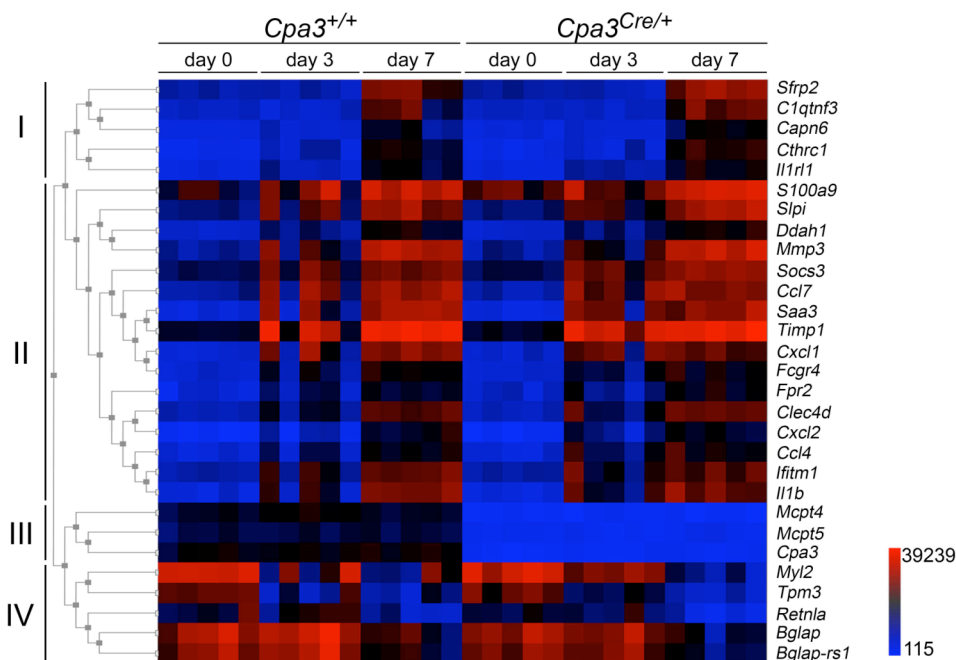


Figure 16 | Gene expression profiling in ankle tissue during serum transfer arthritis

RNA of ankle joints from naïve (day 0) *Cpa3^{+/+}* and *Cpa3^{Cre/+}* mice and from mice three (day 3) and seven days (day 7) after first K/BxN serum injection was analyzed for kinetic changes in gene expression. For each genotype and time point, a total of five joints from three to four individual mice were analyzed. Differentially expressed genes were grouped by hierarchical clustering and four distinct kinetic patterns were identified as indicated on the left (I - IV). Pattern 3 shows lack of mast cell products in ankles from *Cpa3^{Cre/+}* mice at all analyzed time points.

The gene expression patterns 1, 2 and 4 obtained from *Cpa3^{+/+}* and *Cpa3^{Cre/+}* mice were comparable and further supported the comparable clinical and histopathological findings that were monitored during the disease in these two

strains. However, genes of pattern 3, which encode for the mast cell proteases Mcpt4, Mcpt5 and Cpa3, were completely absent in *Cpa3^{Cre/+}* mice at any time point. Of note, they were only slightly expressed in joints of wild type mice and their expression did not change over time (Figure 16).

Hence, induction of K/BxN serum-transferred arthritis did not provoke mast cell products in joints of *Cpa3^{Cre/+}* mice, confirming the absence of mast cells from this mouse strain even under these inflammatory conditions.

Altogether, disease evaluation by clinical scoring, histopathology and gene expression analyses in Kit-proficient mast cell-deficient mice and comparison to the corresponding parameters of wild type littermates does not support the idea of a crucial role for mast cells in the antibody-mediated model of rheumatoid arthritis.

3.3.3 *Cpa3^{Cre/+}* and *Kit^{W/Wv}* mice are fully susceptible to EAE

Multiple sclerosis is a chronic inflammatory disease in which the immune system attacks the myelin sheaths around the nerve fibers of the CNS, leading to demyelination and scarring. Damage of myelin and the axons themselves results in impairment of axonal conduction in the CNS, which causes a broad spectrum of symptoms. Experimental autoimmune encephalomyelitis is a well-characterized murine model of multiple sclerosis that is extensively used to understand the role of specific molecules and cell subsets in disease pathology. EAE critically depends on pro-inflammatory T helper cells¹⁴¹, but experiments in mast cell-deficient *Kit^{W/Wv}* mice suggested also an essential role for mast cells in the pathogenesis of this autoimmune model. In particular, *Kit^{W/Wv}* mice develop EAE later and less severely than control mice in response to immunization with MOG₃₅₋₅₅ peptide⁹⁶. However, there are other reports of an even exacerbated EAE development in *Kit^{W/Wv}* mice compared to wild type mice^{105,106}.

These contradictory observations prompted us to re-evaluate the contribution of mast cells in MOG-induced EAE in Kit-proficient mast cell-lacking mice. To this end *Cpa3^{+/+}*, *Cpa3^{Cre/+}* and *Kit^{W/Wv}* mice were immunized with MOG₃₅₋₅₅ peptide in complete Freund's adjuvant, and onset, severity, and incidence of disease as well as

the number of moribund mice were monitored. *Cpa3*^{+/+} and *Cpa3*^{Cre/+} mice were mixed littermates that were clinically scored without prior knowledge of their genotype. MOG-immunized wild type mice developed chronic progressive EAE in which first symptoms of disease were observed around day 11 post-immunization. Response curves of mast cell-deficient *Cpa3*^{Cre/+}, *Kit*^{W/W^v} mice and wild type mice were nearly congruent, and thus all three genotypes were equally susceptible to EAE induction (Figure 17A). Based on a two-way ANOVA considering time and genotypes, no significant differences were found between any of the strains. A total of three independent experiments confirmed comparable days of onset, maximal clinical scores and 100 % incidence in all three mouse strains (Table 8). Of note, clearly more moribund animals were observed among *Kit*^{W/W^v} mice (46 %) compared to *Cpa3*^{Cre/+} mice (16 %) and wild type controls (21 %) (Figure 17B and Table 8).

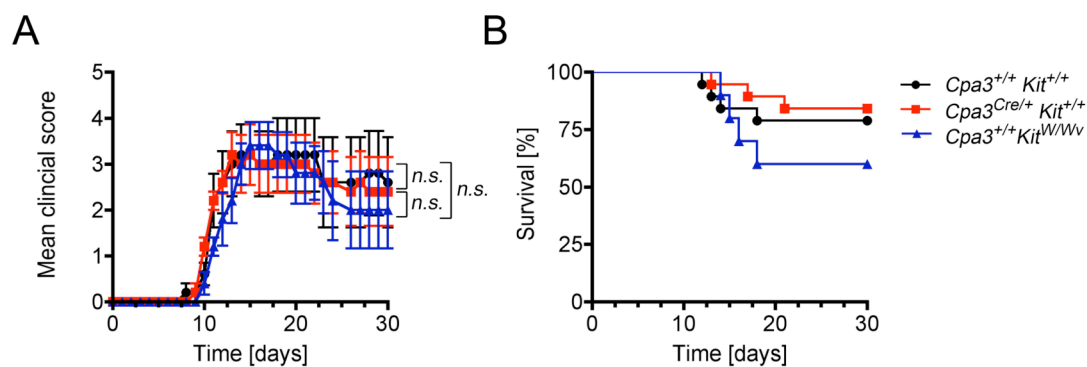


Figure 17 | Clinical disease development in MOG-induced EAE

Mice of the indicated genotypes were subjected to MOG-induced EAE and clinical scores were monitored over a period of 30 days. In detail, mice were subcutaneously immunized with MOG₃₅₋₅₅ peptide in complete Freund's adjuvant on day 0 and intravenously treated with pertussis toxin on experimental days 0 and 2, respectively. **(A)** Immunized mice were scored daily and data represent mean clinical score \pm SEM. Data were obtained from five mice per genotype. Statistical analyses by two-way ANOVA considering time and genotype revealed no significant differences between tested strains ($p = 0.92$ for *Cpa3*^{+/+} versus *Cpa3*^{Cre/+}, $p = 0.69$ for *Cpa3*^{+/+} versus *Kit*^{W/W^v} and $p = 0.74$ for *Cpa3*^{Cre/+} versus *Kit*^{W/W^v}). **(B)** Mice that were not able to straighten up were considered as moribund (score 5) and were sacrificed during the ongoing experiment. The survival curve summarizes data from three independent experiments with 19 mice per genotype except for *Kit*^{W/W^v} mice ($n = 11$).

From these observations it can be concluded that initiation and progression of EAE occurs independently of mast cells. Furthermore, the lack of Kit expression has no protective effect in this disease model but rather seems to exacerbate the susceptibility to EAE induced morbidity.

Table 8 | Summary of MOG₃₅₋₅₅-induced EAE in mast cell-deficient mouse strains

Mouse genotype	Incidence	Day of onset (mean ± s.d.)	Maximum clinical score (mean ± s.d.)	Moribund
<i>Cpa3</i> ^{+/+} <i>Kit</i> ^{+/+}	19/19 (100%)	10.63 ± 1.12	3.68 ± 1.00	4/19 (21%)
<i>Cpa3</i> ^{Cre/+} <i>Kit</i> ^{+/+}	19/19 (100%)	11.05 ± 1.62	3.32 ± 0.89	3/19 (16%)
<i>Cpa3</i> ^{+/+} <i>Kit</i> ^{W/Wv}	11/11 (100%)	11.09 ± 0.94	3.82 ± 1.40	5/11 (46%)

3.3.4 Neither mast cell nor Kit deficiency affect MOG-specific T cell responses

Apart from clinical parameters, it was also examined whether the initial antigen-specific T cell activation during EAE induction might be compromised in a mast cell-deficient environment, as it was observed by others in *Kit*^{W/Wv} mice¹⁴². To answer this question, the proliferative potential and IFN- γ production of splenic MOG-specific T cells was evaluated in *Cpa3*^{+/+}, *Cpa3*^{Cre/+} and *Kit*^{W/Wv} mice 11 days after immunization with MOG₃₅₋₅₅ peptide. In detail, splenocytes from naïve and immunized mice were labeled with CFSE and re-stimulated ex vivo with MOG₃₅₋₅₅ peptide, which contains multiple CD4⁺ and CD8⁺ T cell epitopes¹⁴³. Antigen re-stimulated CD4⁺ and CD8⁺ T cells from immunized mice showed augmented proliferation compared to cells from naïve mice (Figure 18A). In naïve mice only two percent of the splenic CD4⁺ and CD8⁺ T cells proliferated in response to stimulation with MOG₃₅₋₅₅ peptide, respectively. Generally, more CD8⁺ T cells (12 %) proliferated in response to MOG₃₅₋₅₅ peptide than CD4⁺ T cells (6 %). MOG-specific CD4⁺ and CD8⁺ T cells from immunized mast cell-deficient *Cpa3*^{Cre/+} and *Kit*^{W/Wv} mice proliferated comparable to wild type controls (Figure 18A). To evaluate MOG-specific IFN- γ responses, cells were directly re-stimulated ex vivo with MOG₃₅₋₅₅ peptide prior to analysis by intracellular staining and flow cytometry. A comparable frequency

(~ 3 %) of splenic CD4⁺ IFN- γ -producing T cells was found in MOG-primed mice from all three analyzed genotypes (Figure 18B).

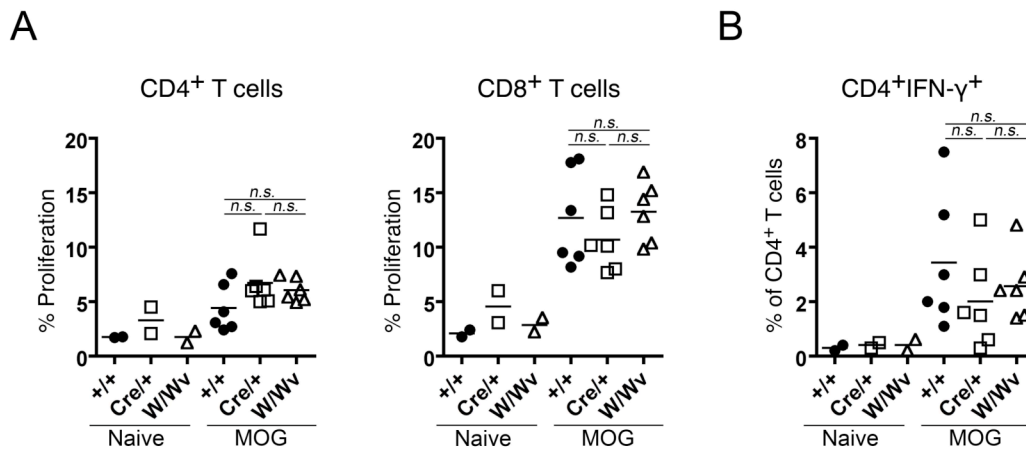


Figure 18 | MOG-specific proliferation and IFN- γ response in the spleen

Spleens from *Cpa3*^{+/+} (+/+), *Cpa3*^{Cre/+} (Cre/+) and *Kit*^{W/Wv} (W/Wv) mice were harvested 11 days after immunization with MOG₃₅₋₅₅ peptide/CFA and splenocytes were re-stimulated ex vivo with MOG₃₅₋₅₅ peptide prior to analyses for proliferation (A) and IFN γ production (B). Cells from naïve mice of the indicated genotypes served as controls. **(A)** Proliferative response of splenic CD4⁺ (left) and CD8⁺ T cells (right). Splenocytes were labeled with CFSE and re-stimulated with MOG₃₅₋₅₅ peptide for three days. Proliferation was measured by analysis of CFSE dilution. **(B)** For analyses of MOG-specific IFN γ expression, splenocytes were re-stimulated with MOG₃₅₋₅₅ peptide over night and intracellularly stained against IFN- γ . The percentage of IFN- γ ⁺CD4⁺ T cells was analyzed by flow cytometry. Data in A - B summarize two independent experiments with a total of two naïve mice per genotype and six immunized mice per genotype. The indicated genotypes of all MOG-immunized mice were statistically compared by unpaired t test and none were found significantly different.

Taken together, parameters of cellular activation of splenic MOG-specific T cells were not altered in immunized *Cpa3*^{Cre/+} or *Kit*^{W/Wv} mice compared to wild type mice. Thus, there was no evidence that mast cells or Kit signalling might influence the primary MOG-specific T cell response after MOG-immunization.

3.3.5 Mast cell and Kit deficiency have no impact on the inflammatory immune response in the CNS

Recent studies led to the assumption that mast cell-derived mediators initiate the inflammatory cell influx of neutrophils and T cells into the central nervous system (CNS) and thus drive disease progression of EAE¹⁴⁴. It was therefore tested whether mast cell-deficient *Cpa3*^{Cre/+} mice might show modified cell entry into the CNS despite normal disease progression. The composition of infiltrating immune cells in brain and spinal cord was analyzed in mast cell-deficient mouse strains and in control mice, and was compared to the naïve status. The analysis was performed 11 days after immunization with MOG₃₅₋₅₅ peptide. Hematopoietic cells in the CNS can be divided into CD45^{low} resident microglia and infiltrating CD45^{high} cells¹⁴⁵. Under normal conditions, one finds only a minor population of infiltrating immune cells in the CNS. Indeed, an increase of CD45^{high} cells was observed in the CNS of MOG-immunized mice compared to naïve mice with all three analyzed mouse strains showing the same extent of CD45^{high} CNS infiltrations (Figure 19A). Further analyses of the different subpopulations represented among these CD45^{high} infiltrates revealed no significant differences in the total numbers of infiltrated activated (CD44⁺CD62L⁻) CD4⁺ and CD8⁺ T cells in *Cpa3*^{Cre/+}, *Kit*^{W/W^v} or control mice (Figure 19B). As expected for an acute immune response, the percentage of T cells with an activated phenotype among all analyzed T cells was near 100 % (data not shown). Also neutrophils (Ly6G⁺Ly6C^{low}) and inflammatory monocytes (Ly6G⁻Ly6C^{high}) make up a substantial proportion of the early cell inflammatory infiltrate in the CNS in acute EAE^{144,146-148}. At day 11 the number of infiltrating myeloid Gr-1⁺ cells was not significantly different between *Cpa3*^{+/+}, *Cpa3*^{Cre/+} or *Kit*^{W/W^v} mice (Figure 19C).

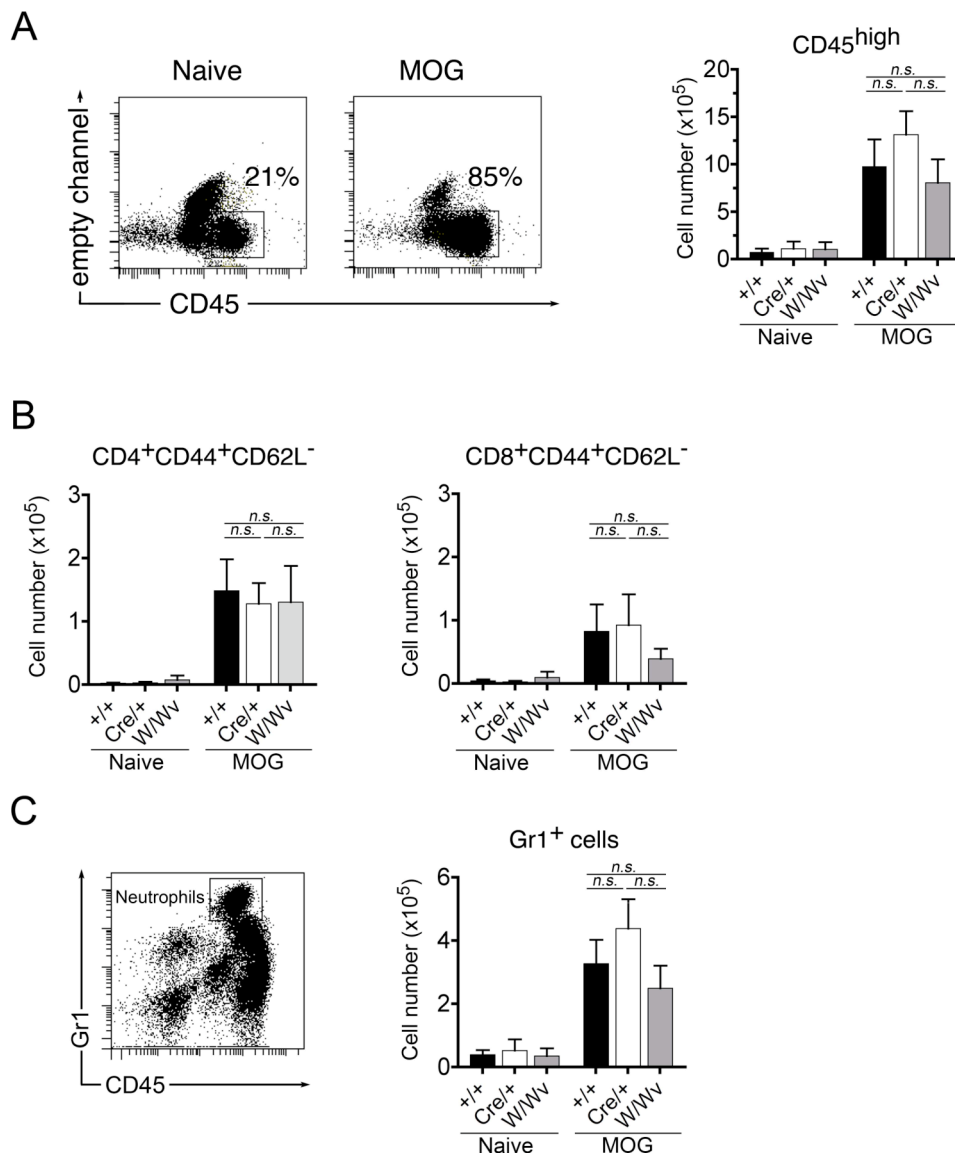


Figure 19 | Inflammatory cell response in the CNS of MOG-immunized mice

(A - C) Inflammatory cells were isolated from pooled brain and spinal cord samples by percoll gradient centrifugation and assessed by flow cytometry 11 days after MOG₃₅₋₅₅ peptide/CFA immunization. Naïve mice served as controls. **(A)** Dot plots on the left demonstrate CD45⁺ and CD45^{high} lymphocytes in the CNS of naïve and MOG-immunized wild type mice. Numbers represent percentage of CD45^{high} cells in the gated regions. Quantification of total CNS-infiltrating CD45^{high} lymphocytes in naïve (naïve) and MOG-immunized (MOG) *Cpa3*^{+/+} (+/+), *Cpa3*^{Cre/+} (Cre/+) and *Kit*^{W/Wv} (W/Wv) mice is shown on the right. **(B)** Total numbers of activated (CD44⁺CD62L⁻) CD4⁺ (left) and CD8⁺ (right) T cells were compared between naïve and immunized mice of the indicated genotypes. **(C)** Dot plot on the left demonstrates infiltrated CD45^{high}Gr1⁺ cells in the CNS after MOG-immunization. Quantification of total CNS-infiltrated Gr1⁺ cells is shown on the left. Data in A - C summarize two independent experiments with a total of two naïve mice per genotype and six immunized mice per genotype. Bar graphs show the mean ± SEM. The indicated genotypes of all MOG-immunized mice were statistically compared by unpaired t test and none were found significantly different.

In the present study, the antibody clone RB6-8C5 was used to recognize infiltrating CD45^{high} cells expressing the myeloid differentiation antigen Gr-1. Since this antibody reacts with a common epitope on Ly6G and Ly6C it does not allow a differentiation between neutrophils (Ly6G⁺Ly6C^{low}) and inflammatory monocytes (Ly6G⁻Ly6C^{high}). However, according to the literature inflammatory monocytes in the CNS are highest on day four after immunization with MOG-peptide, whereas later in disease neutrophils become dominant¹⁴⁷. Thus, the Gr1⁺ cells that were recognized in the CNS on day 11 were most likely neutrophils.

Consistent with their full susceptibility to MOG-induced EAE, no diminution in the entry of inflammatory cells into the CNS of *Cpa3*^{Cre/+} or *Kit*^{W/Wv} mice was observed. In summary, these data lead to the conclusion that neither mast cell nor Kit deficiency affect immunological parameters and disease manifestation in EAE.

4 Discussion

Although mast cells have been discovered already over 130 years ago, they are still one of the most mysterious cells of our immune system. Current research still concentrates on uncovering the physiological functions of mast cells, aside from their unfavourable involvement in allergic disorders.

Selective mast cell deficiency models versus *Kit* mutants

To investigate the function of cell lineages in vivo, selective lineage ablation models serve as important tools. In particular, an ideal mast cell ablation model for studying the immunological role of mast cells should meet the following criteria:

- I. Constitutive lack of CTMC and MMC under physiological and pathological conditions (e.g. inflammation)
- II. No developmental or functional defects in lineages other than the mast cell lineage

The discovery that *Kit* mutant mice are genetically mast cell-deficient, gave new impetus to the field of mast cell research. *Kit*^{W/W^v} and *Kit*^{W-sh/W-sh} mice became standard tools for elucidating in vivo functions of the mast cell lineage^{68,69}. Since *Kit* is not only expressed on mast cells, mutations affecting the functionality of this tyrosine kinase receptor cause defects in diverse cellular compartments. These global *Kit*-related defects might influence biological responses of the *Kit* mutants. That could lead to experimental misinterpretations in which defects are assigned to mast cells, which in fact are caused by *Kit* deficiency. Hence, the development of a *Kit*-independent mast cell-deficient mouse model would be a major advance in the field of mast cell research.

Recent technical progress in transgenesis and gene targeting facilitated the development of genetically defined mutants that could meet the requirements for selective mast cell deficiency much better than the naturally occurring *Kit* mutated

strains. Prerequisite for the generation of genetically defined mast cell-deficient mouse mutants is the identification of genes selectively expressed in this cell lineage. Mast cell carboxypeptidase (*Cpa3*) is suited for genetic manipulation of the mast cell lineage because it is already strongly expressed in the earliest committed mast cell progenitor but not in hematopoietic stem cells¹⁵.

***Cpa3*^{Cre/+} mice fulfil the criterion of complete mast cell deficiency**

In the newly generated *Cpa3*^{Cre/+} mice, *Cpa3*-driven Cre expression results in an entire and specific ablation of mast cells¹²². In this study, complete mast cell ablation in skin and peritoneal cavity of naïve *Cpa3*^{Cre/+} mice was demonstrated by several independent methods including flow cytometry, histology, and measurement of mRNA transcripts for mast cell products. Such a comprehensive search for mast cells and associated products has so far not been done in *Kit* mutant strains or other recently published mast cell ablation models (see chapter 1.6). Additionally, the unresponsiveness of *Cpa3*^{Cre/+} mice to IgE-mediated anaphylaxis and correction of this resistance by selective transfer of BMDC further confirmed the mast cell deficiency of this strain on a systemic level.

To test whether *Cpa3*^{Cre/+} mice also remain mast cell-deficient under inflammatory conditions, they were subjected to chronic dermatitis and intestinal parasite infection. These experiments are not part of this thesis but are worth to be discussed here to complement the characterization of our new mast cell-deficient mouse model. Treatment of the skin with phorbol-12-myristate-13-acetate (PMA) induces chronic dermatitis and leads to strong increase of skin mast cell numbers in wild type mice but also in mast cell-deficient *Kit*^{W/W^v} mice^{74,75}. Interestingly, the skin of *Cpa3*^{Cre/+} mice remained free of mast cells after repeated exposure to PMA¹²². Apparently, inflammatory signals can abrogate the block in mast cell development in the skin of *Kit*^{W/W^v} mice but do not overcome Cre-mediated mast cell ablation. In contrast to CTMC, which are constitutively present in the connective tissues under normal conditions, MMC require an inflammatory impulse to expand to a recognisable number. Particularly, the number of MMC increase significantly during a T helper 2

(Th2) type response to parasitic infections of the gut^{149,150}. The expansion of mast cells in the gut may result from a combination of increased recruitment, survival and/or differentiation and maturation of mast cell progenitors, as well as proliferation of mature mast cells resident at that site. To examine whether intestinal mastocytosis can be induced in *Cpa3^{Cre/+}* mice, they were infected with the prototypic Th2 cell-inducing helminth *Nippostrongylus brasiliensis* (*Nb*). As shown by histology as well as analysis of local and systemic levels of Mcpt1 expression, wild type mice generated a mucosal mast cell response to *Nb* infection¹²². In contrast, no MMC induction or MMC-specific marker expression was detectable in *Cpa3^{Cre/+}* mice upon *Nb* infection¹²². Additionally, the absence of mast cell-associated mRNA transcripts in the inflammatory joints of arthritic *Cpa3^{Cre/+}* mice is a further confirmation of their resistance to mast cell generation under inflammatory conditions.

Altogether, *Cpa3^{Cre/+}* mice completely lack both subpopulations of mature mast cells, CTMC and MMC, under physiological as well as pathological conditions and therefore clearly fulfil the main criterion for a conclusive model of mast cell deficiency.

Implications of reduced basophil numbers in *Cpa3^{Cre/+}* mice

To meet the requirement of selectivity, *Cpa3^{Cre/+}* mice should lack only cells of the mast cell lineage without manifestation of any other defects. Given the unanticipated mechanism of Cre-mediated lineage ablation in *Cpa3^{Cre/+}* mice, a prudent characterization of common hematopoietic lineages was mandatory to find out whether *Cpa3*-driven Cre expression also affects the development of other cell populations. Moreover, it should be considered that the complete absence of the mast cell lineage might also influence the composition of other immune cell compartments. The analysis of numerous immune cell subsets in the spleen of naïve heterozygous *Cpa3^{Cre/+}* mice revealed a normal immune system. Thus, the lack of mast cells has no impact on the number and composition of all analyzed cell subsets of the lymphoid and myeloid lineage. An exception are basophils that were reduced to about 35 % compared with the number of basophils in wild type mice. In *Cpa3^{Cre/Cre}* mice, which express two mutated *Cpa3* alleles, basophils in the spleen

were further reduced to about 18 %. As mentioned above, *Kit^{W/W^v}* mice suffer from several hematopoietic aberrancies (reviewed in Grimbaldston et al.⁶⁹). However, regarding basophil numbers, the literature repeatedly stated that *Kit^{W/W^v}* mice exhibit no defects in the basophil compartment^{68,69}. This statement was simply based on an older study that found equal numbers of peripheral blood basophils in *Kit^{W/W^v}* and wild type mice by means of morphological identification¹⁵¹. However, very recently Mancardi et al. reported a marked reduction of basophils in the peripheral blood of *Kit^{W/W^v}* mice based on the flow cytometric identification of DX5⁺Kit⁺FcεRI⁺ basophils¹⁰⁸. Flow cytometry experiments in our laboratory revealed a 10-fold reduction of the number of basophils in the spleen of *Kit^{W/W^v}* mice, demonstrating basophil deficiency also in this peripheral lymphoid organ.

A combined deficiency in the mast cell and basophil lineage is not unique for *Cpa3^{Cre/+}* mice but is also observed in the recently described Mas-TRECK mice^{111,112} and *Cpa3-Cre x Mcl-1^{fl/fl}* mice¹¹⁰. The toxin receptor-mediated conditional cell knock-out (TRECK) system is based on transgenic expression of a diphtheria toxin receptor controlled by assumed mast cell-specific *Il4* gene regulation. But diphtheria toxin treatment completely depletes mast cells and basophils in the Mas-TRECK system^{111,112}. Lilla et al. generated a transgenic mouse strain that expresses Cre recombinase under the control of a 780 bp fragment of the *Cpa3* locus¹¹⁰. Crossing of transgenic *Cpa3-Cre* mice to mice bearing a floxed allele of the anti-apoptotic factor *Mcl-1* resulted in severe mast cell deficiency and marked reduction in basophil numbers. Consequently, mating *Cpa3-Cre* mice to reporter mice revealed high levels of *Cpa3*-driven Cre expression not only in peritoneal mast cells but also in splenic basophils¹¹⁰. Consistent with this observation, *Cpa3* expression was identified in basophils that were purified from the lung of *Nb* infected mice¹⁵². Our laboratory generated a reporter strain that directly visualizes *Cpa3* expression by a cell surface marker. In detail, the cell surface marker human CD4 (hCD4) was inserted into the *Cpa3* locus by homologous recombination and thus *Cpa3*-driven human CD4 expression reflects the transcription of this locus (unpublished data). Based on *Cpa3^{hCD4}* mice, cell surface expression of human CD4 was not only found in the mast cell lineage but also in hematopoietic progenitors of the basophil lineage as well as in mature splenic basophils. Notably, *Cpa3* expression in the basophil and

mast cell lineage supports the model of a common origin of these two lineages in adult murine hematopoiesis, as it was proposed by Arinobu et al¹⁸. Alternatively, the two lineages express *Cpa3* in independent progenitors for each lineage. Hence, Cre-mediated cell ablation affects not only the mast cell lineage but also results in partial reduction of the basophil compartment in *Cpa3*^{Cre/+} mice.

It should be examined whether the remaining basophils are functionally normal and whether their reduction may influence basophil-dependent immunological responses in *Cpa3*^{Cre/+} mice. The induction of IgE-dependent systemic anaphylaxis does not require basophils since adoptive transfer of cultured mast cells completely restored the defective anaphylactic response in *Cpa3*^{Cre/+} mice. Thus, mast cells are the key effector cells of this response, although basophils also express the high affinity IgE receptor FcεRI. Another model of an IgE-dependent allergic reaction, chronic allergic inflammation (CAI), has been shown to be solely dependent on basophils¹⁵³ and this allergic response is abolished in several mouse models of basophil ablation^{110,112,134}. It might be possible that CAI is also suppressed in *Cpa3*^{Cre/+} mice, what still needs to be examined. Instead of CAI, we tested IgG1-dependent passive systemic anaphylaxis in *Cpa3*^{Cre/+} mice to analyze the functional capacity of the remaining basophils. Passively administered IgG1-immune complexes induce anaphylaxis that depends exclusively on interaction with FcγRIII¹³⁸. IgG1-mediated passive systemic anaphylaxis was not abrogated in mast cell-deficient *Kit*^{W-sh/W-sh} mice, whereas depletion of basophils decreased the severity of the anaphylactic response¹³⁶. Hence, basophils have been supposed to be crucial players in this 'alternative pathway of anaphylaxis'. *Cpa3*^{Cre/+} and *Cpa3*^{Cre/Cre} mice, which lack about 65 % to 80 % basophils respectively, were largely resistant to IgG1-mediated anaphylaxis. One would expect a similar reaction in *Kit*^{W/Wv} mice, which lack even 80 % to 90 % of basophils in peripheral blood¹⁰⁸ and spleen, respectively. However, *Kit*^{W/Wv} mice responded by a drastic even though transient drop in body temperature in this anaphylaxis model. It is not known how many basophils are actually required to induce an efficient IgG1-mediated anaphylactic response. Possibly, remaining basophils in *Kit*^{W/Wv} mice are sufficient to orchestrate IgG1-dependent passive anaphylaxis whereas residual basophils in *Cpa3*^{Cre/+} mice are functionally abnormal in ways that limit their ability to induce an efficient anaphylactic response.

Alternatively, alterations of other cell lineages in *Kit* mutant *Kit^{W/W^v}* mice may compensate for the lack of basophils, rendering them responsive to IgG1-mediated anaphylaxis. In summary, *Cpa3^{Cre/+}* mice are not only mast cell-deficient but also exhibit a partial reduction in basophils, which should be considered when immunological functions are investigated in this strain.

Considerations on the mechanism of lineage ablation in *Cpa3^{Cre/+}* mice

What could be the mechanism underlying the loss of mast cells and the reduction of basophils? Cell ablation in *Cpa3^{Cre/+}* mice occurs in heterozygous gene-targeted mice independently of any introduced *loxP* sites, indicating that the lack of cells is unrelated to the disruption of the *Cpa3* locus. In line with this conclusion, *Cpa3^{-/-}* mice have normal numbers of mast cells¹⁵⁴. It seems that Cre expression by itself is responsible for constitutive cell ablation in *Cpa3^{Cre/+}* mice. Consistent with this idea, high levels of Cre expression have been reported to be toxic in certain murine and human cell lines^{132,133,155}. Adverse effects of Cre expression were also observed in vivo. Transgenic mice that express Cre in postmeiotic spermatids display aberrant chromosomal rearrangements in spermatids and suffer from male infertility¹²³. Another report demonstrated that transgenic mice, which express Cre under control of a fragment of the rat insulin II gene promoter (RIP-Cre mice), display glucose intolerance even if no floxed alleles are targeted¹⁵⁶. The authors of this study suggested that Cre toxicity might affect the function of pancreatic beta cells, which then results in impaired insulin secretion. A temporal regulation of Cre activity can be achieved by fusing Cre recombinase to the mutated ligand-binding domain of the estrogen receptor (ER^{T2}), which is highly sensitive to the synthetic ligand tamoxifen. Transgenic mouse lines, in which CreER^{T2} was inserted into the *Rosa26* locus (*R26CreER^{T2}* mice), showed reduced proliferation, increased apoptosis and illegitimate chromosomal rearrangement in hematopoietic lineages after tamoxifen administration¹²⁴. The authors proposed that the observed haematological abnormalities were caused by Cre-mediated toxicity of systemic CreER^{T2} activation. Mammalian genomes contain cryptic (or pseudo) *loxP* sites, which can serve as

functional recombinase recognition sites¹³⁵. A bioinformatics evaluation estimated that such sites are present in the mouse genome at a frequency of 1.2 per megabase (about 3000 sites in the total mouse genome)¹⁵⁷. Cre-induced recombination between cryptic *loxP* sites might account for chromosomal rearrangements and consequently for the frequently observed unintentional effect of aberrant Cre activity in vitro and in vivo. In particular, Higashi et al. demonstrated cleavage of a putative cryptic *loxP* site in the thymus genome of *R26CreER^{T2}* mice after the activation of CreER^{T2}¹²⁴.

Referring to our model, direct verification of Cre-mediated genotoxic effects on mast cells was not feasible in vivo due to the complete lack of this lineage in *Cpa3^{Cre/+}* mice. To investigate Cre toxicity in the mast cell lineage, bone marrow-derived mast cells were generated from *Cpa3^{Cre/+}* mice. Under normal culture conditions in the presence of IL-3 and SCF it was extremely inefficient to generate mast cells from *Cpa3^{Cre/+}* bone marrow compared to wild type bone marrow. Further analyses of *Cpa3^{Cre/+}* BMDC revealed genomic deletions and pseudotrismy, which is supportive of a genotoxic mechanism of mast cell ablation¹²². The genotoxic cell ablation is p53-dependent, as crossing of *Cpa3^{Cre/+}* mice to the p53 knock-out background rescued peritoneal and skin mast cells, at least partially¹²².

Taken together, the Cre-mediated effect is strong and effective enough to result in a complete deletion of the mast cell lineage in *Cpa3^{Cre/+}* mice. The toxic effect of *Cpa3*-driven Cre expression on mast cells is reminiscent of the constitutive and selective ablation of basophils in *Mcpt8-Cre* BAC transgenic mice¹³⁴. Possibly, mast cells and basophils are more sensitive to Cre overexpression than other cell lineages and/or they may not be able to compensate the loss, e.g. through developmental selection and adaptation processes. However, mast cell ablation due to Cre-mediated toxicity is unique to *Cpa3^{Cre/+}* mice because other mouse strains that express Cre recombinase under control of mast cell-specific promoters, such as *Mcpt5-Cre* mice¹⁵⁸, alpha-chymase-Cre transgenic mice (*Chm:Cre*)¹⁵⁹ or even transgenic *Cpa3-Cre* mice¹¹⁰ have normal mast cell numbers. What could be the reasons for the diverse phenotypes of these four different Cre-expressing mouse lines? First of all, in *Cpa3^{Cre/+}* mice Cre recombinase was inserted into the endogenous *Cpa3* locus via gene targeting while *Mcpt5-Cre*, *Chm:Cre* and *Cpa3-Cre* mice are transgenic lines

with random integration into the mouse genome. Transgenic *Cpa3-Cre* mice were constructed to express Cre under control of a 780 bp fragment of the *Cpa3* promoter¹¹⁰ and therefore do not contain all gene regulatory elements of the endogenous *Cpa3* gene. In addition, codon-improved Cre recombinase (iCre), which is mutated according to mammalian codon usage¹⁶⁰, was used for gene targeting in *Cpa3^{Cre/+}* mice. These differences in the construction of *Cpa3^{Cre/+}* mice could increase the expression strength of the Cre recombinase and thus account for Cre-mediated mast cell ablation specifically in this strain.

Finally, expression of the *Cpa3* locus is very strong in mature mast cells as shown by the analysis of human CD4 surface expression in *Cpa3^{hCD4/CD4}* mice. The *Cpa3* locus was weakly expressed in the bipotent basophil and mast cell progenitor (BMCP) and its expression level increased with further lineage development of both, mast cells and basophils. Progressive increase of *Cpa3* expression was paralleled by the loss of cells. The observed correlation between *Cpa3*-driven Cre expression and cell loss indirectly confirms the conclusion that cell ablation in *Cpa3^{Cre/+}* mice occurs due to toxic effects of Cre activation. Of note, *Cpa3* expression in progenitor T cells does not affect T cell development in *Cpa3^{Cre/+}* mice, they display normal numbers in all T cell subsets analyzed, probably because *Cpa3* expression in the T cell lineage is very weak and only transient¹²¹. These findings, together with the detailed analysis of immune cell subsets, show that Cre activation in *Cpa3^{Cre/+}* mice does not exert an aberrant effect on cells aside from of the mast cell and basophil lineages.

Kit deficiency rather than mast cell deficiency impacts susceptibility to K/BxN serum transfer arthritis

The *Cpa3^{Cre/+}* strain represents a novel, in-depth characterized model of mast cell deficiency. Given its advantages over the *Kit* mutant mast cell-deficient mouse models, the *Cpa3^{Cre/+}* strain serves as valuable tool for the investigation of mast cell functions in vivo.

Lee et al. reported that *Kit^{W/W^v}* mice were resistant to the development of joint inflammation in the K/BxN serum transfer arthritis⁹⁸. Since BMCC engraftment restored disease susceptibility, mast cells were considered to be a key effector

population in the pathogenesis of this experimental model of rheumatoid arthritis⁹⁸. Our own experiments with K/BxN serum-treated *Kit*^{W/Wv} mice confirmed the findings from Lee and colleagues that this mutant is highly resistant in this disease model. However, mast cell-deficient *Cpa3*^{Cre/+} mice were fully susceptible to serum transfer arthritis by clinical and histopathological criteria. In addition, wild type mice did not upregulate mast cell-associated products in the inflammatory joints during the disease course. In summary, these observations do not support the view that mast cells or their products are critically involved in the development of pathogenic arthritis in this model. In addition, a recent report demonstrated that *Kit*^{W-sh/W-sh} mice and *FcγRIIIB/IIIA*^{-/-}*FcεRI/II*^{-/-} mice, whose mast cells could not be activated directly by autoantibodies from K/BxN serum, develop full-blown arthritis after serum injection¹⁰⁸. The authors found that the activating IgG2 receptor FcγRIV, which is expressed by monocytes, macrophages and neutrophils, was the only Fc receptor required for disease induction¹⁰⁸. Altogether, these findings further indicate that mast cells are not mandatory for the development of K/BxN serum-transferred arthritis. Different disease outcomes in *Kit*^{W/Wv} and *Kit*^{W-sh/W-sh} mice have also been reported in the context of anti-collagen/LPS-induced arthritis¹⁶¹. Injection of anti-collagen monoclonal antibodies and LPS resulted in full arthritis in *Kit*^{W-sh/W-sh} mice and full resistance in *Kit*^{W/Wv} mice¹⁶¹.

Kit^{W/Wv} and *Kit*^{W-sh/W-sh} mice have hematopoietic abnormalities, which could influence the arthritic phenotype. Mainly, higher neutrophil¹⁶¹ and/or monocyte¹⁰⁸ numbers in *Kit*^{W-sh/W-sh} than in *Kit*^{W/Wv} mice may explain the observed differences in arthritis susceptibility. In support of this hypothesis, it was recently reported that adoptive transfer of neutrophils is sufficient to induce serum transfer arthritis in *Kit*^{W/Wv} mice¹⁶². Lower than normal numbers of neutrophils in *Kit*^{W/Wv} mice¹⁶¹ may thus protect from K/BxN serum transfer arthritis. Under conditions of neutropenia, mast cells could play a role, since mast cell engraftment restored disease susceptibility in *Kit*^{W/Wv} mice⁹⁸, and BMNC reconstitution of *Kit*^{W/Wv} mice failed to correct the peripheral neutropenia¹⁴⁴. Alternatively, myeloid and megakaryocyte expansion in the *Kit*^{W-sh/W-sh} mice may compensate for the lack of mast cells⁷⁹.

Taken together, the different responses of *Kit* mutant *Kit*^{W/Wv} and *Kit*^{W-sh/W-sh} mice in models of antibody-mediated arthritis suggest that factors other than mast cell

deficiency can determine the disease development. To obtain unambiguous results, it is mandatory to review the findings from *Kit* mutant strains in mast cell-deficient models with intact Kit function. We observed that mast cell-deficient mice with a normal immune system were fully susceptible to serum-transferred arthritis, which led us to question the contribution of mast cells in this autoimmune model.

EAE development is independent of mast cells and Kit signalling

A report from the year 2000 initiated a series of studies on the functional role of mast cells in the context of experimental autoimmune encephalomyelitis. This report stated that *Kit^{W/W^v}* mice develop attenuated and delayed MOG-induced EAE, and that this phenotype could be reversed by reconstitution with wild type BMMC⁹⁶. The access of neutrophils to the CNS, which is diminished in *Kit^{W/W^v}* mice, might be regulated by meningeal mast cell-secreted TNF- α ¹⁴⁴. Stelekati et al. published that EAE severity is also decreased in *Kit^{W-sh/W-sh}* mice which could be restored following mast cell reconstitution¹⁶³. According to these reports, it seemed very clear that mast cells contribute significantly to disease development in EAE. However, recent studies illustrate a more complex picture. Bennett and colleagues were the first to show that mast cell-deficient Kit mutants are completely susceptible to the development of EAE¹⁰⁵. Additionally, Li et al reported exacerbated disease severity in *Kit^{W-sh/W-sh}* mice compared to wild type controls¹⁰⁷. Here we have shown that *Cpa3^{Cre/+}* mice as well as *Kit^{W/W^v}* mice developed full-blown EAE. Remarkably, we noticed more moribund mice in the *Kit^{W/W^v}* group than in wild type controls and mast cell-deficient *Cpa3^{Cre/+}* mice. Moreover, we observed the same extent of immune cell infiltration into the CNS and peripheral MOG-specific T cell response in mast cell-deficient strains and wild type animals.

The divergent results obtained by different research groups might be related to different immunization protocols used to induce EAE. At least for the *Kit^{W/W^v}* model, it has been shown that the dose of adjuvant or peptide in the immunization protocol can affect the extent of mast cell involvement in experimental models of asthma¹⁶⁴ and contact hypersensitivity¹⁶⁵. Accordingly, it was demonstrated that *Kit^{W/W^v}* mice

were differentially susceptible to EAE induction depending on the strength of the immunization protocol whereas *Kit*^{W-sh/W-sh} mice developed exacerbated EAE under all tested conditions of immunization¹⁰⁶. We induced EAE in *Kit*^{W/Wv} mice under rather mild conditions similar to those described in the literature¹⁰⁶, and observed an exacerbated disease course compared to wild type controls. However, in their recent publication Brown and colleagues also described reduced EAE severity in *Kit*^{W/Wv} mice when applying a milder immunization protocol¹⁴⁴. Thus, different protocols of EAE induction seem to be not the only factor that determines the results obtained by different groups investigating EAE susceptibility in the *Kit*^{W/Wv} strain. Further factors, which might have an influence on the disease outcome in *Kit* mutant models, include age of the mice¹⁶⁶, potential exposure of the mice to environmental stress or pathogens during disease course^{167,168}, housing conditions, or the composition of the gut microflora¹⁶⁹. Furthermore, the observed divergences between *Kit*^{W/Wv} and *Kit*^{W-sh/W-sh} mice may depend on the complex and diverse hematopoietic alterations in these strains. In general, it is hard to draw a clear conclusion about the involvement of mast cells in EAE pathology when mast cell dependency varies with the experimental conditions or the impact of Kit mutation. Our results from EAE induction in Kit-proficient *Cpa3*^{Cre/+} mice do not support a major role of mast cells in this autoimmune model.

In summary, the *Cpa3*^{Cre/+} strain is a new mouse model that constitutively lacks mast cells independent of Kit mutations or toxin applications. A detailed analysis of their immunological status under steady-state conditions revealed that *Cpa3*^{Cre/+} mice do not suffer from hematopoietic abnormalities except for a partial reduction in the number of splenic basophils. In contrast to published findings based on experiments with *Kit* mutant *Kit*^{W/Wv} mice, mast cell deficiency in *Cpa3*^{Cre/+} mice had no impact on disease susceptibility to antibody-mediated arthritis and EAE. This observation indicates that Kit deficiency rather than the lack of mast cells in *Kit*^{W/Wv} mice influences the disease outcome in these autoimmune models.

Hence, *Cpa3*^{Cre/+} mice represent a new cornerstone in the field of mast cell research for the re-evaluation of the immunomodulatory functions of mast cells in a Kit-proficient genetically mast cell-deficient environment.

5 References

1. Ehrlich, P. Beiträge zur Theorie und Praxis der Histologischen Färbung. *Thesis, Leipzig University* (1878).
2. Portier P., R.C. De l'action anaphylactique de certains venins. *C. R. Soc. Bio.* **54**, 170 - 172 (1902).
3. Riley, J.F. & West, G.B. Histamine in tissue mast cells. *J Physiol* **117**, 72P-73P (1952).
4. Riley, J.F. & West, G.B. The presence of histamine in tissue mast cells. *J Physiol* **120**, 528-537 (1953).
5. Riley, J.F. & West, G.B. Mast cells and histamine in normal and pathological tissues. *J Physiol* **119**, 44P (1953).
6. Riley, J.F. & West, G.B. Tissue mast cells: studies with a histamine-liberator of low toxicity (compound 48/80). *J Pathol Bacteriol* **69**, 269-282 (1955).
7. Mota, I. & Vugman, I. Effects of anaphylactic shock and compound 48/80 on the mast cells of the guinea pig lung. *Nature* **177**, 427-429 (1956).
8. Ishizaka, K. & Campbell, D.H. Biologic activity of soluble antigen-antibody complexes. IV. The inhibition of the skin reactivity of soluble complexes and the PCA reaction by heterologous complexes. *J Immunol* **83**, 116-126 (1959).
9. Ishizaka, K. & Ishizaka, T. Identification of gamma-E-antibodies as a carrier of reaginic activity. *J Immunol* **99**, 1187-1198 (1967).
10. Kulczycki, A., Jr., Isersky, C. & Metzger, H. The interaction of IgE with rat basophilic leukemia cells. I. Evidence for specific binding of IgE. *J Exp Med* **139**, 600-616 (1974).
11. Conrad, D.H., Berczi, I. & Froese, A. Characterization of the target cell receptor for IgE-I. Solubilization of IgE-receptor complexes from rat mast cells and rat basophilic leukemia cells. *Immunochemistry* **13**, 329-332 (1976).
12. Barsumian, E.L., Isersky, C., Petrino, M.G. & Siraganian, R.P. IgE-induced histamine release from rat basophilic leukemia cell lines: isolation of releasing and nonreleasing clones. *Eur J Immunol* **11**, 317-323 (1981).
13. Fewtrell, C. Comparative aspects of secretion from tumor and normal mast cells. *Adv. Inflam. Res.* **1**, 205-221 (1979).
14. Kitamura, Y., Shimada, M., Hatanaka, K. & Miyano, Y. Development of mast cells from grafted bone marrow cells in irradiated mice. *Nature* **268**, 442-443 (1977).

15. Rodewald, H.R., Dessing, M., Dvorak, A.M. & Galli, S.J. Identification of a committed precursor for the mast cell lineage. *Science* **271**, 818-822 (1996).
16. Chen, C.C., Grimaldeston, M.A., Tsai, M., Weissman, I.L. & Galli, S.J. Identification of mast cell progenitors in adult mice. *Proc Natl Acad Sci U S A* **102**, 11408-11413 (2005).
17. Jamur, M.C., *et al.* Identification and characterization of undifferentiated mast cells in mouse bone marrow. *Blood* **105**, 4282-4289 (2005).
18. Arinobu, Y., *et al.* Developmental checkpoints of the basophil/mast cell lineages in adult murine hematopoiesis. *Proc Natl Acad Sci U S A* **102**, 18105-18110 (2005).
19. Sonoda, T., Kitamura, Y., Haku, Y., Hara, H. & Mori, K.J. Mast-cell precursors in various haematopoietic colonies of mice produced in vivo and in vitro. *Br J Haematol* **53**, 611-620 (1983).
20. Tsai, M., *et al.* Induction of mast cell proliferation, maturation, and heparin synthesis by the rat c-kit ligand, stem cell factor. *Proc Natl Acad Sci U S A* **88**, 6382-6386 (1991).
21. Kitamura, Y., Go, S. & Hatanaka, K. Decrease of mast cells in W/Wv mice and their increase by bone marrow transplantation. *Blood* **52**, 447-452 (1978).
22. Kitamura, Y. & Go, S. Decreased production of mast cells in S1/S1d anemic mice. *Blood* **53**, 492-497 (1979).
23. Razin, E., *et al.* Interleukin 3: A differentiation and growth factor for the mouse mast cell that contains chondroitin sulfate E proteoglycan. *J Immunol* **132**, 1479-1486 (1984).
24. Eklund, K.K., *et al.* Mouse bone marrow-derived mast cells (mBMMC) obtained in vitro from mice that are mast cell-deficient in vivo express the same panel of granule proteases as mBMMC and serosal mast cells from their normal littermates. *J Exp Med* **180**, 67-73 (1994).
25. Lantz, C.S., *et al.* Role for interleukin-3 in mast-cell and basophil development and in immunity to parasites. *Nature* **392**, 90-93 (1998).
26. Galli, S.J., Grimaldeston, M. & Tsai, M. Immunomodulatory mast cells: negative, as well as positive, regulators of immunity. *Nat Rev Immunol* **8**, 478-486 (2008).
27. Goldstein, S.M., *et al.* Detection and partial characterization of a human mast cell carboxypeptidase. *J Immunol* **139**, 2724-2729 (1987).
28. Schechter, N.M., *et al.* Identification of a chymotrypsin-like proteinase in human mast cells. *J Immunol* **137**, 962-970 (1986).

29. Schwartz, L.B., Lewis, R.A. & Austen, K.F. Tryptase from human pulmonary mast cells. Purification and characterization. *J Biol Chem* **256**, 11939-11943 (1981).
30. Gordon, J.R. & Galli, S.J. Mast cells as a source of both preformed and immunologically inducible TNF-alpha/cachectin. *Nature* **346**, 274-276 (1990).
31. Metz, M., *et al.* Mast cells can enhance resistance to snake and honeybee venoms. *Science* **313**, 526-530 (2006).
32. Akahoshi, M., *et al.* Mast cell chymase reduces the toxicity of Gila monster venom, scorpion venom, and vasoactive intestinal polypeptide in mice. *J Clin Invest* **121**, 4180-4191 (2011).
33. Schneider, L.A., Schlenner, S.M., Feyerabend, T.B., Wunderlin, M. & Rodewald, H.R. Molecular mechanism of mast cell mediated innate defense against endothelin and snake venom sarafotoxin. *J Exp Med* **204**, 2629-2639 (2007).
34. Piliponsky, A.M., *et al.* Neurotensin increases mortality and mast cells reduce neurotensin levels in a mouse model of sepsis. *Nat Med* **14**, 392-398 (2008).
35. Huang, C., *et al.* Induction of a selective and persistent extravasation of neutrophils into the peritoneal cavity by tryptase mouse mast cell protease 6. *J Immunol* **160**, 1910-1919 (1998).
36. Knight, P.A., Wright, S.H., Lawrence, C.E., Paterson, Y.Y. & Miller, H.R. Delayed expulsion of the nematode *Trichinella spiralis* in mice lacking the mucosal mast cell-specific granule chymase, mouse mast cell protease-1. *J Exp Med* **192**, 1849-1856 (2000).
37. McDermott, J.R., *et al.* Mast cells disrupt epithelial barrier function during enteric nematode infection. *Proc Natl Acad Sci U S A* **100**, 7761-7766 (2003).
38. Thakurdas, S.M., *et al.* The mast cell-restricted tryptase mMCP-6 has a critical immunoprotective role in bacterial infections. *J Biol Chem* **282**, 20809-20815 (2007).
39. Roberts, L.J., 2nd, Lewis, R.A., Oates, J.A. & Austen, K.F. Prostaglandin thromboxane, and 12-hydroxy-5,8,10,14-eicosatetraenoic acid production by ionophore-stimulated rat serosal mast cells. *Biochim Biophys Acta* **575**, 185-192 (1979).
40. Razin, E., Mencia-Huerta, J.M., Lewis, R.A., Corey, E.J. & Austen, K.F. Generation of leukotriene C4 from a subclass of mast cells differentiated in vitro from mouse bone marrow. *Proc Natl Acad Sci U S A* **79**, 4665-4667 (1982).

41. Plaut, M., *et al.* Mast cell lines produce lymphokines in response to cross-linkage of Fc epsilon RI or to calcium ionophores. *Nature* **339**, 64-67 (1989).
42. Enerback, L. Mast cells in rat gastrointestinal mucosa. 2. Dye-binding and metachromatic properties. *Acta Pathol Microbiol Scand* **66**, 303-312 (1966).
43. Enerback, L. Berberine sulphate binding to mast cell polyanions: a cytofluorometric method for the quantitation of heparin. *Histochemistry* **42**, 301-313 (1974).
44. Bienenstock, J., *et al.* Mast cell heterogeneity. *Monogr Allergy* **18**, 124-128 (1983).
45. Friend, D.S., *et al.* Mast cells that reside at different locations in the jejunum of mice infected with *Trichinella spiralis* exhibit sequential changes in their granule ultrastructure and chymase phenotype. *J Cell Biol* **135**, 279-290 (1996).
46. Friend, D.S., *et al.* Reversible expression of tryptases and chymases in the jejunal mast cells of mice infected with *Trichinella spiralis*. *J Immunol* **160**, 5537-5545 (1998).
47. Abe, T., Swieter, M., Imai, T., Hollander, N.D. & Befus, A.D. Mast cell heterogeneity: two-dimensional gel electrophoretic analyses of rat peritoneal and intestinal mucosal mast cells. *Eur J Immunol* **20**, 1941-1947 (1990).
48. Reynolds, D.S., *et al.* Different mouse mast cell populations express various combinations of at least six distinct mast cell serine proteases. *Proc Natl Acad Sci U S A* **87**, 3230-3234 (1990).
49. Xing, W., Austen, K.F., Gurish, M.F. & Jones, T.G. Protease phenotype of constitutive connective tissue and of induced mucosal mast cells in mice is regulated by the tissue. *Proc Natl Acad Sci U S A* **108**, 14210-14215 (2011).
50. Enerback, L. & Lundin, P.M. Ultrastructure of mucosal mast cells in normal and compound 48-80-treated rats. *Cell Tissue Res* **150**, 95-105 (1974).
51. Metcalfe, D.D., Baram, D. & Mekori, Y.A. Mast cells. *Physiol Rev* **77**, 1033-1079 (1997).
52. Okayama, Y. & Kawakami, T. Development, migration, and survival of mast cells. *Immunol Res* **34**, 97-115 (2006).
53. Stead, R.H., *et al.* Intestinal mucosal mast cells in normal and nematode-infected rat intestines are in intimate contact with peptidergic nerves. *Proc Natl Acad Sci U S A* **84**, 2975-2979 (1987).
54. Galli, S.J., Maurer, M. & Lantz, C.S. Mast cells as sentinels of innate immunity. *Curr Opin Immunol* **11**, 53-59 (1999).

55. McLachlan, J.B., *et al.* Mast cell-derived tumor necrosis factor induces hypertrophy of draining lymph nodes during infection. *Nat Immunol* **4**, 1199-1205 (2003).
56. Mazzoni, A., Young, H.A., Spitzer, J.H., Visintin, A. & Segal, D.M. Histamine regulates cytokine production in maturing dendritic cells, resulting in altered T cell polarization. *J Clin Invest* **108**, 1865-1873 (2001).
57. Jawdat, D.M., Rowden, G. & Marshall, J.S. Mast cells have a pivotal role in TNF-independent lymph node hypertrophy and the mobilization of Langerhans cells in response to bacterial peptidoglycan. *J Immunol* **177**, 1755-1762 (2006).
58. McCurdy, J.D., Lin, T.J. & Marshall, J.S. Toll-like receptor 4-mediated activation of murine mast cells. *J Leukoc Biol* **70**, 977-984 (2001).
59. Matsushima, H., Yamada, N., Matsue, H. & Shimada, S. TLR3-, TLR7-, and TLR9-mediated production of proinflammatory cytokines and chemokines from murine connective tissue type skin-derived mast cells but not from bone marrow-derived mast cells. *J Immunol* **173**, 531-541 (2004).
60. Supajatura, V., *et al.* Differential responses of mast cell Toll-like receptors 2 and 4 in allergy and innate immunity. *J Clin Invest* **109**, 1351-1359 (2002).
61. Supajatura, V., *et al.* Protective roles of mast cells against enterobacterial infection are mediated by Toll-like receptor 4. *J Immunol* **167**, 2250-2256 (2001).
62. Orinska, Z., *et al.* TLR3-induced activation of mast cells modulates CD8+ T-cell recruitment. *Blood* **106**, 978-987 (2005).
63. Heib, V., *et al.* Mast cells are crucial for early inflammation, migration of Langerhans cells, and CTL responses following topical application of TLR7 ligand in mice. *Blood* **110**, 946-953 (2007).
64. Tkaczyk, C., Okayama, Y., Metcalfe, D.D. & Gilfillan, A.M. Fcγ receptors on mast cells: activatory and inhibitory regulation of mediator release. *Int Arch Allergy Immunol* **133**, 305-315 (2004).
65. Johnson, A.R., Hugli, T.E. & Muller-Eberhard, H.J. Release of histamine from rat mast cells by the complement peptides C3a and C5a. *Immunology* **28**, 1067-1080 (1975).
66. Marshall, J.S. Mast-cell responses to pathogens. *Nat Rev Immunol* **4**, 787-799 (2004).
67. Dawicki, W. & Marshall, J.S. New and emerging roles for mast cells in host defence. *Curr Opin Immunol* **19**, 31-38 (2007).

68. Galli, S.J. & Kitamura, Y. Genetically mast-cell-deficient W/W^v and Sl/Sl^d mice. Their value for the analysis of the roles of mast cells in biologic responses in vivo. *Am J Pathol* **127**, 191-198 (1987).
69. Grimbaldeston, M.A., *et al.* Mast cell-deficient W-sash c-kit mutant Kit W-sh/W-sh mice as a model for investigating mast cell biology in vivo. *Am J Pathol* **167**, 835-848 (2005).
70. Galli, S.J., Arizono, N., Murakami, T., Dvorak, A.M. & Fox, J.G. Development of large numbers of mast cells at sites of idiopathic chronic dermatitis in genetically mast cell-deficient WBB6F1-W/W^v mice. *Blood* **69**, 1661-1666 (1987).
71. Kitamura, Y., Yokoyama, M., Matsuda, H. & Shimada, M. Coincidental development of forestomach papilloma and prepyloric ulcer in nontreated mutant mice of W/W^v and Sl/Sl^d genotypes. *Cancer Res* **40**, 3392-3397 (1980).
72. Shimada, M., *et al.* Spontaneous stomach ulcer in genetically mast-cell depleted W/W^v mice. *Nature* **283**, 662-664 (1980).
73. Yokoyama, M., Tatsuta, M., Baba, M. & Kitamura, Y. Bile reflux: a possible cause of stomach ulcer in nontreated mutant mice of W/W^v genotype. *Gastroenterology* **82**, 857-863 (1982).
74. Gordon, J.R. & Galli, S.J. Phorbol 12-myristate 13-acetate-induced development of functionally active mast cells in W/W^v but not Sl/Sl^d genetically mast cell-deficient mice. *Blood* **75**, 1637-1645 (1990).
75. Waskow, C., Bartels, S., Schlenner, S.M., Costa, C. & Rodewald, H.R. Kit is essential for PMA-inflammation-induced mast-cell accumulation in the skin. *Blood* **109**, 5363-5370 (2007).
76. Lyon, M.F. & Glenister, P.H. A new allele sash (Wsh) at the W-locus and a spontaneous recessive lethal in mice. *Genet Res* **39**, 315-322 (1982).
77. Duttlinger, R., *et al.* W-sash affects positive and negative elements controlling c-kit expression: ectopic c-kit expression at sites of kit-ligand expression affects melanogenesis. *Development* **118**, 705-717 (1993).
78. Nagle, D.L., Kozak, C.A., Mano, H., Chapman, V.M. & Bucan, M. Physical mapping of the Tec and Gabrb1 loci reveals that the Wsh mutation on mouse chromosome 5 is associated with an inversion. *Hum Mol Genet* **4**, 2073-2079 (1995).
79. Nigrovic, P.A., *et al.* Genetic inversion in mast cell-deficient (Wsh) mice interrupts corin and manifests as hematopoietic and cardiac aberrancy. *Am J Pathol* **173**, 1693-1701 (2008).

80. Yamazaki, M., *et al.* C-kit gene is expressed by skin mast cells in embryos but not in puppies of Wsh/Wsh mice: age-dependent abolishment of c-kit gene expression. *Blood* **83**, 3509-3516 (1994).
81. Berrozpe, G., *et al.* A distant upstream locus control region is critical for expression of the Kit receptor gene in mast cells. *Mol Cell Biol* **26**, 5850-5860 (2006).
82. Chan, J.C., *et al.* Hypertension in mice lacking the proatrial natriuretic peptide convertase corin. *Proc Natl Acad Sci U S A* **102**, 785-790 (2005).
83. Zsebo, K.M., *et al.* Stem cell factor is encoded at the Sl locus of the mouse and is the ligand for the c-kit tyrosine kinase receptor. *Cell* **63**, 213-224 (1990).
84. Nakano, T., *et al.* Fate of bone marrow-derived cultured mast cells after intracutaneous, intraperitoneal, and intravenous transfer into genetically mast cell-deficient W/W^v mice. Evidence that cultured mast cells can give rise to both connective tissue type and mucosal mast cells. *J Exp Med* **162**, 1025-1043 (1985).
85. Lu, L.F., *et al.* Mast cells are essential intermediaries in regulatory T-cell tolerance. *Nature* **442**, 997-1002 (2006).
86. Heissig, B., *et al.* Low-dose irradiation promotes tissue revascularization through VEGF release from mast cells and MMP-9-mediated progenitor cell mobilization. *J Exp Med* **202**, 739-750 (2005).
87. Coussens, L.M., *et al.* Inflammatory mast cells up-regulate angiogenesis during squamous epithelial carcinogenesis. *Genes Dev* **13**, 1382-1397 (1999).
88. Sun, J., *et al.* Mast cells promote atherosclerosis by releasing proinflammatory cytokines. *Nat Med* **13**, 719-724 (2007).
89. Toms, R., Weiner, H.L. & Johnson, D. Identification of IgE-positive cells and mast cells in frozen sections of multiple sclerosis brains. *J Neuroimmunol* **30**, 169-177 (1990).
90. Ibrahim, M.Z., Reder, A.T., Lawand, R., Takash, W. & Sallouh-Khatib, S. The mast cells of the multiple sclerosis brain. *J Neuroimmunol* **70**, 131-138 (1996).
91. Neuman, J. Über das Vorkommen der sogenannten "Mastzellen" bei pathologischen Veränderungen des Gehirns. *Arch. Pathol. Anat. Physiol. Virchows* **122**, 378-381 (1890).
92. Lock, C., *et al.* Gene-microarray analysis of multiple sclerosis lesions yields new targets validated in autoimmune encephalomyelitis. *Nat Med* **8**, 500-508 (2002).

93. Rozniecki, J.J., Hauser, S.L., Stein, M., Lincoln, R. & Theoharides, T.C. Elevated mast cell tryptase in cerebrospinal fluid of multiple sclerosis patients. *Ann Neurol* **37**, 63-66 (1995).
94. Brenner, T., Soffer, D., Shalit, M. & Levi-Schaffer, F. Mast cells in experimental allergic encephalomyelitis: characterization, distribution in the CNS and in vitro activation by myelin basic protein and neuropeptides. *J Neurol Sci* **122**, 210-213 (1994).
95. Dietsch, G.N. & Hinrichs, D.J. The role of mast cells in the elicitation of experimental allergic encephalomyelitis. *J Immunol* **142**, 1476-1481 (1989).
96. Secor, V.H., Secor, W.E., Gutekunst, C.A. & Brown, M.A. Mast cells are essential for early onset and severe disease in a murine model of multiple sclerosis. *J Exp Med* **191**, 813-822 (2000).
97. Woolley, D.E. & Tetlow, L.C. Mast cell activation and its relation to proinflammatory cytokine production in the rheumatoid lesion. *Arthritis Res* **2**, 65-74 (2000).
98. Lee, D.M., *et al.* Mast cells: a cellular link between autoantibodies and inflammatory arthritis. *Science* **297**, 1689-1692 (2002).
99. Kouskoff, V., *et al.* Organ-specific disease provoked by systemic autoimmunity. *Cell* **87**, 811-822 (1996).
100. Korganow, A.S., *et al.* From systemic T cell self-reactivity to organ-specific autoimmune disease via immunoglobulins. *Immunity* **10**, 451-461 (1999).
101. Wipke, B.T. & Allen, P.M. Essential role of neutrophils in the initiation and progression of a murine model of rheumatoid arthritis. *J Immunol* **167**, 1601-1608 (2001).
102. Ji, H., *et al.* Critical roles for interleukin 1 and tumor necrosis factor alpha in antibody-induced arthritis. *J Exp Med* **196**, 77-85 (2002).
103. Malfait, A.M., *et al.* The beta2-adrenergic agonist salbutamol is a potent suppressor of established collagen-induced arthritis: mechanisms of action. *J Immunol* **162**, 6278-6283 (1999).
104. Xu, D., *et al.* IL-33 exacerbates antigen-induced arthritis by activating mast cells. *Proc Natl Acad Sci U S A* **105**, 10913-10918 (2008).
105. Bennett, J.L., *et al.* Bone marrow-derived mast cells accumulate in the central nervous system during inflammation but are dispensable for experimental autoimmune encephalomyelitis pathogenesis. *J Immunol* **182**, 5507-5514 (2009).

106. Piconese, S., *et al.* Exacerbated experimental autoimmune encephalomyelitis in mast-cell-deficient Kit W-sh/W-sh mice. *Lab Invest* **91**, 627-641 (2011).
107. Li, H., *et al.* Kit (W-sh) mice develop earlier and more severe experimental autoimmune encephalomyelitis due to absence of immune suppression. *J Immunol* **187**, 274-282 (2011).
108. Mancardi, D.A., *et al.* Cutting Edge: The murine high-affinity IgG receptor FcγR4 is sufficient for autoantibody-induced arthritis. *J Immunol* **186**, 1899-1903 (2011).
109. Dudeck, A., *et al.* Mast cells are key promoters of contact allergy that mediate the adjuvant effects of haptens. *Immunity* **34**, 973-984 (2011).
110. Lilla, J.N., *et al.* Reduced mast cell and basophil numbers and function in Cpa3-Cre; Mcl-1^{fl/fl} mice. *Blood* **118**, 6930-6938 (2011).
111. Otsuka, A., *et al.* Requirement of interaction between mast cells and skin dendritic cells to establish contact hypersensitivity. *PLoS One* **6**, e25538 (2011).
112. Sawaguchi, M., *et al.* Role of mast cells and basophils in IgE responses and in allergic airway hyperresponsiveness. *J Immunol* **188**, 1809-1818 (2012).
113. Feyerabend, T.B., *et al.* Cre-mediated cell ablation contests mast cell contribution in models of antibody- and T cell-mediated autoimmunity. *Immunity* **35**, 832-844 (2011).
114. Palmiter, R.D., *et al.* Cell lineage ablation in transgenic mice by cell-specific expression of a toxin gene. *Cell* **50**, 435-443 (1987).
115. Saito, M., *et al.* Diphtheria toxin receptor-mediated conditional and targeted cell ablation in transgenic mice. *Nat Biotechnol* **19**, 746-750 (2001).
116. Mitamura, T., Higashiyama, S., Taniguchi, N., Klagsbrun, M. & Mekada, E. Diphtheria toxin binds to the epidermal growth factor (EGF)-like domain of human heparin-binding EGF-like growth factor/diphtheria toxin receptor and inhibits specifically its mitogenic activity. *J Biol Chem* **270**, 1015-1019 (1995).
117. Sauer, B. & Henderson, N. The cyclization of linear DNA in *Escherichia coli* by site-specific recombination. *Gene* **70**, 331-341 (1988).
118. Buch, T., *et al.* A Cre-inducible diphtheria toxin receptor mediates cell lineage ablation after toxin administration. *Nat Methods* **2**, 419-426 (2005).
119. Voehringer, D., Liang, H.E. & Locksley, R.M. Homeostasis and effector function of lymphopenia-induced "memory-like" T cells in constitutively T cell-depleted mice. *J Immunol* **180**, 4742-4753 (2008).

120. Zhou, P., *et al.* Mcl-1 in transgenic mice promotes survival in a spectrum of hematopoietic cell types and immortalization in the myeloid lineage. *Blood* **92**, 3226-3239 (1998).
121. Feyerabend, T.B., *et al.* Deletion of Notch1 converts pro-T cells to dendritic cells and promotes thymic B cells by cell-extrinsic and cell-intrinsic mechanisms. *Immunity* **30**, 67-79 (2009).
122. Feyerabend, T.B., Weiser, A. & al., e. Cre-mediated cell ablation contests mast cell contribution in models of antibody- and T cell-mediated autoimmunity. *Immunity* **35**, 832-844 (2011).
123. Schmidt, E.E., Taylor, D.S., Prigge, J.R., Barnett, S. & Capecchi, M.R. Illegitimate Cre-dependent chromosome rearrangements in transgenic mouse spermatids. *Proc Natl Acad Sci U S A* **97**, 13702-13707 (2000).
124. Higashi, A.Y., *et al.* Direct hematological toxicity and illegitimate chromosomal recombination caused by the systemic activation of CreERT2. *J Immunol* **182**, 5633-5640 (2009).
125. Tawfik, D.S., Chap, R., Eshhar, Z. & Green, B.S. pH on-off switching of antibody-hapten binding by site-specific chemical modification of tyrosine. *Protein Eng* **7**, 431-434 (1994).
126. Karasuyama, H. & Melchers, F. Establishment of mouse cell lines which constitutively secrete large quantities of interleukin 2, 3, 4 or 5, using modified cDNA expression vectors. *Eur J Immunol* **18**, 97-104 (1988).
127. FA, R.E.a.L. Selection and inbreeding for longevity of a lethal type. *J Hered* **50** 19-25 (1959).
128. Bernstein SE, R.E., Keighley G. Two hereditary mouse anemias (Sl/Sld and W/Wv) deficient in response to erythropoietin. *Annals of the New York Academy of Sciences* **149**, 475-485 (1968).
129. Piconese, S., *et al.* Mast cells counteract regulatory T-cell suppression through interleukin-6 and OX40/OX40L axis toward Th17-cell differentiation. *Blood* **114**, 2639-2648 (2009).
130. Piconese, S., Valzasina, B. & Colombo, M.P. OX40 triggering blocks suppression by regulatory T cells and facilitates tumor rejection. *J Exp Med* **205**, 825-839 (2008).
131. Paul A. Chervenick†, D.R.B. Decreased neutrophils and megakaryocytes in anemic mice of genotype W/Wv. *Journal of Cellular Physiology* **73**, 25-30 (1969).

132. Loonstra, A., *et al.* Growth inhibition and DNA damage induced by Cre recombinase in mammalian cells. *Proc Natl Acad Sci U S A* **98**, 9209-9214 (2001).
133. Silver, D.P. & Livingston, D.M. Self-excising retroviral vectors encoding the Cre recombinase overcome Cre-mediated cellular toxicity. *Mol Cell* **8**, 233-243 (2001).
134. Ohnmacht, C., *et al.* Basophils orchestrate chronic allergic dermatitis and protective immunity against helminths. *Immunity* **33**, 364-374 (2010).
135. Thyagarajan, B., Guimaraes, M.J., Groth, A.C. & Calos, M.P. Mammalian genomes contain active recombinase recognition sites. *Gene* **244**, 47-54 (2000).
136. Tsujimura, Y., *et al.* Basophils play a pivotal role in immunoglobulin-G-mediated but not immunoglobulin-E-mediated systemic anaphylaxis. *Immunity* **28**, 581-589 (2008).
137. Strait, R.T., Morris, S.C., Yang, M., Qu, X.W. & Finkelman, F.D. Pathways of anaphylaxis in the mouse. *J Allergy Clin Immunol* **109**, 658-668 (2002).
138. Jonsson, F., *et al.* Mouse and human neutrophils induce anaphylaxis. *J Clin Invest* **121**, 1484-1496 (2011).
139. Benoist, C. & Mathis, D. Mast cells in autoimmune disease. *Nature* **420**, 875-878 (2002).
140. Jacobs, J.P., *et al.* Deficiency of CXCR2, but not other chemokine receptors, attenuates autoantibody-mediated arthritis in a murine model. *Arthritis Rheum* **62**, 1921-1932 (2010).
141. Hickey, W.F. Migration of hematogenous cells through the blood-brain barrier and the initiation of CNS inflammation. *Brain Pathol* **1**, 97-105 (1991).
142. Gregory, G.D., Robbie-Ryan, M., Secor, V.H., Sabatino, J.J., Jr. & Brown, M.A. Mast cells are required for optimal autoreactive T cell responses in a murine model of multiple sclerosis. *Eur J Immunol* **35**, 3478-3486 (2005).
143. Sun, D., *et al.* Myelin antigen-specific CD8⁺ T cells are encephalitogenic and produce severe disease in C57BL/6 mice. *J Immunol* **166**, 7579-7587 (2001).
144. Sayed, B.A., Christy, A.L., Walker, M.E. & Brown, M.A. Meningeal mast cells affect early T cell central nervous system infiltration and blood-brain barrier integrity through TNF: a role for neutrophil recruitment? *J Immunol* **184**, 6891-6900 (2010).
145. Ford, A.L., Goodsall, A.L., Hickey, W.F. & Sedgwick, J.D. Normal adult ramified microglia separated from other central nervous system macrophages

- by flow cytometric sorting. Phenotypic differences defined and direct ex vivo antigen presentation to myelin basic protein-reactive CD4⁺ T cells compared. *J Immunol* **154**, 4309-4321 (1995).
146. Ajami, B., Bennett, J.L., Krieger, C., McNagny, K.M. & Rossi, F.M. Infiltrating monocytes trigger EAE progression, but do not contribute to the resident microglia pool. *Nat Neurosci* **14**, 1142-1149 (2011).
 147. Denney, L., *et al.* Activation of invariant NKT cells in early phase of experimental autoimmune encephalomyelitis results in differentiation of Ly6Chi inflammatory monocyte to M2 macrophages and improved outcome. *J Immunol* **189**, 551-557 (2012).
 148. Mildner, A., *et al.* CCR2+Ly-6Chi monocytes are crucial for the effector phase of autoimmunity in the central nervous system. *Brain* **132**, 2487-2500 (2009).
 149. Irani, A.M., *et al.* Deficiency of the tryptase-positive, chymase-negative mast cell type in gastrointestinal mucosa of patients with defective T lymphocyte function. *J Immunol* **138**, 4381-4386 (1987).
 150. Ruitenbergh, E.J. & Elgersma, A. Absence of intestinal mast cell response in congenitally athymic mice during *Trichinella spiralis* infection. *Nature* **264**, 258-260 (1976).
 151. Jacoby, W., Cammarata, P.V., Findlay, S. & Pincus, S.H. Anaphylaxis in mast cell-deficient mice. *J Invest Dermatol* **83**, 302-304 (1984).
 152. Voehringer, D., Shinkai, K. & Locksley, R.M. Type 2 immunity reflects orchestrated recruitment of cells committed to IL-4 production. *Immunity* **20**, 267-277 (2004).
 153. Mukai, K., *et al.* Basophils play a critical role in the development of IgE-mediated chronic allergic inflammation independently of T cells and mast cells. *Immunity* **23**, 191-202 (2005).
 154. Feyerabend, T.B., *et al.* Loss of histochemical identity in mast cells lacking carboxypeptidase A. *Mol Cell Biol* **25**, 6199-6210 (2005).
 155. de Alboran, I.M., *et al.* Analysis of C-MYC function in normal cells via conditional gene-targeted mutation. *Immunity* **14**, 45-55 (2001).
 156. Lee, J.Y., *et al.* RIP-Cre revisited, evidence for impairments of pancreatic beta-cell function. *J Biol Chem* **281**, 2649-2653 (2006).
 157. Semprini, S., *et al.* Cryptic loxP sites in mammalian genomes: genome-wide distribution and relevance for the efficiency of BAC/PAC recombineering techniques. *Nucleic Acids Res* **35**, 1402-1410 (2007).

158. Scholten, J., *et al.* Mast cell-specific Cre/loxP-mediated recombination in vivo. *Transgenic Res* **17**, 307-315 (2008).
159. Musch, W., Wege, A.K., Mannel, D.N. & Hehlgans, T. Generation and characterization of alpha-chymase-Cre transgenic mice. *Genesis* **46**, 163-166 (2008).
160. Shimshek, D.R., *et al.* Codon-improved Cre recombinase (iCre) expression in the mouse. *Genesis* **32**, 19-26 (2002).
161. Zhou, J.S., Xing, W., Friend, D.S., Austen, K.F. & Katz, H.R. Mast cell deficiency in Kit(W-sh) mice does not impair antibody-mediated arthritis. *J Exp Med* **204**, 2797-2802 (2007).
162. Tsuboi, N., *et al.* Regulation of human neutrophil Fcγ receptor IIa by C5a receptor promotes inflammatory arthritis in mice. *Arthritis Rheum* **63**, 467-478 (2011).
163. Stelekati, E., *et al.* Mast cell-mediated antigen presentation regulates CD8+ T cell effector functions. *Immunity* **31**, 665-676 (2009).
164. Williams, C.M. & Galli, S.J. Mast cells can amplify airway reactivity and features of chronic inflammation in an asthma model in mice. *J Exp Med* **192**, 455-462 (2000).
165. Norman, M.U., *et al.* Mast cells regulate the magnitude and the cytokine microenvironment of the contact hypersensitivity response. *Am J Pathol* **172**, 1638-1649 (2008).
166. Smith, M.E., Eller, N.L., McFarland, H.F., Racke, M.K. & Raine, C.S. Age dependence of clinical and pathological manifestations of autoimmune demyelination. Implications for multiple sclerosis. *Am J Pathol* **155**, 1147-1161 (1999).
167. Poliak, S., *et al.* Stress and autoimmunity: the neuropeptides corticotropin-releasing factor and urocortin suppress encephalomyelitis via effects on both the hypothalamic-pituitary-adrenal axis and the immune system. *J Immunol* **158**, 5751-5756 (1997).
168. La Flamme, A.C., Ruddenklau, K. & Backstrom, B.T. Schistosomiasis decreases central nervous system inflammation and alters the progression of experimental autoimmune encephalomyelitis. *Infect Immun* **71**, 4996-5004 (2003).
169. Ochoa-Reparaz, J., *et al.* Role of gut commensal microflora in the development of experimental autoimmune encephalomyelitis. *J Immunol* **183**, 6041-6050 (2009).

Acknowledgements

I am very grateful to Prof. Dr. Hans-Reimer Rodewald for giving me the opportunity to work on this project. I thank him for his supervision, continuous support and encouragement during the last years. His question 'Was gibt es Neues?' was the source for many extensive and constructive discussions.

I would like to thank Prof. Dr. Bernd Arnold for his second opinion on this thesis, and him and Prof. Dr. Hans-Jörg Fehling for their willingness to participate in my thesis advisory committee and for providing useful guidance.

I would like to address special thanks to Dr. Thorsten Feyerabend for his scientific advice and for acquainting me with various methods in the lab. Some of the results presented in my thesis were generated in collaboration with Thorsten. Last but not least, this study would not have been possible without his preliminary work, since he developed the mouse strains, which were the focus of my project.

I am grateful to the members of the DKFZ Microarray Core Facility for their helpful assistance with the mRNA expression profiling, Axel Benner for help with the statistical analyses, Dr. Marcus Feuerer and Martin Teichert for assisting in the analysis of the mRNA expression data, and all our collaborators in Germany and overseas for supporting us with cells, sera and expertise. I thank all present and former members of the Rodewald group in Ulm and in Heidelberg for their intensive support, for their help and the fun that we had inside and outside the lab.

My private thanks I would like to address to my family and my wonderful friends for their constant encouragement over my years of education and training. Thank you for being there for me and undergoing the ups and downs of life with me.